3-manifolds, q-series, and topological strings

Thesis by
Sunghyuk Park

In Partial Fulfillment of the Requirements for the
Degree of
Doctor of Philosophy in Mathematics

CALIFORNIA INSTITUTE OF TECHNOLOGY
Pasadena, California

2022
Defended May 3, 2022

Sunghyuk Park
ORCID: 0000-0002-6132-0871

ACKNOWLEDGEMENTS

First and foremost, I would like to thank my adviser, Sergei Gukov, for his tremendous support and guidance. He introduced me to this beautiful subject of quantum topology and mathematical physics, taught me how to become an independent researcher, and encouraged me when I needed it the most.

Research is a lot more fun when I get to discuss the problem and share ideas with other people, and I was lucky to have many collaborators: Sungbong Chun, Tobias Ekholm, Angus Gruen, Sergei Gukov, Po-Shen Hsin, Piotr Kucharski, Hiraku Nakajima, Du Pei, Pavel Putrov, Nikita Sopenko, Marko Stosic, and Piotr Sulkowski. I would like to thank them all for enjoyable collaborations. I look forward to more collaborations with them and with many others in the future.

I would also like to express my gratitude to Tobias Ekholm, Sergei Gukov, Tom Hutchcroft, Ciprian Manolescu, and Yi Ni for kindly serving in my thesis defense committee.

Fortunately, I have had opportunities to present my work at various seminars and conferences, online and offline. I am very grateful to the organizers for the invitation and to those who attended my talks and asked a lot of questions. Especially, I had wonderful times visiting Stanford, USC, UC Berkeley, and UT Austin in person, and I would like to thank Ciprian Manolescu, Cris Negron, Miroslav Rapcak, Mina Aganagic, and Dan Freed for their hospitality. I truly appreciate it.

I gratefully acknowledge the generous support from Kwanjeong Educational Foundation over the five years of my PhD, which allowed me to focus on research rather than spending too much time on TAing.

Last, but certainly not least, my life in the past five years was more fun because of my officemates and colleagues (Forte Shinko, Tamir Hemo, Nathaniel Sagman, Bowen Yang, Alex de Faveri, Frid Fu, and many others), roommates (Omar Mehio, Aidan Fenwick, and Bryan Gerber), friends from the badminton club (Sumit Goel, Jag Boddapati, Ashish Goel, Cathy Miao, Silvia Kim, Tung Wongwaitayakornkul, Masami Hazu, Shawn Yoshida, and many others), and the Chamber Music and Glee Club at Caltech (from which I should thank the directors and instructors: Maia Jasper White, Robert Ward, and Nancy Sulahian). They made a huge difference, and I thank them all. Finally, I dedicate my thesis to my mom and dad, for their love and support.

ABSTRACT

$\hat{Z}$ is a 3d TQFT whose existence was predicted by S. Gukov, D. Pei, P. Putrov, and C. Vafa in 2017. To each 3-manifold equipped with a spin^c structure, $\hat{Z}$ is supposed to assign a q-series with integer coefficients that is categorifiable and provides an analytic continuation of the Witten-Reshetikhin-Turaev invariants. In 2019, S. Gukov and C. Manolescu initiated a program to mathematically construct $\hat{Z}$ via Dehn surgery, and as part of that they conjectured that the Melvin-Morton-Rozansky expansion of the colored Jones polynomials can be re-summed into a two-variable series $F_K(x, q)$, which is $\hat{Z}$ for the knot complement. Following those developments, in this thesis we develop further and generalize the theory of $\hat{Z}$. Some of the main results are:

1. Proof of Gukov-Manolescu conjecture for a big class of links, including all homogeneous braid links, which gives a mathematical definition of $\hat{Z}$ for the complements of those links;

2. Generalization of Gukov-Pei-Putrov-Vafa formula for $\hat{Z}$ for negative-definite plumbed 3-manifolds to general Lie algebra;

3. Various conjectures coming out of the interpretation of $F_K(x, q)$ in terms of topological strings, such as the HOMFLY-PT analogue (i.e., a-deformation) of $F_K(x, q)$ and the holomorphic Lagrangian generalizing the A-polynomial.

PUBLISHED CONTENT AND CONTRIBUTIONS

[Ekh+22] Tobias Ekholm, Angus Gruen, Sergei Gukov, Piotr Kucharski, Sunghyuk Park, Marko Stošić, and Piotr Sułkowski. "Branches, quivers, and ideals for knot complements". In: *Journal of Geometry and Physics* 177 (2022), p. 104520. ISSN: 0393-0440. DOI: 10.1016/j.geomphys.2022.104520.

[Par20a] Sunghyuk Park. "Higher rank $\hat{Z}$ and F_K". In: *SIGMA Symmetry Integrability Geom. Methods Appl.* 16 (2020), Paper No. 044, 17. DOI: 10.3842/SIGMA.2020.044.

[Par20b] Sunghyuk Park. "Large color R-matrix for knot complements and strange identities". In: *J. Knot Theory Ramifications* 29.14 (2020), pp. 2050097, 32. ISSN: 0218-2165. DOI: 10.1142/S0218216520500972.

TABLE OF CONTENTS

Chapter 1

OVERVIEW

1.1 Introduction

"If a smooth 4-manifold is homeomorphic to S^4, then does it follow that it is diffeomorphic to S^4?" This is a major open problem in topology known as the smooth Poincaré conjecture in dimension four. The fact that such a fundamental question remains open to date shows how little is known about the differential topology in dimension four. In order to develop an understanding of smooth 4-manifolds, it is vital to construct an invariant of smooth 4-manifolds that is strong and easily computable.

A *categorification* of an invariant of n-manifolds assigns a graded vector space $\mathcal{H}(Y) = \oplus_{i\in\mathbb{Z}}\mathcal{H}_i(Y)$, instead of a number, to each n-manifold Y in such a way that the Euler characteristic $\sum_{i\in\mathbb{Z}}(-1)^i \dim \mathcal{H}_i(Y)$ of the graded vector space recovers the original invariant. For each cobordism X from Y_1 to Y_2, the categorification assigns a linear map from $\mathcal{H}(Y_1)$ to $\mathcal{H}(Y_2)$. In particular, it assigns a number to each closed $(n+1)$-manifold X, which can be considered as a cobordism from an empty manifold to itself. The idea of categorification has revolutionized the study of low-dimensional topology, as it provides a way to construct much stronger invariants of manifolds. For instance, Rasmussen's s-invariant of a knot [Ras10], which provides a lower bound to the slice genus of the knot, can be derived from Khovanov homology [Kho00], a categorification of the Jones polynomial.

To date, however, most research on categorification has been limited to invariants of knots, instead of 3-manifolds. While categorification of knot invariants has provided new insights on smooth surfaces in the 4-ball, it does not tell us much about general smooth 4-manifolds. In order to construct novel invariants of smooth 4-manifolds, it is desirable to categorify topological invariants of 3-manifolds, instead of knots. The main challenge has been to find the right candidate of an invariant of 3-manifolds that can be categorified.

Physics provides a promising idea to answer this question. There is a construction in string theory and M-theory that takes an n-dimensional manifold Y and an ADE type Lie algebra $\mathfrak{g}$ as an input and produces a $(6-n)$-dimensional quantum field theory $T_{\mathfrak{g}}[Y]$ that contains a wealth of information about the manifold Y itself. When the manifold Y is 3-dimensional, there is an invariant $\hat{Z}^{\mathfrak{g}}_Y$ of Y derived from $T_{\mathfrak{g}}[Y]$ known as the *homological block* [GPV17; Guk+20]. Physically, the homological block is a certain count of what is known as the *Bogomol'nyi–Prasad–Sommerfield (BPS) states*. This means that the vector space of BPS states provides a natural categorification of the homological block of 3-manifolds. In other words, the homological block $\hat{Z}^{\mathfrak{g}}$ is the sought-after invariant of 3-dimensional manifolds that can be categorified.

This provides a research program to construct a novel invariant of smooth 4-dimensional manifolds by categorifying the homological block, in a mathematically rigorous way.

Problem 1.1.1. Mathematically construct and categorify the homological block. This problem can be divided into two parts:

1. Mathematically construct the homological block $\hat{Z}^{\mathfrak{g}}$ as an invariant of 3-manifolds.
2. Mathematically construct the vector space of BPS states as a categorification of the homological block.

It should be noted that it is a highly non-trivial problem to "translate" the physical construction into mathematics. This is because, for one thing, quantum field theory is not yet mathematically rigorously defined, and for another, not much is known about the physics of the quantum field theory $T_{\mathfrak{g}}[Y]$ for a general 3-manifold Y. Hence, completing this research problem would not only be impactful in low-dimensional topology but also would shed light on the physics of the quantum field theory $T_{\mathfrak{g}}[Y]$.

1.2 This thesis

What this thesis is about

This thesis is about the first part of the Problem 1.1.1; that is, we focus on constructing the q-series invariant $\hat{Z}$ of 3-manifolds, leaving the categorification problem for the future. While this problem has not been solved completely yet, we have been able to make significant progress. For simplicity, assume $\mathfrak{g} = \mathfrak{sl}_2$ for now. The main ingredient in our construction is the *large-color R-matrix* [Par20b; Par] that we introduce in Chapter 3. It is the R-matrix describing the braiding of Verma modules of $U_q(\mathfrak{sl}_2)$. Using Verma modules and the R-matrix, we construct $\hat{Z}$ for a large class of 3-manifolds, that includes all complements of homogeneous braid links.

Theorem 1.2.1 ([Par]). *For any homogeneous braid link $L \subset S^3$, there is a well-defined invariant $\hat{Z}_{S^3 \setminus L}$ that can be computed from a state sum model on the homogeneous braid diagram.*

A braid is called *homogeneous* if it can be presented by a braid word $\sigma_{i_1}^{\epsilon_1} \cdots \sigma_{i_l}^{\epsilon_l}$, $\epsilon_k \in \{\pm 1\}$, where each Artin generator σ_j always appears with the same sign. A link is called a *homogeneous braid link* if it is a closure of a homogeneous braid. For example, the figure-eight knot $\mathbf{4}_1$ is a homogeneous braid knot, as it is the closure of the homogeneous braid $\sigma_1 \sigma_2^{-1} \sigma_1 \sigma_2^{-1}$. It is well-known [Sta78] that any link L can be made into a homogeneous braid link $L' = L \cup K$ by adding an auxiliary unknot component K with any desired linking number with each component of L. Combined with the classical theorem of Lickorish and Wallace [Lic62; Lic63; Wal60] that any closed, oriented, connected 3-manifold can be obtained by performing Dehn surgery on a framed link in S^3 (with ± 1 surgery coefficients), it implies that for any 3-manifold Y, there is a link $L \subset Y$ such that the complement $Y \setminus L$ is homeomorphic to the complement of a homogeneous braid link $L' \subset S^3$. Therefore, our theorem has the following corollary.

Corollary 1.2.2. *For any 3-manifold Y, there is a link $L \subset Y$ for which we can compute $\hat{Z}_{Y \setminus L}$.*

In other words, the first part of the Problem 1.1.1 is now reduced to the problem of finding a Dehn surgery formula for $\hat{Z}$. While a fully general Dehn surgery formula is not available yet, there are many hints. One of them is the conjectural $\frac{p}{r}$-surgery formula of Gukov and Manolescu [GM21], which can be applied whenever $-\frac{r}{p}$ is sufficiently large. Another one is the conjectural regularized surgery formula coming from the *inverted Habiro series*. We review them in Chapter 2 and 4.

Another main result of this thesis is the study of the dependence of $\hat{Z}$ on the choice of Lie algebra $\mathfrak{g}$, which is the topic of Chapter 5. The following result generalizes the result of [Guk+20] and [GM21] from $\mathfrak{sl}_2$ to an arbitrary simple Lie algebra.

Theorem 1.2.3 ([Par20a]). *Fix a simple Lie algebra $\mathfrak{g}$. For any negative definite plumbed 3-manifold (or any negative definite plumbed knot complement) Y, there is a well-defined invariant $\hat{Z}^{\mathfrak{g}}_Y$.*

When $\mathfrak{g} = \mathfrak{sl}_N$ and $Y = S^3 \setminus K$ is the complement of a torus knot $K = T_{s,t}$, after specializing to symmetric representations, it can be checked that

$$\hat{A}_K(\hat{x}, \hat{y}, a, q)\Big|_{a=q^N} \hat{Z}^{\mathfrak{sl}(N)}_{S^3\setminus K}(x, q) = 0,$$

where $\hat{A}_K(\hat{x}, \hat{y}, a, q)$ is a q-difference operator known as the a-deformed quantum A-polynomial of K [FGS13]. In view of such a regular behavior of $\hat{Z}_{S^3\setminus K}$ under the change of the rank of the Lie algebra, it is natural to conjecture that for any knot K, there is a three-variable invariant $\hat{Z}_{S^3\setminus K}(x, a, q)$ that interpolates all the $\mathfrak{sl}_N$ invariants $\hat{Z}^{\mathfrak{sl}_N}_{S^3\setminus K}(x, q)$.

From the physics point of view, there is a natural interpretation of such a three-variable invariant [Ekh+; Ekh+22] as a count of open topological strings. This is based on the well-known duality [Wit95; GV98; OV00] between Chern-Simons theory and topological string theory. The novelty in our case is that we need to use the knot complement Lagrangian instead of the usual knot conormal Lagrangian. While the physical description of $\hat{Z}^{\mathfrak{sl}_N}_{S^3\setminus K}(x, q)$ is not mathematically rigorous, it allows us to formulate a number of concrete mathematical conjectures which can be explicitly checked for some simple knots. We review them in Chapter 6.

How this thesis is organized

In Chapter 2, we review the necessary background, including quantum groups, their representations, quantum invariants of links and 3-manifolds. We then review the definition of $\hat{Z}$ for negative definite plumbed 3-manifolds [Guk+20] as well as the conjectures of Gukov-Manolescu [GM21] on $\hat{Z}$ for knot complements and Dehn surgery formulas.

In Chapter 3 (based on [Par20b; Par]), we introduce the large-color R-matrix. Given a link diagram, the large-color R-matrix determines a state sum model, but due to the infinite-dimensional nature of Verma modules, it is a highly non-trivial problem to make sense of these infinite sums. We introduce the notion of *inverted state sums*, and show that if a link admits a link diagram on which the inverted state sum converges absolutely, then the inverted state sum is a well-defined invariant of the link. Any homogeneous braid link admits such a link diagram. This link invariant satisfies the expected properties of $\hat{Z}$ for link complements and therefore provides a definition of $\hat{Z}$ for those link complements.

In Chapter 4 (based on [Par]), we introduce the notion of *inverted Habiro series*. We present some q-series identities, which can be used to study $\hat{Z}$ of certain Dehn surgeries on a knot.

In Chapter 5 (based on [Par20a]), we present a generalization of the works [Guk+20; GM21] reviewed in Chapter 2 to any simple Lie algebra $\mathfrak{g}$. We also provide simple formulas of $\hat{Z}^{\mathfrak{g}}$ for some 3-manifolds, including Seifert manifolds with 3 singular fibers and torus knot complements.

In Chapter 6 (based on [Ekh+; Ekh+22]), we present some conjectures on $\hat{Z}_{S^3\setminus K}(x, a, q)$ that are motivated from the physics of topological strings.

Chapter 2

BACKGROUND

2.1 Chern-Simons theory

Quantum topology, now a mature field of study of more than 30 years of history, started with the discovery of Jones polynomial [Jon85] and its interpretation as the expectation value of the Wilson line defect in Chern-Simons theory [Wit89]. Chern-Simons theory is a prominent example of a 3-dimensional topological quantum field theory (TQFT) [Ati88; Wit88], and it can be defined mathematically using the representation theory of quantum groups [RT91]. There are numerous textbooks on this topic, such as [Ati90; Koh02; Tur94; BK01], so we will not review in detail what Chern-Simons theory is. Instead, let us briefly review what *colored Jones polynomials* and *Witten-Reshetikhin-Turaev invariants* are, which will be useful for the readers in reading the later chapters.

Quantum groups

Quantum $\mathfrak{sl}_2$, $U_q(\mathfrak{sl}_2)$, is an associative algebra over $\mathbb{C}(q^{\frac{1}{4}})$ generated by $E, F, K^{\pm\frac{1}{2}}(= q^{\pm\frac{H}{4}})$ with relations[1]

$$K^{\frac{1}{2}}E = q^{\frac{1}{2}}EK^{\frac{1}{2}}, \quad K^{\frac{1}{2}}F = q^{-\frac{1}{2}}FK^{\frac{1}{2}}, \quad [E,F] = \frac{K-K^{-1}}{q^{\frac{1}{2}}-q^{-\frac{1}{2}}}.$$

In fact, $U_q(\mathfrak{sl}_2)$ is not just an associate algebra, but it is a quasitriangular Hopf algebra. This means, first of all, that it is a Hopf algebra with the following coproduct, counit and antipode

$$\Delta(E) = E\otimes K^{\frac{1}{2}} + K^{-\frac{1}{2}}\otimes E, \quad \Delta(F) = F\otimes K^{\frac{1}{2}} + K^{-\frac{1}{2}}\otimes F, \quad \Delta(K^{\frac{1}{2}}) = K^{\frac{1}{2}}\otimes K^{\frac{1}{2}},$$

$$\epsilon(E) = \epsilon(F) = 0, \quad \epsilon(K^{\frac{1}{2}}) = 1,$$

$$S(E) = -q^{\frac{1}{2}}E, \quad S(F) = -q^{-\frac{1}{2}}F, \quad S(K^{\frac{1}{2}}) = K^{-\frac{1}{2}},$$

and moreover that it admits a universal R-matrix

$$R = q^{\frac{H\otimes H}{4}}\sum_{k\geq 0} q^{-\frac{k(k+1)}{4}}\frac{(q^{\frac{1}{2}}-q^{-\frac{1}{2}})^k}{[k]!}(K^{\frac{k}{2}}E^k\otimes K^{-\frac{k}{2}}F^k) \in U_q(\mathfrak{sl}_2)\hat{\otimes}U_q(\mathfrak{sl}_2).$$

[1] Here we are following the "balanced" convention used in [KM91] which uses a square root of K. It is possible to work only with integral powers of K as in [Hab02] by choosing the "unbalanced" generators $E_{Habiro} = E_{KM}K^{\frac{1}{2}}$, $F_{Habiro} = K^{-\frac{1}{2}}F_{KM}$ instead.

For each $n \geq 1$, let V_n be the n-dimensional $U_q(\mathfrak{sl}_2)$-module with basis $\{v^0, \cdots, v^{n-1}\}$ on which the generators act by

$$Ev^j = [j]v^{j-1}, \quad Fv^j = [n-1-j]v^{j+1}, \quad Kv^j = q^{\frac{n-1-2j}{2}}v^j,$$

where $[m] := \frac{q^{\frac{m}{2}} - q^{-\frac{m}{2}}}{q^{\frac{1}{2}} - q^{-\frac{1}{2}}}$ for any $m \in \mathbb{Z}$.

Applying the universal R-matrix to V_n (followed by a flip $v \otimes w \mapsto w \otimes v$), we obtain an automorphism $\check{R} \in \mathrm{Aut}(V_n \otimes V_n)$ given by

$$\check{R}(v^i \otimes v^j) = q^{\frac{n^2-1}{4}} \sum_{k \geq 0} q^{-\frac{(i+j-k+1)(n-1)}{2} + (i-k)j} \begin{bmatrix} i \\ k \end{bmatrix}_q \prod_{1 \leq l \leq k} (1 - q^{-n+j+l}) v^{j+k} \otimes v^{i-k}$$

that satisfies the Yang-Baxter equation

$$\check{R}_{12}\check{R}_{23}\check{R}_{12} = \check{R}_{23}\check{R}_{12}\check{R}_{23},$$

where $\check{R}_{12} := \check{R} \otimes \mathrm{Id}_{V_n}$ and $\check{R}_{23} := \mathrm{Id}_{V_n} \otimes \check{R}$. The Yang-Baxter equation can be thought of diagrammatically as in Figure 2.1. Therefore, for any s (the number of

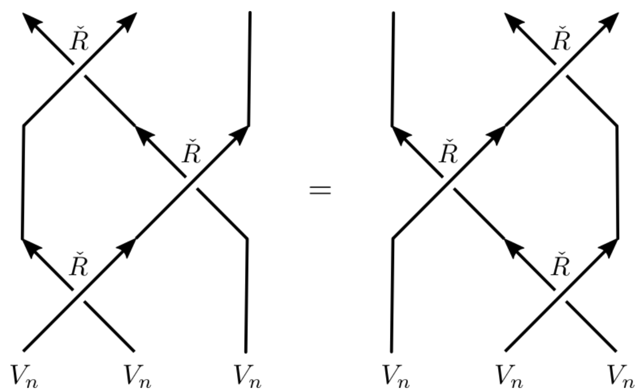

Figure 2.1: Yang-Baxter equation encodes the braid relation.

strands), the R-matrix induces a representation of the braid group

$$\varphi_{n,s} : B_s \longrightarrow \mathrm{Aut}(V_n^{\otimes s})$$

by applying $\check{R}$ for each positive crossing and $\check{R}^{-1}$ for each negative crossing.

Colored Jones polynomials

For any $U_q(\mathfrak{sl}_2)$-module V and an endomorphism $f \in \mathrm{End}(V)$, the *quantum trace* of f is defined to be

$$\mathrm{Tr}_q(f) := \mathrm{Tr}\big(K^{\otimes s} f\big).$$

The *quantum dimension* of a $U_q(\mathfrak{sl}_2)$-module V is simply the quantum trace of the identity map. In particular,

$$\mathrm{qdim}(V_n) = \mathrm{Tr}_q(\mathrm{Id}_{V_n}) = [n].$$

Let L be a link which can be presented as the closure of a braid β with s strands. The *unreduced n-colored Jones polynomial* $\tilde{J}_{L,n}(q)$ is the quantum trace of the automorphism $\varphi_{n,s}(\beta)$. That is,

$$\tilde{J}_{L,n}(q) := \mathrm{Tr}_q(\varphi_{n,s}(\beta)).$$

It can be shown that this is independent of the choice of a braid representing the link. Instead of the full quantum trace, we can also consider the partial quantum trace, which is taken by closing up the braid to the right, except for the left-most strand which we leave open. See Figure 2.2 for an example of the trefoil knot. Since V_n is

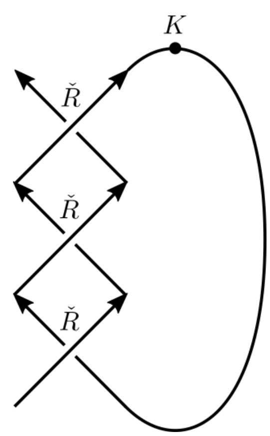

Figure 2.2: Partial quantum trace of the trefoil knot.

irreducible, by Schur's lemma, this partial quantum trace of $\varphi_{n,s}(\beta)$ is a constant times the identity map Id_{V_n}. The *reduced n-colored Jones polynomial* $J_{L,n}(q)$ is defined to be this constant. By closing up the remaining strand, we see that

$$J_{L,n}(q) = \frac{1}{[n]}\tilde{J}_{L,n}(q).$$

From now on, we will refer to the reduced n-colored Jones polynomial simply as the *n-colored Jones polynomial*. For any 0-framed (Seifert-framed) knot K, it can be shown that

$$J_{K,n}(q) \in \mathbb{Z}[q, q^{-1}].$$

Witten-Reshetikhin-Turaev invariants

Let Y be a closed 3-manifold obtained by performing a Dehn surgery on a framed link $L \in S^3$ with s components, and let ζ_k a primitive k-th root of unity. The *Witten-Reshetikhin-Turaev (WRT) invariant* $WRT_Y(\zeta_k)$ of Y at ζ_k is a topological invariant of Y that can be defined as a certain linear combination of $\tilde{J}_{L,n_1,\cdots,n_s}(\zeta_k)$ for $1 \leq n_1, \cdots, n_s \leq k-1$:

$$WRT_Y(\zeta_k) := C^{\sigma(L)} \sum_{1 \leq n_1, \cdots, n_s \leq k-1} S_{0n_s} \cdots S_{0n_s} \tilde{J}_{L,n_1,\cdots,n_s}(\zeta_k),$$

where $C^{\sigma(L)}$ is the framing factor, S_{0n_j}'s are the S-matrix elements, etc. The precise definition is not so important for the purpose of this thesis; interested readers can learn more by reading the standard textbooks such as [Tur94; BK01; Koh02] instead. What is important for us is that, while WRT invariants are natural analogues of the colored Jones polynomials for 3-manifolds, unlike colored Jones polynomials WRT invariants have no apparent integrality.

A crucial observation was made by Lawrence and Zaiger [LZ99]. They discovered that the WRT invariants of the Poincaré homology sphere (and some other Seifert 3-manifolds) can be obtained as, up to a simple overall factor, the limit of a power series in q with integer coefficients, as q approaches each root of unity radially from inside the unit disk.

Theorem 2.1.1 ([LZ99])**.** *Let $P = \Sigma(2,3,5)$ be the Poincaré homology sphere. Then*[2]

$$WRT_P(\zeta_k) = \lim_{q \to \zeta_k} \frac{\hat{Z}_P(q)}{2(q^{\frac{1}{2}} - q^{-\frac{1}{2}})},$$

where

$$\begin{aligned} \hat{Z}_P(q) &= q^{-\frac{3}{2}} \sum_{n \geq 0} \frac{(-1)^n q^{\frac{n(3n-1)}{2}}}{\prod_{1 \leq j \leq n}(1-q^{n+j})} \qquad (2.1) \\ &= q^{-\frac{3}{2}}(1 - q - q^3 - q^7 + q^8 + q^{14} + \cdots). \end{aligned}$$

Similar results for more general Seifert 3-manifolds can be found in a series of work by Hikami [Hik05a; Hik05b; Hik06b; Hik06a].

The important point is that, while integrality was not visible for WRT invariants, the "analytic continuation" of the WRT invariants has integer coefficients, making

[2]As we will see later, the denominator $2(q^{\frac{1}{2}} - q^{-\frac{1}{2}})$ is in fact $\hat{Z}_{S^3}(q)$.

it suitable for categorification. Homological blocks, that we introduce in the next section, can be thought of as a generalization of these analytically continued WRT invariants.

2.2 Homological blocks

As briefly described in the Introduction, the *homological blocks* were first introduced in the physics literature by Gukov, Pei, Putrov, and Vafa [GPV17; Guk+20] in their study of 3d/3d correspondence. The idea is to consider the 6d $\mathcal{N} = (0,2)$ theory (the world-volume theory of M5-branes) of type $\mathfrak{g}$ on $Y \times \mathbb{C} \times S^1$, where Y is a 3-manifold. Reducing the theory on Y, it becomes a 3d $\mathcal{N} = 2$ superconformal field theory $T_{\mathfrak{g}}[Y]$ on $\mathbb{C} \times S^1$. Viewing S^1 as the time direction, the physics "definition" of $\hat{Z}_Y$ is a count of BPS states:

$$\hat{Z}_{Y,b}(q) = \sum_{i,j} (-1)^i q^j \dim \mathcal{H}^{i,j}_{T_{\mathfrak{g}}[Y]}(\mathbb{C}, b),$$

where i is the R-charge, j is the spin, and b is a charge (superselection sector) of the M2-branes (ending on the M5-branes) that give rise to the BPS particles of $T_{\mathfrak{g}}[Y]$.

While it is not easy to make sense of this physics "definition" mathematically, the following conjecture proposes a precise relation between $\hat{Z}$ and WRT invariants.

Conjecture 2.2.1 ([Guk+20])**.** *Let Y be a 3-manifold with $b_1(Y) = 0$, and set $\mathfrak{g} = \mathfrak{sl}_2$ for simplicity. Then the WRT invariant of Y can be decomposed into a certain linear combination of $q \to e^{\frac{2\pi i}{k}}$ limit of $\hat{Z}_{Y,b}$. More explicitly,*

$$WRT_Y(e^{\frac{2\pi i}{k}}) = \sum_{a \in H_1(Y;\mathbb{Z})/\mathbb{Z}_2} e^{2\pi i k CS(a)} \sum_{b \in \mathrm{Spin}^c(Y)/\mathbb{Z}_2} S_{ab} \lim_{q \to e^{\frac{2\pi i}{k}}} \frac{\hat{Z}_{Y,b}(q)}{2(q^{\frac{1}{2}} - q^{-\frac{1}{2}})},$$

where S_{ab} is a matrix determined by the linking pairing of Y that does not depend on k. (See [Guk+20] for the explicit form of the matrix S_{ab}.)

This conjecture can be motivated in various ways, including resurgence in complex Chern-Simons theory around abelian flat connections [GMP16] and a string theory realization of Chern-Simons theory (nicely reviewed in [FP20, Sec. 2.1]).

In view of this conjecture, $\hat{Z}$ can be thought of as an "analytic continuation" of the WRT invariants, generalizing what we briefly reviewed in the previous section. What is perhaps a little surprising is that, according to this conjecture, in order to analytically continue the WRT invariant we need to decompose it into parts labeled by spin^c-structures on Y.

$\hat{Z}$ for negative definite plumbed 3-manifolds

There is a class of 3-manifolds called negative definite plumbed 3-manifolds for which there is a simple mathematical definition of $\hat{Z}$.

For any tree Γ whose vertices are labeled by integers (called the *plumbing graph*), there is a naturally associated framed link obtained by replacing each vertex by an unknot, framing it by the number labeling the vertex, and linking two unknots in the simplest possible way whenever the corresponding two vertices are connected by an edge. See Figure 2.3 for an example. By performing a Dehn surgery along that

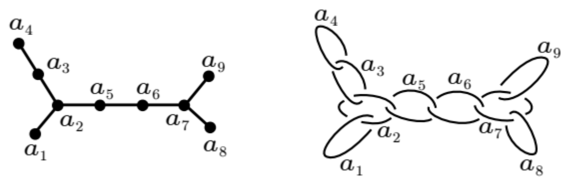

Figure 2.3: A plumbing graph and the corresponding surgery link.

framed link, we obtain a 3-manifold Y_Γ, called the *plumbed* 3-*manifold*.

Different plumbing graphs can give rise to the same 3-manifold, and such an equivalence relation between plumbing graphs is generated by a finite set of moves depicted in Figure 2.4 known as the *Neumann moves* [Neu81]; they are analogues of the Kirby moves [Kir78].

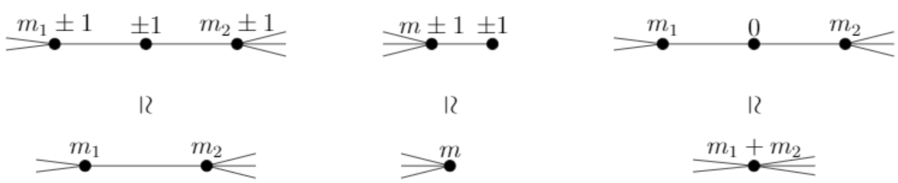

Figure 2.4: Neumann moves.

Let B be the adjacency matrix of the plumbing graph, with the integers labeling the vertices on the diagonal. That is, if $s = |V|$ and m_v's are the integers labeling the vertices, then B is the $s \times s$ matrix defined by

$$B_{vw} = \begin{cases} m_v & \text{if } v = w \\ 1 & \text{if } (v, w) \in E(\Gamma) \\ 0 & \text{otherwise} \end{cases}.$$

We call a plumbed 3-manifold *negative definite* if B is negative definite.

Definition 2.2.2 ([Guk+20])**.** For a negative definite plumbed 3-manifold Y_Γ, define

$$\hat{Z}_{Y_\Gamma,b}(q) = q^{-\frac{3s+\sum_v m_v}{4}} \oint \prod_{v\in V} \frac{dx_v}{2\pi i x_v}\left(\prod_{v\in V}(x_v^{\frac{1}{2}} - x_v^{-\frac{1}{2}})^{2-\deg v} \sum_{\ell\in 2B\mathbb{Z}^V+b} q^{-\frac{1}{4}(\ell,B^{-1}\ell)} x^{\frac{\ell}{2}}\right), \tag{2.2}$$

where

$$b \in (2\mathbb{Z}^V + \delta)/2B\mathbb{Z}^V \cong \mathrm{Spin}^c(Y_\Gamma),$$

and δ is the degree vector whose v-th coordinate is $\delta_v = \deg v$.

Theorem 2.2.3 ([GM21])**.** *The above definition is invariant under Neumann moves, and therefore it is a well-defined invariant of negative definite plumbed* 3*-manifolds.*

The expression (2.2) should be interpreted in the following way:

1. Take the symmetric expansion (i.e., average of the power series expansions near 0 and near ∞) of the rational function $(x_v^{\frac{1}{2}} - x_v^{-\frac{1}{2}})^{2-\deg v}$, and take product over all vertices $v \in V$. The result is a formal bilateral series in s variables.
2. Multiply it with the theta function $\sum_{\ell\in 2B\mathbb{Z}^V+b} q^{-\frac{1}{4}(\ell,B^{-1}\ell)} x^{\frac{\ell}{2}}$.
3. The contour integral $\oint \prod_{v\in V} \frac{dx_v}{2\pi i x_v}$ picks out the constant term of this formal series. Multiply it by $q^{-\frac{3s+\sum_v m_v}{4}}$, and we get $\hat{Z}_{Y_\Gamma,b}(q) \in 2^{-t}q^{\Delta}\mathbb{Z}[[q]]$, where t is the number of vertices with degree ≥ 3 and
$$\Delta = -\frac{3s+\sum_v m_v}{4} + \min_{\ell\in 2B\mathbb{Z}^V+b} \frac{-(\ell,B^{-1}\ell)}{4} \in \mathbb{Q}. \tag{2.3}$$

Note, negative definiteness of B ensures that the resulting q-series converges inside the unit disk $|q| < 1$.

Example 2.2.4.

- S^3: a single vertex labeled by -1.
$$\hat{Z}_{S^3}(q) = 2(q^{\frac{1}{2}} - q^{-\frac{1}{2}}).$$
- $L(8,3)$: two vertices both labeled by -3 connected by an edge.
$$\hat{Z}_{L(8,3)}(q) = \{q^{\frac{1}{4}}, q^{-\frac{1}{8}}, 0, 0, 0\}.$$
- $P = \Sigma(2,3,5)$: Y-shaped plumbing with four vertices, with the center vertex labeled by 1 and the other three vertices labeled by 2, 3, 5, respectively.
$$\begin{aligned}\hat{Z}_{\Sigma(2,3,5)}(q) &= q^{-\frac{3}{2}}(1 - q - q^3 - q^7 + q^8 + q^{14} + \cdots)\\ &= q^{-\frac{3}{2}} \sum_{n\geq 0} \frac{(-1)^n q^{\frac{n(3n-1)}{2}}}{\prod_{1\leq j\leq n}(1-q^{n+j})} = (2.1).\end{aligned}$$

- $\Sigma(2,3,7)$: Y-shaped plumbing with four vertices, with the center vertex labeled by -1 and the other three vertices labeled by $-2, -3, -7$, respectively, as in Figure 2.5.

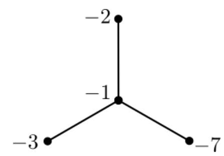

Figure 2.5: $\Sigma(2,3,7)$.

$$\begin{aligned}\hat{Z}_{\Sigma(2,3,7)}(q) &= q^{\frac{1}{2}}(1 - q - q^5 + q^{10} - q^{11} + q^{18} + \cdots) \\ &= q^{\frac{1}{2}} \sum_{n\geq 0} \frac{(-1)^n q^{\frac{n(n+1)}{2}}}{\prod_{1\leq j\leq n}(1-q^{n+j})}. \end{aligned} \tag{2.4}$$

Remark 2.2.5. This definition has various generalizations; see [Chu20; Par20a; FP20] for the generalization to general Lie algebras and Lie superalgebras, and [AJK21] for a common generalization of $\hat{Z}$ and lattice cohomology for negative definite plumbed 3-manifolds.

Remark 2.2.6. Conjecture 2.2.1 relating $\hat{Z}$ and WRT invariants is proven in many cases by now. See e.g., [AM22; Fuj+21; MM21].

Remark 2.2.7. Also, it is known that in many examples, they provide examples of quantum modular forms. See e.g., [BMM20b; BMM20a; Bri+21].

Remark 2.2.8. The overall shift of q-degree (2.3) is closely related to the ρ-invariant. See [GPP21].

Toward $\hat{Z}$ for general 3-manifolds

While negative definite plumbed 3-manifolds form a nice class of 3-manifolds, they are all examples of graph manifolds, and in particular none of them are hyperbolic. How do we generalize further? Since every closed, connected, oriented 3-manifold can be obtained by performing a Dehn surgery on a link in S^3, one possible approach is to

1. study $\hat{Z}$ for link complements, and then

2. study how it behaves under Dehn surgery.

This is the approach initiated by Gukov and Manolescu in [GM21]. By studying $\hat{Z}$ for plumbed knot complements, they proved that

Theorem 2.2.9 ([GM21])**.** *For the complement of a torus knot $K = T(s,t)$, there is a two-variable series*

$$\hat{Z}_{S^3\setminus K}(x,q) = F_K(x,q)$$

and a Dehn surgery formula

$$\hat{Z}_{S^3_{p/r}(K),b}(q) = \epsilon q^d \oint \frac{dx}{2\pi i x}\left((x^{\frac{1}{2r}} - x^{-\frac{1}{2r}}) F_K(x,q) \sum_{u\in \frac{p}{r}\mathbb{Z}+\frac{b}{r}} q^{-\frac{r}{p}u^2} x^u \right), \tag{2.5}$$

for some $\epsilon \in \{\pm 1\}$ and $d \in \mathbb{Q}$, provided that the right-hand side converges (i.e., when $-\frac{r}{p}$ is big enough).

They conjectured that such two-variable series invariant exists for all knots. In order to state their conjecture, we need to review the Melvin-Morton-Rozansky (MMR) expansion of colored Jones polynomials.

Theorem 2.2.10 (Conjectured by [MM95; Roz97], proved by [BG96; Roz98])**.** *Set $q = e^{\hbar}$. Consider the limit where $\hbar \to 0$ and $n \to \infty$ while $n\hbar$ is fixed. In this large-color limit, the colored Jones polynomial has the following expansion:*

$$J_{K,n}(q) = \frac{1}{\Delta_K(x)} + \frac{P_1(x)}{\Delta_K(x)^3}\hbar + \frac{P_2(x)}{\Delta_K(x)^5}\frac{\hbar^2}{2!} + \cdots,$$

where $x = q^n = e^{n\hbar}$, $\Delta_K(x)$ is the Alexander polynomial, and $P_j(x) \in \mathbb{Z}[x, x^{-1}]$ are Laurent polynomials invariant under Weyl symmetry $x \leftrightarrow x^{-1}$.

Conjecture 2.2.11 ([GM21])**.** *For any knot K, there is a two-variable series invariant $F_K(x,q)$ such that the $\hbar$-expansion of $\frac{F_K(x,e^{\hbar})}{x^{\frac{1}{2}}-x^{-\frac{1}{2}}}$ agrees with the MMR expansion of colored Jones polynomials. That is,*

$$\frac{F_K(x,e^{\hbar})}{x^{\frac{1}{2}}-x^{-\frac{1}{2}}} = \sum_{j\geq 0} \frac{P_j(x)}{\Delta_K(x)^{2j+1}}\frac{\hbar^j}{j!}$$

where the right-hand side is understood as the symmetric expansion (i.e., the average of its power series expansions near $x = 0$ and $x = \infty$), and $F_K(x,q)$ is a formal series of the form $\frac{1}{2}\sum_{m\in 2\mathbb{Z}+1} f_m(q) x^{\frac{m}{2}}$ with $f_m(q) \in \mathbb{Z}((q))$ and $f_{-m}(q) = -f_m(q)$.

Moreover,

$$\hat{A}_K(\hat{x},\hat{y},q)F_K(x,q) = 0,$$

where $\hat{A}_K$ is the quantum A-polynomial for the unreduced colored Jones polynomials of K.

This two-variable series $F_K(x,q)$ should really be thought of as $\hat{Z}$ for the knot complement $S^3 \setminus K$. It is conjectured [GM21, Conjecture 1.7] that the same Dehn surgery formula (2.5) can be applied to obtain the $\hat{Z}$ for the 3-manifold $S^3_{p/r}(K)$ obtained by performing the $\frac{p}{r}$-Dehn surgery on K whenever $-\frac{r}{p}$ is big enough.

Example 2.2.12 (Unknot)**.** For the unknot $\mathbf{0}_1$,

$$F_{\mathbf{0}_1}(x,q) = x^{\frac{1}{2}} - x^{-\frac{1}{2}}.$$

Example 2.2.13 (Figure-eight knot)**.** For the figure-eight knot $\mathbf{4}_1$,

$$\begin{aligned} J_{\mathbf{4}_1,n}(q) &= \sum_{0\le m\le n} \prod_{1\le j\le m} (q^n + q^{-n} - q^j - q^{-j}) \\ &= 1 \\ &\quad + (-1+n^2)\hbar^2 \\ &\quad + \left(\frac{47}{12} - 5n^2 + \frac{13}{12}n^4\right)\hbar^4 \\ &\quad + \cdots \\ &= \frac{1}{-x+3-x^{-1}} + \frac{x^2-4x+5-4x^{-1}+x^{-2}}{(-x+3-x^{-1})^5}\hbar^2 + \cdots . \end{aligned}$$

Expanding and resumming, we get

$$F_{\mathbf{4}_1}(x,q) = \frac{1}{2}\sum_{\substack{m\ge 0\\ \text{odd}}} f_m(q)\left(x^{\frac{m}{2}} - x^{-\frac{m}{2}}\right),$$

where

$$\begin{aligned} f_1 &= 1, \\ f_3 &= 2, \\ f_5 &= q^{-1} + 3 + q, \\ f_7 &= 2q^{-2} + 2q^{-1} + 5 + 2q + 2q^2, \end{aligned}$$

and so on.

Applying the (conjectural) -1-surgery formula,

$$\begin{aligned} \hat{Z}_{-\Sigma(2,3,7)}(q) &= -q^{-\frac{1}{2}}(1 + q + q^3 + q^4 + q^5 + 2q^7 + q^8 + 2q^9 + \cdots) \\ &= -q^{-\frac{1}{2}} \sum_{n\ge 0} \frac{q^{n^2}}{\prod_{1\le j\le n}(1-q^{n+j})}. \end{aligned} \tag{2.6}$$

This is one of Ramanujan's mock theta functions!

Remark 2.2.14. Compare (2.6) with (2.4). Up to sign, one expression can be obtained from another by replacing q with q^{-1}, which is exactly what is expected of $\hat{Z}$ under orientation reversal of the 3-manifold, from its connection to WRT invariants. Of course, it is a highly non-trivial problem to extend a q-series defined inside the unit disk $|q| < 1$ to outside the unit disk $|q| > 1$. We will see in Chapter 4 how *inverted Habiro expansion* of $F_K(x, q)$ can help constructing such pairs.

Chapter 3

LARGE-COLOR R-MATRIX

3.1 The large-color R-matrix

We would like to solve Conjecture 2.2.11. Since it is about the large-color asymptotics of colored Jones polynomials and since colored Jones polynomials can be obtained from R-matrices, it is natural to study the large-color limit of the R-matrices.

In the large-color limit, the finite-dimensional representations V_n become an infinite-dimensional *Verma module* V_∞ with a generic highest (or lowest) weight. We will mostly focus on the highest weight Verma modules, but the story is analogous for the lowest weight Verma modules (they are related via the Weyl symmetry $x \leftrightarrow x^{-1}$).

Let $V_\infty(x)$ denote the highest weight Verma module with the highest weight $\lambda = \log_q x - 1$. It has a basis $\{v_j\}_{j\geq 0}$ on which the generators of $U_q(\mathfrak{sl}_2)$ act by

$$Ev_j = [j]v_{j-1}, \quad Fv_j = [\lambda - j]v_{j+1}, \quad Kv_j = q^{\frac{\lambda-2j}{2}}v_j.$$

Definition 3.1.1. The *large-color R-matrix* is the R-matrix for these Verma modules (i.e., the universal R-matrix applied to the Verma modules[1]). Explicitly,

$$\begin{aligned}\check{R}(x_1,x_2) : V_\infty(x_1)\otimes V_\infty(x_2) &\to V_\infty(x_2)\otimes V_\infty(x_1)\\ v_i\otimes v_j &\mapsto \sum_{i',j'\geq 0} \check{R}(x_1,x_2)_{i,j}^{i',j'}\, v_{i'}\otimes v_{j'},\end{aligned}$$

where

$$\check{R}(x_1,x_2)_{i,j}^{i',j'} = \delta_{i+j,i'+j'}\, q^{(j+\frac{1}{2})(j'+\frac{1}{2})} x_1^{\frac{-i'-j-1}{4}} x_2^{\frac{i-3j'-1}{4}} \begin{bmatrix} i \\ j' \end{bmatrix}_q \prod_{1\leq l\leq i-j'} (1-q^{j+l}x_2^{-1}). \tag{3.1}$$

When the two strands are both $V_\infty(x)$, define also

$$\begin{aligned}\check{R}(x)_{i,j}^{i',j'} &:= q^{\frac{1}{4}}\check{R}(x,x)_{i,j}^{i',j'}\\ &= \delta_{i+j,i'+j'}\, q^{jj'+\frac{j+j'+1}{2}} x^{-\frac{j+j'+1}{2}} \begin{bmatrix} i \\ j' \end{bmatrix}_q \prod_{1\leq l\leq i-j'} (1-q^{j+l}x^{-1}).\end{aligned}$$

[1] To be more precise, we have divided it out by the framing factor so that when we apply this for a knot we automatically get an invariant associated to the canonical 0-framing.

The large-color R-matrix describes the braiding of the Verma modules, and it satisfies the Yang-Baxter equation, meaning it induces a representation of the braid group

$$\varphi_{x,s} : B_s \longrightarrow \mathrm{Aut}(V_\infty(x)^{\otimes s}),$$

and, if we use different x-parameters for different strands, a representation of the corresponding subgroup of the braid group (such as the pure braid group)

$$\varphi_{x_1,\cdots,x_s} : P_s \longrightarrow \mathrm{Aut}(V_\infty(x_1) \otimes \cdots \otimes V_\infty(x_s)).$$

An invariant of annular braid closures from the large-color R-matrix

Since we have a braid group representation coming from the large-color R-matrix, the most natural and naive guess would be that the two-variable series $F_K(x,q)$ in Conjecture 2.2.11 for a knot K (presented as the closure of a braid β with s strands) is the (partial) quantum trace of $\varphi_{x,s}(\beta)$. However, in general the quantum trace does not converge due to the infinite-dimensional nature of the Verma module.

There is a way to make sense of the trace, by making use of the fact $V_\infty(x)^{\otimes s}$ is graded by the total weight. For a vector $v_{i_1} \otimes \cdots \otimes v_{i_s} \in V_\infty(x)^{\otimes s}$, let its *total weight* be $w = \sum_{1\le k\le s} i_k$. Let $\left(V_\infty(x)^{\otimes s}\right)_w$ be the span of the vectors of total weight w. Then

$$V_\infty(x)^{\otimes s} = \oplus_{w\ge 0}\left(V_\infty(x)^{\otimes s}\right)_w.$$

The large-color R-matrix preserves the total weight, so the finite-dimensional subspaces $\left(V_\infty(x)^{\otimes s}\right)_w$ themselves are representations of the braid group B_s.

Definition 3.1.2. Define the *z-graded trace* of $\varphi_{x,s}(\beta)$ to be

$$\mathrm{Tr}_z(\varphi_{x,s}(\beta)) := \sum_{w\ge 0} z^w \,\mathrm{Tr}\left(\varphi_{x,s}(\beta)\big|_{\left(V_\infty(x)^{\otimes s}\right)_w}\right) \in q^{\frac{s+1}{2}} x^{\frac{s+1}{2}} \mathbb{Z}[x^{\pm 1}, q^{\pm 1}][[z]].$$

Clearly, this is invariant under braid isotopy and conjugation of the braid, and therefore it is an invariant of the annular closure of β (that is, the closure of β in the solid torus, where the braid goes around the S^1 direction of the solid torus). Moreover, our discussion so far in this subsection has an obvious generalization to braids whose closures are links, so from the z-graded trace we obtain an invariant of any annular braid closure.

The complement of the annular link $(D^2\times S^1)\setminus L$ is homeomorphic to the complement $S^3 \setminus L'$ of the link $L' = L \cup O$ obtained by adding an unknot component O to $L \subset S^3$ so that the braid β goes around the meridian of O once, as in Figure 3.1. We can

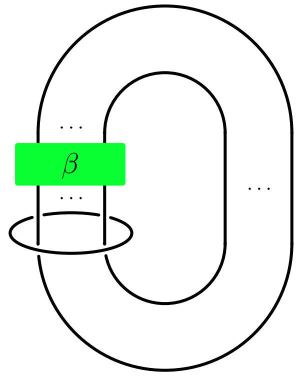

Figure 3.1: The link L'.

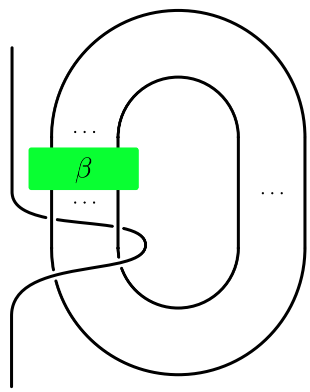

Figure 3.2: L' as a $(1,1)$-tangle.

open up the unknot component and draw L' as the $(1,1)$-tangle as in Figure 3.2. It turns out, the corresponding partial quantum trace converges absolutely to a power series in z^{-1}, if z is the parameter for the Verma module $V_\infty(z)$ assigned to the open strand. This can be seen by putting the vector v_0 on the ends of the open strand. It is easy to see that all the arcs of the open strand should carry v_0 as well. Using the fact that

$$\check{R}(z,x)^{a,0}_{0,a}\check{R}(x,z)^{0,a}_{a,0}x^{\frac{1}{2}}q^{-\frac{1}{2}-a} = z^{-a-\frac{1}{2}}$$

for any x and a, we see that the partial quantum trace multiplied by $(z^{\frac{1}{2}} - z^{-\frac{1}{2}})$ is exactly

$$F_{L'}(z,x,q) = (z^{\frac{1}{2}} - z^{-\frac{1}{2}})z^{-\frac{s}{2}}\,\mathrm{Tr}_{z^{-1}}(\varphi_{x,s}(\beta)).$$

This is in fact $\hat{Z}$ for the complement of the link L' in the sense that it satisfies all the properties in Conjecture 2.2.11! This can be shown using a proof similar to that of Rozansky's proof of MMR conjecture [Roz98]. We will give a more elaborate version of the state sum later in this chapter, as well as the proof of Conjecture 2.2.11 for a big class of links. In case of annular braid closures, what is special about L' is that its complement is fibered over S^1, with the fiber being a disk with s punctures. The fibered structure is what makes the state sum converge absolutely to a power series (in the variable associated to the S^1-direction) whose coefficients are polynomials. We will comment more about this in the next section.

Geometrical meaning of the parameter x

Geometrically, the parameters x_1 and x_2 are the (squares of the) *holonomy eigenvalues* around the meridians of the two strands, in $SL_2(\mathbb{C})$ Chern-Simons theory at the abelian branch. See [Eli+89] for a relevant discussion. For this reason, the R-matrix elements $\check{R}(x_1,x_2)_{i,j}^{i',j'}$ and $\check{R}^{-1}(x_1,x_2)_{i,j}^{i',j'}$ can be drawn diagrammatically as in Figure 3.3.

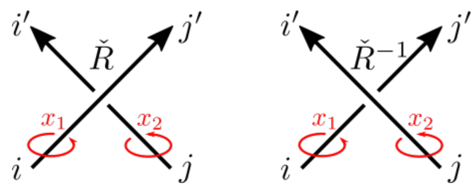

Figure 3.3: $\check{R}(x_1,x_2)_{i,j}^{i',j'}$ and $\check{R}^{-1}(x_1,x_2)_{i,j}^{i',j'}$.

Define the pairing and copairing by Figure 3.4. So, for instance, when we are taking

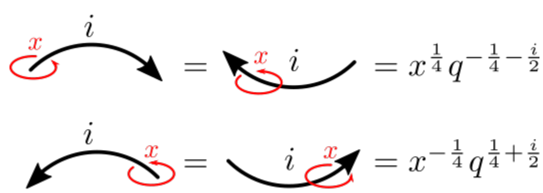

Figure 3.4: Pairing and copairing.

the right-closure of a braid, for each strand with holonomy x and spin i, we get the weight of $(x^{\frac{1}{4}} q^{-\frac{1}{4}-\frac{i}{2}})^2 = x^{\frac{1}{2}} q^{-\frac{1}{2}-i}$, which is the correct weight for taking the quantum trace.

Extension of the large-color R-matrix

The large-color R-matrix element (3.1) is originally defined for $i, j, i', j' \geq 0$, but the domain of i, j, i', j' can be naturally extended to the set of all integers. Explicitly,

$$\check{R}(x)_{i,j}^{i',j'} = \begin{cases} \delta_{i+j,i'+j'} q^{\frac{j+j'+1}{2}} x^{-\frac{j+j'+1}{2}} q^{jj'} \begin{bmatrix} i \\ i-j' \end{bmatrix}_q \prod_{1\leq l\leq i-j'} (1-q^{j+l}x^{-1}) & \text{if } \begin{array}{c} i \geq j' \geq 0 \\ \text{or} \\ 0 > i \geq j' \end{array} \\ \delta_{i+j,i'+j'} q^{\frac{j+j'+1}{2}} x^{-\frac{j+j'+1}{2}} q^{jj'} \begin{bmatrix} i \\ j' \end{bmatrix}_q \frac{1}{\prod_{0\leq l\leq j'-i-1}(1-q^{j-l}x^{-1})} & \text{if } j' \geq 0 > i \\ 0 & \text{otherwise} \end{cases},$$

$$\check{R}^{-1}(x)_{i,j}^{i',j'} = \begin{cases} \delta_{i+j,i'+j'} q^{-\frac{i+i'+1}{2}} x^{\frac{i+i'+1}{2}} q^{-ii'} \begin{bmatrix} j \\ j-i' \end{bmatrix}_{q^{-1}} \prod_{1\leq l\leq j-i'} (1-q^{-i-l}x) & \text{if } \begin{array}{c} j \geq i' \geq 0 \\ \text{or} \\ 0 > j \geq i' \end{array} \\ \delta_{i+j,i'+j'} q^{-\frac{i+i'+1}{2}} x^{\frac{i+i'+1}{2}} q^{-ii'} \begin{bmatrix} j \\ i' \end{bmatrix}_{q^{-1}} \frac{1}{\prod_{0\leq l\leq i'-j-1}(1-q^{-i+l}x)} & \text{if } i' \geq 0 > j \\ 0 & \text{otherwise} \end{cases},$$

and

$$\check{R}(x,y)_{i,j}^{i',j'} = \begin{cases} \delta_{i+j,i'+j'} q^{\frac{j+j'+\frac{1}{2}}{2}} x^{-\frac{i'+j+1}{4}} y^{-\frac{3j'-i+1}{4}} q^{jj'} \begin{bmatrix} i \\ i-j' \end{bmatrix}_q \prod_{1\leq l\leq i-j'} (1-q^{j+l}y^{-1}) & \text{if } \begin{array}{c} i \geq j' \geq 0 \\ \text{or} \\ 0 > i \geq j' \end{array} \\ \delta_{i+j,i'+j'} q^{\frac{j+j'+\frac{1}{2}}{2}} x^{-\frac{i'+j+1}{4}} y^{-\frac{3j'-i+1}{4}} q^{jj'} \begin{bmatrix} i \\ j' \end{bmatrix}_q \frac{1}{\prod_{0\leq l\leq j'-i-1}(1-q^{j-l}y^{-1})} & \text{if } j' \geq 0 > i \\ 0 & \text{otherwise} \end{cases},$$

$$\check{R}^{-1}(x,y)_{i,j}^{i',j'} = \begin{cases} \delta_{i+j,i'+j'} q^{-\frac{i+i'+\frac{1}{2}}{2}} x^{\frac{3i'-j+1}{4}} y^{\frac{j'+i+1}{4}} q^{-ii'} \begin{bmatrix} j \\ j-i' \end{bmatrix}_{q^{-1}} \prod_{1\leq l\leq j-i'} (1-q^{-i-l}x) & \text{if } \begin{array}{c} j \geq i' \geq 0 \\ \text{or} \\ 0 > j \geq i' \end{array} \\ \delta_{i+j,i'+j'} q^{-\frac{i+i'+\frac{1}{2}}{2}} x^{\frac{3i'-j+1}{4}} y^{\frac{j'+i+1}{4}} q^{-ii'} \begin{bmatrix} j \\ i' \end{bmatrix}_{q^{-1}} \frac{1}{\prod_{0\leq l\leq i'-j-1}(1-q^{-i+l}x)} & \text{if } i' \geq 0 > j \\ 0 & \text{otherwise.} \end{cases}$$

As power series in x^{-1}, we have

$$\check{R}(x)_{i,j}^{i',j'} = O(x^{-\frac{j+j'+1}{2}}), \quad \check{R}^{-1}(x)_{i,j}^{i',j'} = O(x^{\frac{j+j'+1}{2}}). \tag{3.2}$$

These bounds in x-degree will be used later to show that certain state sums converge absolutely to a power series in x^{-1}.

Meaning of the extension

Before extension, "the space of spin states" assigned to each strand of a braid in our state sum model is the highest weight Verma module $V_\infty(x)$ with the highest weight $\lambda = \log_q x - 1$. The basis vectors $\{v_j\}_{j\geq 0}$ are labeled by non-negative integers, where each v_j is an element of the weight subspace $V_\infty(x)\big|_{K=q^{\frac{\lambda-2j}{2}}}$. We can describe this highest weight Verma module diagrammatically as

$$\cdots \underset{F}{\overset{E}{\rightleftharpoons}} \operatorname{span}(v_1) \underset{F}{\overset{E}{\rightleftharpoons}} \operatorname{span}(v_0).$$

Now, extending j to negative values means we consider new vectors v_j for $n < 0$ on which K acts as $q^{\frac{\lambda-2j}{2}}$ as usual. That is, the highest weight Verma module is extended to the principal series module

$$\cdots \underset{F}{\overset{E}{\rightleftharpoons}} \operatorname{span}(v_1) \underset{F}{\overset{E}{\rightleftharpoons}} \operatorname{span}(v_0) \underset{F}{\overset{E}{\rightleftharpoons}} \operatorname{span}(v_{-1}) \underset{F}{\overset{E}{\rightleftharpoons}} \operatorname{span}(v_{-2}) \underset{F}{\overset{E}{\rightleftharpoons}} \cdots .$$

The new upper-half part of this module,

$$\operatorname{span}(v_{-1}) \underset{F}{\overset{E}{\rightleftharpoons}} \operatorname{span}(v_{-2}) \underset{F}{\overset{E}{\rightleftharpoons}} \cdots ,$$

which can be seen as the quotient of the principal series by the highest weight module, is actually the lowest weight Verma module $V_\infty^*(x^{-1})$ with the lowest weight $\lambda + 2 = \log_q x + 1$. To see this, observe that, for $j \geq 0$,

$$Ev_{-j-1} = [-j-1]v_{-(j+1)-1}, \quad Fv_{-j-1} = [\lambda+j+1]v_{-(j-1)-1}, \quad Kv_{-j-1} = q^{\frac{(\lambda+2)+2j}{2}}v_{-j-1}.$$

If we rescale the basis and define

$$w_j = \frac{[j]!}{\prod_{k=0}^{j-1}[\lambda+2+k]}v_{-j-1},$$

then

$$Ew_j = [-(\lambda+2)-j]w_{j+1}, \quad Fw_j = [j]w_{j-1}, \quad Kw_j = q^{\frac{(\lambda+2)+2j}{2}}w_j,$$

which is the standard action of $U_q(\mathfrak{sl}_2)$ on the basis $\{w_j\}_{j\geq 0}$ of the lowest weight Verma module with lowest weight $\lambda + 2 = \log_q x + 1$.

In terms of diagrams, this allows us to identify an arc labeled by spin i with the orientation-reversed arc labeled by spin $-1-i$, as in Figure 3.5.

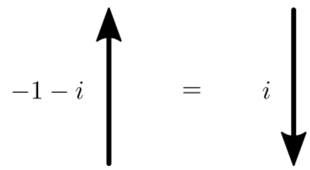

Figure 3.5: Inverting the domain of i from $\mathbb{Z}_{\geq 0}$ to $\mathbb{Z}_{<0}$ is the same as inverting the orientation of the strand.

Symmetries of the large-color R-matrix

The large-color R-matrix satisfies all the symmetries that are natural from the diagrammatic point of view. In particular, it is straightforward to check the following identities:

Proposition 3.1.3.

$$\check{R}(x_1,x_2)^{i',-1-j'}_{-1-i,j} = q^{\frac{i-j'}{2}}\check{R}^{-1}(x_2,x_1^{-1})^{i,i'}_{j,j'}, \tag{3.3}$$

$$\check{R}(x_1,x_2)^{-1-i',j'}_{i,-1-j} = q^{\frac{i'-j}{2}}\check{R}^{-1}(x_2^{-1},x_1)^{j',j}_{i',i}, \tag{3.4}$$

$$\check{R}(x_1,x_2)^{-1-i',-1-j'}_{-1-i,-1-j} = \check{R}(x_1^{-1},x_2^{-1})^{j,i}_{j',i'}, \tag{3.5}$$

$$\check{R}^{-1}(x_1,x_2)^{i',-1-j'}_{-1-i,j} = q^{\frac{i-j'}{2}}\check{R}(x_2,x_1^{-1})^{i,i'}_{j,j'}, \tag{3.6}$$

$$\check{R}^{-1}(x_1,x_2)^{-1-i',j'}_{i,-1-j} = q^{\frac{i'-j}{2}}\check{R}(x_2^{-1},x_1)^{j',j}_{i',i}, \tag{3.7}$$

$$\check{R}^{-1}(x_1,x_2)^{-1-i',-1-j'}_{-1-i,-1-j} = \check{R}^{-1}(x_1^{-1},x_2^{-1})^{j,i}_{j',i'}. \tag{3.8}$$

The first identity (3.3), for instance, can be diagrammatically understood as in Figure 3.6. Note, the factor $q^{\frac{i-j'}{2}} = (x_1^{\frac{1}{4}}q^{\frac{1}{4}+\frac{i}{2}})(x_1^{-\frac{1}{4}}q^{-\frac{1}{4}-\frac{j'}{2}})$ comes from the pairing

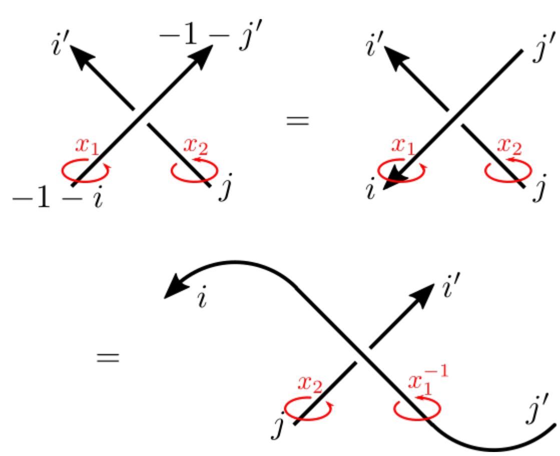

Figure 3.6: A symmetry of the R-matrix.

and copairing (Figure 3.4). All the other identities have similar diagrammatic interpretation as well.

3.2 Inverted state sum

By inverting some arcs, we get not only the rotated versions of the standard positive and negative crossings but also some non-standard crossings where the orientation of the strands change across the crossing; see Figure 3.7.

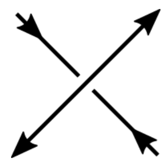

Figure 3.7: A new type of crossing.

Let L be an oriented link, and let D be its diagram as a $(1,1)$-tangle. An *inversion datum* I on D is an orientation of each arc of D such that each crossing looks like one of the crossings in Figure 3.8 or their rotated versions.

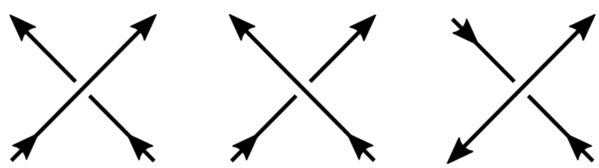

Figure 3.8: Allowed crossings.

A diagram D with an inversion datum I determines a state sum that we call an *inverted state sum*. That is, given a spin configuration (i.e., labeling of the arcs), its weight is given by the product of R-matrix elements, pairing, and the copairings. The inverted state sum $Z(D,I)$ is the sum of such weights over all spin configurations (i.e., indices $i \geq 0$) of the internal arcs. Since this is an infinite sum, convergence is not always guaranteed.

Definition 3.2.1. A link is *nice* if it admits a link diagram with an inversion datum such that the inverted state sum $Z(D,I)$ is absolutely convergent in $\mathbb{Z}[q,q^{-1}][[x^{-1}]]$.

We will prove the following theorem in the next section.

Theorem 3.2.2 ([Par]). *Gukov-Manolescu conjecture (Conjecture 2.2.11) is true for any nice link.*

In fact, we will show that for a nice link L,

$$F_L = \epsilon(x^{\frac{1}{2}} - x^{-\frac{1}{2}})Z(D, I),$$

where x is the holonomy parameter associated to the open strand, and $\epsilon \in \{\pm 1\}$ is a sign determined in the following way:

1. Consider the usual orientation of the link compatible with the choice of orientation of the meridian of each link component. Comparing it with the inversion datum I, let S be the set of arcs of the link diagram D whose orientation is inverted by the inversion datum I.

2. For each crossing, if exactly two out of four arcs are in S, then connect the ends of the two arcs. If all four arcs are in S, then connect the ends of the arcs of the same strand (i.e., same as in the link). Let $\tilde{S}$ be the resulting tangle made out of the arcs in S.

3. Define $\epsilon = (-1)^{\#\text{ of closed components of }\tilde{S}}$.

The class of nice links is quite big. As briefly mentioned in the introduction, a braid is called *homogeneous* if it can be presented as a braid word where all the Artin generators σ_j, for fixed j, appears with either postive or negative power. A link is called a *homogeneous braid link* if it is a closure of a homogeneous braid.

Proposition 3.2.3. *Homogeneous braid links are nice.*

Proof. Given any homogeneous braid, we can orient its arcs in such a way that for any positive crossing, the two arcs on the right are oriented upward, and for any negative crossing, the two arcs on the right are oriented downward. In other words, we invert the right-arcs of the negative crossings. We close up the braid to the right, leaving the left-most strand open. See Figure 3.9 for an example of the figure-eight knot. Thanks to the bound (3.2), only finitely many spin configurations contribute to the coefficient of a fixed power of x^{-1}, and therefore the resulting inverted state sum converges absolutely. □

Homogeneous braid link examples

Example 3.2.4 (Figure-eight knot)**.** Take the braid $\sigma_1\sigma_2^{-1}\sigma_1\sigma_2^{-1}$ from bottom to top. We close up the second and the third strand while leaving the first strand open.

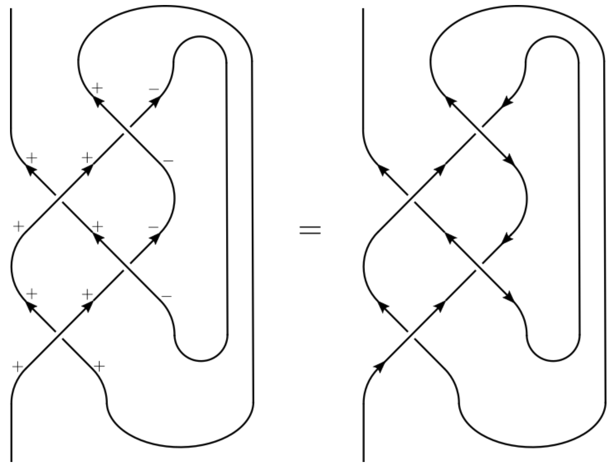

Figure 3.9: An inversion datum for the figure-eight knot.

We use the inversion datum as in Figure 3.9. In this case, $\epsilon = -1$, because there is only one closed component of $\tilde{S}$ made out of the arcs labeled by minus sign. Before closing up the braid, let's say the indices of the three open strands are $0, m, k$ from left to right. In this case, these three indices uniquely determine all the internal indices. Summing over $m \geq 0$ and $k < 0$, we get the following expression for $F_{\mathbf{4}_1}$:

$$F_{\mathbf{4}_1}(x,q) = -(x^{\frac{1}{2}} - x^{-\frac{1}{2}}) \sum_{\substack{m \geq 0 \\ k<0}} \check{R}(x)^{m,0}_{0,m} \check{R}^{-1}(x)^{0,k}_{0,k} \check{R}(x)^{0,m}_{m,0} \check{R}^{-1}(x)^{m,k}_{m,k} \cdot x^{\frac{1}{2}} q^{-\frac{1}{2}-m} \cdot x^{\frac{1}{2}} q^{-\frac{1}{2}-k}$$

$$= -x^{-\frac{1}{2}} - 2x^{-\frac{3}{2}} - (\frac{1}{q} + 3 + q)x^{-\frac{5}{2}} - (\frac{2}{q^2} + \frac{2}{q} + 5 + 2q + 2q^2)x^{-\frac{7}{2}} + O(x^{-\frac{9}{2}})$$

$$= -(x^{\frac{1}{2}} - x^{-\frac{1}{2}}) \sum_{n \geq 0} \frac{1}{\prod_{0 \leq j \leq n}(x + x^{-1} - q^j - q^{-j})}.$$

In [GM21] this series was computed term by term using recursion, but we have found a closed formula!

Example 3.2.5 (6_2 knot)**.** Take the braid $\sigma_1^3 \sigma_2^{-1} \sigma_1 \sigma_2^{-1}$ from bottom to top. Computing the inverted state sum, we get

$$F_{\mathbf{6}_2}(x,q) = -qx^{-\frac{3}{2}} - 2qx^{-\frac{5}{2}} + (-1 - 3q + q^2)x^{-\frac{7}{2}} + (-\frac{2}{q} - 2 - 4q + 2q^2)x^{-\frac{9}{2}} + O(x^{-\frac{11}{2}}).$$

Example 3.2.6 (6_3 knot)**.** Take the braid $\sigma_1^2 \sigma_2^{-1} \sigma_1 \sigma_2^{-2}$ from bottom to top. Computing the inverted state sum, we get

$$F_{\mathbf{6}_3}(x,q) = x^{-\frac{3}{2}} + 2x^{-\frac{5}{2}} + (-\frac{1}{q} + 3 - q)x^{-\frac{7}{2}} + (-\frac{2}{q^2} - \frac{2}{q} + 4 - 2q - 2q^2)x^{-\frac{9}{2}} + O(x^{-\frac{11}{2}}).$$

Note that each coefficient has $q \leftrightarrow q^{-1}$ symmetry, which is due to amphichirality of $\mathbf{6}_3$.

Example 3.2.7 (Whitehead link)**.** Take the braid $\sigma_1\sigma_2^{-1}\sigma_1\sigma_2^{-1}\sigma_1$ from bottom to top. Computing the inverted state sum, we get

$$F_{\mathbf{Wh}}(x_1,x_2,q) = -q^{\frac{1}{2}} \sum_{n,m\geq 0} f_{n,m}^{\mathbf{Wh}} x_1^{-n-\frac{1}{2}} x_2^{-m-\frac{1}{2}},$$

where

$$f^{\mathbf{Wh}} = \begin{pmatrix} 1 & 1 & 1 & 1 & \cdots \\ 1 & \frac{1}{q}+1-q & \frac{1}{q^2}+\frac{1}{q}+1-q-q^2 & \frac{1}{q^3}+\frac{1}{q^2}+\frac{1}{q}+1-q-q^2-q^3 & \cdots \\ 1 & \frac{1}{q^2}+\frac{1}{q}+1-q-q^2 & \frac{1}{q^4}+\frac{1}{q^3}+\frac{2}{q^2}+\frac{1}{q}-2q-2q^2 & \frac{1}{q^6}+\frac{1}{q^5}+\frac{2}{q^4}+\frac{2}{q^3}+\frac{2}{q^2}-1-3q-3q^2-q^3+q^5 & \cdots \\ 1 & \frac{1}{q^3}+\frac{1}{q^2}+\frac{1}{q}+1-q-q^2-q^3 & \frac{1}{q^6}+\frac{1}{q^5}+\frac{2}{q^4}+\frac{2}{q^3}+\frac{2}{q^2}-1-3q-3q^2-q^3+q^5 & \begin{matrix}\frac{1}{q^9}+\frac{1}{q^8}+\frac{2}{q^7}+\frac{3}{q^6}+\frac{3}{q^5}+\frac{3}{q^4}+\frac{2}{q^3} \\ -\frac{3}{q}-4-6q-4q^2-2q^3+q^4+2q^5+q^6+q^7\end{matrix} & \cdots \\ \vdots & \vdots & \vdots & \vdots & \ddots \end{pmatrix}.$$

Example 3.2.8 (Borromean rings)**.** Take the braid $\sigma_1\sigma_2^{-1}\sigma_1\sigma_2^{-1}\sigma_1\sigma_2^{-1}$ from bottom to top. Computing the inverted state sum, we get

$$F_{\mathbf{Bor}}(x_1,x_2,x_3,q) = \sum_{n,m,l\geq 0} f_{n,m,l}^{\mathbf{Bor}} x_1^{-n-\frac{1}{2}} x_2^{-m-\frac{1}{2}} x_3^{-l-\frac{1}{2}},$$

where

$$f_0^{\mathbf{Bor}} = \begin{pmatrix} 1 & 1 & 1 & \cdots \\ 1 & 1 & 1 & \cdots \\ 1 & 1 & 1 & \cdots \\ \vdots & \vdots & \vdots & \ddots \end{pmatrix},$$

$$f_1^{\mathbf{Bor}} = \begin{pmatrix} 1 & 1 & 1 & \cdots \\ 1 & -\frac{1}{q^2}+3-q^2 & -\frac{1}{q^3}-\frac{1}{q^2}+\frac{1}{q}+3+q-q^2-q^3 & \cdots \\ 1 & -\frac{1}{q^3}-\frac{1}{q^2}+\frac{1}{q}+3+q-q^2-q^3 & -\frac{1}{q^4}-\frac{2}{q^3}-\frac{1}{q^2}+\frac{2}{q}+5+2q-q^2-2q^3-q^4 & \cdots \\ \vdots & \vdots & \vdots & \ddots \end{pmatrix},$$

$$f_2^{\mathbf{Bor}} = \begin{pmatrix} 1 & 1 & 1 & \cdots \\ 1 & -\frac{1}{q^3}-\frac{1}{q^2}+\frac{1}{q}+3+q-q^2-q^3 & -\frac{1}{q^4}-\frac{2}{q^3}-\frac{1}{q^2}+\frac{2}{q}+5+2q-q^2-2q^3-q^4 & \cdots \\ 1 & -\frac{1}{q^4}-\frac{2}{q^3}-\frac{1}{q^2}+\frac{2}{q}+5+2q-q^2-2q^3-q^4 & \frac{1}{q^7}-\frac{1}{q^5}-\frac{5}{q^4}-\frac{6}{q^3}-\frac{1}{q^2}+\frac{6}{q}+13+6q-q^2-6q^3-5q^4-q^5+q^7 & \cdots \\ \vdots & \vdots & \vdots & \ddots \end{pmatrix},$$

and so on. Note that the coefficients have $q \leftrightarrow q^{-1}$ symmetry due to amphichirality of the Borromean rings.

Example 3.2.9 (**L7a1**)**.** Take the braid $\sigma_1^2\sigma_2^{-1}\sigma_1\sigma_2^{-1}\sigma_1\sigma_2^{-1}$ from bottom to top. Among the three strands that are open before closing up, let's say x_1 is the variable associated with the first two strands (they are connected once we close up the braid) and x_2 is the variable associated with the third strand. Computing the inverted state sum, we get

$$F_{\mathbf{L7a1}}(x_1,x_2,q) = q^{\frac{1}{2}} \sum_{n,m\geq 0} f_{n,m}^{\mathbf{L7a1}} x_1^{-n-\frac{1}{2}} x_2^{-m-\frac{1}{2}},$$

where

$$f^{\mathbf{L7a1}} = \begin{pmatrix} 0 & 0 & 0 & 0 & \cdots \\ 1 & 1 & 1 & 1 & \cdots \\ 2 & 2 & 2 & 2 & \cdots \\ 3-q & -\frac{1}{q^2}+4-q & -\frac{1}{q^3}-\frac{1}{q^2}+4 & -\frac{1}{q^4}-\frac{1}{q^3}-\frac{1}{q^2}+4+q^2 & \cdots \\ \vdots & \vdots & \vdots & \vdots & \ddots \end{pmatrix}.$$

The link **L7a1** consists of two unknots linked together with linking number 0. See Figure 3.10. So by doing $\frac{1}{r}$-surgery on one of the components, we can obtain various

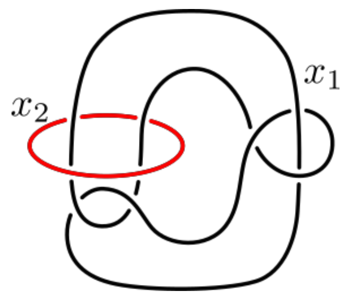

Figure 3.10: The link **L4a1**.

knots. For instance, -1, $+1$, $-\frac{1}{2}$. and $+\frac{1}{2}$-surgery on the x_2-component gives $\mathbf{6_3}$, $\mathbf{6_2}$, $\mathbf{8}_8$, and $\mathbf{8}_6$, respectively. These are good consistency checks, and indeed applying the partial $+1$ and -1 surgery formula (which can be found in Chapter 4 of this thesis), we get the same result as in Examples 3.2.5 and 3.2.6.

Homogenization of braids

As pointed out in [Sta78], for any link L, we can add an additional unknot component O (with any desired linking number with each component of L) so that $L' = L \cup O$ is a homogeneous braid link. It follows that the problem of defining F_L for all links is reduced to the following problem of finding an ∞-surgery formula.

Question 3.2.10. Let L' be a link obtained by adding a new component O to a link L. Is there a formula for $F_{L'}$ in terms of F_L?

Remark 3.2.11. In [Tur02], there is a nice ∞-surgery formula for the torsion, or equivalently the Alexander-Conway polynomial in our case of link complements, when the $\mathrm{lk}(L, O)$ is non-zero. Written in terms of the inverse torsions, the ∞-surgery formula is given by

$$\frac{1}{\tau(S^3 \setminus L)} = \frac{[O]-1}{\mathrm{in}(\tau(S^3 \setminus L'))}, \tag{3.9}$$

where $[O]$ is the homology class of O in $S^3 \setminus L$, and $\mathrm{in} : \mathbb{Z}[H_1(S^3 \setminus L')] \to \mathbb{Z}[H_1(S^3 \setminus L)]$ is the inclusion homomorphism. So, Question 3.2.10 is asking if there is a q-deformation of the equation (3.9).

If a link L can be obtained by performing $-\frac{1}{r}$-surgery on an unknot component of a link L', and if L' is a homogeneous braid link, then we can compute F_L by using the partial surgery formula that we will review in Chapter 4. This has been a useful strategy in computing F_K for a variety of knots; for instance, double twist knots can be obtained by $\frac{1}{m}, \frac{1}{n}$ surgery on the Borromean rings, which is a homogeneous braid link.

Fibered knots

According to KnotInfo [LM], there are 117 fibered knots up to 10 crossings. Using their minimum braid representatives in Knot Atlas [Atl], we see that 74 of them are homogeneous braids, and the other 43 of them are non-homogeneous braids. It turns out, all of them are good knots!

Proposition 3.2.12. *All fibered knots up to 10 crossings are nice.*

We summarize the inversion data in Table 3.1. In the table, each inversion datum shows how each elementary braid in the braid word looks like. The green arcs represent the ones labeled with − signs (i.e., the ones whose orientation gets inverted) and the black arcs represent the ones labeled with + signs. For example, the inversion datum for $\mathbf{8}_{20}$ can be translated into the diagram in Figure 3.11. In each case, one can show that the inverted state sum converges absolutely using the bound (3.2) on the order of x^{-1} for the R-matrix elements.

Based on this observation, we conjecture the following:

Conjecture 3.2.13 ([Par]). *For any fibered knot K, the coefficients of $F_K(x, q)$ are in $\mathbb{Z}[q, q^{-1}]$ (rather than $\mathbb{Z}((q))$).*

Remark 3.2.14. If K has a non-monic Alexander polynomial (in which case K must be non-fibered), $\frac{1}{\Delta_K(x)}$ has non-integral coefficients as a power series in x (or x^{-1}). Therefore, in this case, the coefficients of $F_K(x, q)$ cannot be polynomials. It is known that up to 10 crossings, a knot has a monic Alexander polynomial iff it is fibered. Therefore, for knots with at most 10 crossings, the coefficients of $F_K(x, q)$ are polynomials iff K is fibered.

This conjecture is motivated by enumerative geometry too. As we will say more in Chapter 6, F_K can be thought of a count of open topological strings [Ekh+], a setup similar to [OV00] for HOMFLY-PT polynomials, except that we use the *knot complement Lagrangian* instead of the usual knot conormal Lagrangian. When the

Knot	Braid	Inversion data
$\mathbf{8}_{20}$	$\sigma_1^{-1}\sigma_2^{-3}\sigma_1^{-1}\sigma_2^{3}$	
$\mathbf{8}_{21}$	$\sigma_1^{-2}\sigma_2^{2}\sigma_1^{-1}\sigma_2^{-3}$	
$\mathbf{9}_{42}$	$\sigma_1\sigma_2^{-1}\sigma_1\sigma_3^{-2}\sigma_2^{-1}\sigma_3^{3}$	
$\mathbf{9}_{44}$	$\sigma_1\sigma_2^{-1}\sigma_1\sigma_3^{2}\sigma_2^{-1}\sigma_3^{-3}$	
$\mathbf{9}_{45}$	$\sigma_1^{-1}\sigma_2\sigma_1^{-1}\sigma_3^{-1}\sigma_2^{-1}\sigma_3\sigma_2^{-1}\sigma_3^{-2}$	
$\mathbf{9}_{48}$	$\sigma_1^{-1}\sigma_2\sigma_3^{-1}\sigma_2\sigma_1^{-1}\sigma_3\sigma_2\sigma_3^{-1}\sigma_2\sigma_3^{2}$	
$\mathbf{10}_{60}$	$\sigma_1^{-1}\sigma_2\sigma_1^{-1}\sigma_2^{2}\sigma_3^{-1}\sigma_2\sigma_3^{-1}\sigma_2^{-1}\sigma_4^{-1}\sigma_3\sigma_4^{-1}$	
$\mathbf{10}_{69}$	$\sigma_1\sigma_2^{-1}\sigma_3\sigma_2^{-1}\sigma_4\sigma_1\sigma_3\sigma_2^{-1}\sigma_4^{-1}\sigma_3\sigma_4^{2}$	
$\mathbf{10}_{73}$	$\sigma_1^{-1}\sigma_2\sigma_1^{-1}\sigma_2\sigma_3^{-1}\sigma_2\sigma_4^{-1}\sigma_3^{-1}\sigma_4\sigma_3^{-1}\sigma_4^{-2}$	
$\mathbf{10}_{75}$	$\sigma_1\sigma_2^{-1}\sigma_1\sigma_2^{-1}\sigma_3\sigma_2^{-2}\sigma_4\sigma_3^{-1}\sigma_2\sigma_4\sigma_3$	
$\mathbf{10}_{78}$	$\sigma_1^{-2}\sigma_2\sigma_1^{-1}\sigma_3^{-1}\sigma_2\sigma_4^{-1}\sigma_3^{-1}\sigma_4\sigma_3^{-1}\sigma_4^{-2}$	
$\mathbf{10}_{81}$	$\sigma_1^{2}\sigma_2^{-1}\sigma_1\sigma_3\sigma_2^{2}\sigma_4^{-1}\sigma_3^{-3}\sigma_4^{-1}$	
$\mathbf{10}_{89}$	$\sigma_1^{-1}\sigma_2^{-1}\sigma_3\sigma_2^{-1}\sigma_4^{-1}\sigma_1^{-1}\sigma_3^{-1}\sigma_2\sigma_3\sigma_4^{-1}\sigma_3\sigma_4^{-1}$	
$\mathbf{10}_{96}$	$\sigma_1\sigma_2^{-1}\sigma_3\sigma_2^{-1}\sigma_4\sigma_1\sigma_2^{-1}\sigma_3\sigma_2^{-1}\sigma_4\sigma_3\sigma_4^{-1}$	
$\mathbf{10}_{105}$	$\sigma_1^{2}\sigma_2^{-1}\sigma_1\sigma_3\sigma_2^{2}\sigma_4^{-1}\sigma_3^{-1}\sigma_2\sigma_3^{-1}\sigma_4^{-1}$	
$\mathbf{10}_{107}$	$\sigma_1^{-2}\sigma_2\sigma_1^{-1}\sigma_3\sigma_2^{2}\sigma_4^{-1}\sigma_3\sigma_2^{-1}\sigma_3\sigma_4^{-1}$	
$\mathbf{10}_{110}$	$\sigma_1^{-1}\sigma_2\sigma_1^{-1}\sigma_3^{-1}\sigma_2^{-3}\sigma_4\sigma_3\sigma_2^{-1}\sigma_3\sigma_4$	
$\mathbf{10}_{115}$	$\sigma_1\sigma_2^{-1}\sigma_1\sigma_3\sigma_2^{2}\sigma_4^{-1}\sigma_3^{-1}\sigma_2\sigma_3^{-2}\sigma_4^{-1}$	
$\mathbf{10}_{125}$	$\sigma_1^{-1}\sigma_2^{-3}\sigma_1^{-1}\sigma_2^{5}$	
$\mathbf{10}_{126}$	$\sigma_1^{-1}\sigma_2^{3}\sigma_1^{-1}\sigma_2^{-5}$	
$\mathbf{10}_{127}$	$\sigma_1^{-2}\sigma_2^{2}\sigma_1^{-1}\sigma_2^{-5}$	
$\mathbf{10}_{132}$	$\sigma_1^{-1}\sigma_2^{-1}\sigma_3^{-1}\sigma_2\sigma_1^{3}\sigma_3^{-2}\sigma_2^{-1}\sigma_1^{-1}$	
$\mathbf{10}_{133}$	$\sigma_1^{-2}\sigma_2\sigma_1^{-1}\sigma_2^{-1}\sigma_3^{2}\sigma_2^{-1}\sigma_3^{-3}$	
$\mathbf{10}_{136}$	$\sigma_1\sigma_2^{-1}\sigma_1\sigma_3^{2}\sigma_2^{-1}\sigma_3^{-1}\sigma_4\sigma_3^{-1}\sigma_4$	
$\mathbf{10}_{137}$	$\sigma_1\sigma_2^{-1}\sigma_1\sigma_3^{-2}\sigma_2^{-1}\sigma_3\sigma_4^{-1}\sigma_3\sigma_4^{-1}$	
$\mathbf{10}_{140}$	$\sigma_1^{-1}\sigma_2^{-1}\sigma_3^{-1}\sigma_2\sigma_1^{3}\sigma_3^{-1}\sigma_2^{-1}\sigma_1^{-2}$	
$\mathbf{10}_{141}$	$\sigma_1^{-2}\sigma_2^{-3}\sigma_1^{-1}\sigma_2^{4}$	
$\mathbf{10}_{143}$	$\sigma_1^{-2}\sigma_2^{3}\sigma_1^{-1}\sigma_2^{-4}$	
$\mathbf{10}_{145}$	$\sigma_1^{-1}\sigma_2^{-1}\sigma_3\sigma_2^{-1}\sigma_1^{-1}\sigma_3^{-1}\sigma_2^{-1}\sigma_3\sigma_2^{-1}\sigma_3^{-2}$	
$\mathbf{10}_{148}$	$\sigma_1^{-1}\sigma_2\sigma_1^{-1}\sigma_2^{2}\sigma_1^{-1}\sigma_2^{-4}$	
$\mathbf{10}_{149}$	$\sigma_1^{-2}\sigma_2\sigma_1^{-1}\sigma_2\sigma_1^{-1}\sigma_2^{-4}$	
$\mathbf{10}_{150}$	$\sigma_2\sigma_1\sigma_3^{-1}\sigma_2^{-1}\sigma_1\sigma_3^{2}\sigma_2^{-1}\sigma_3^{3}$	
$\mathbf{10}_{151}$	$\sigma_2^{-1}\sigma_1\sigma_3\sigma_2^{-1}\sigma_1\sigma_3^{-2}\sigma_2\sigma_3^{3}$	
$\mathbf{10}_{153}$	$\sigma_1^{-3}\sigma_2^{-1}\sigma_1^{-2}\sigma_3\sigma_2^{3}\sigma_3$	
$\mathbf{10}_{154}$	$\sigma_1\sigma_2^{3}\sigma_1\sigma_3\sigma_2\sigma_3^{-1}\sigma_2\sigma_3^{2}$	
$\mathbf{10}_{155}$	$\sigma_1\sigma_2^{-2}\sigma_1\sigma_2^{-2}\sigma_1\sigma_2^{3}$	
$\mathbf{10}_{156}$	$\sigma_1^{-1}\sigma_2^{-1}\sigma_3\sigma_2^{-1}\sigma_1^{-1}\sigma_3^{2}\sigma_2\sigma_3^{-3}$	
$\mathbf{10}_{157}$	$\sigma_1^{2}\sigma_2^{-1}\sigma_1\sigma_2^{-1}\sigma_1^{2}\sigma_2^{3}$	
$\mathbf{10}_{158}$	$\sigma_1\sigma_2\sigma_3^{-1}\sigma_2\sigma_1\sigma_3^{2}\sigma_2^{-1}\sigma_3^{-3}$	
$\mathbf{10}_{159}$	$\sigma_1^{-2}\sigma_2^{2}\sigma_1^{-1}\sigma_2\sigma_1^{-1}\sigma_2^{-3}$	
$\mathbf{10}_{160}$	$\sigma_1^{-1}\sigma_2\sigma_3^{-1}\sigma_2\sigma_1^{-1}\sigma_3^{2}\sigma_2\sigma_3^{3}$	
$\mathbf{10}_{161}$	$\sigma_1^{-2}\sigma_2^{-2}\sigma_1^{-1}\sigma_2\sigma_1^{-1}\sigma_2^{-3}$	
$\mathbf{10}_{163}$	$\sigma_1\sigma_2^{2}\sigma_3^{-1}\sigma_2\sigma_1\sigma_3^{-2}\sigma_2^{-1}\sigma_3^{2}$	

Table 3.1: Fibered knots up to 10 crossings that are possibly not homogeneous braid knots.

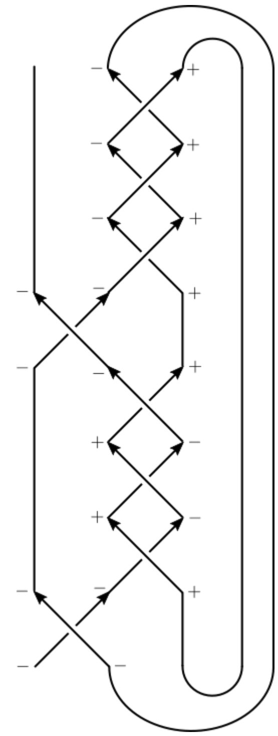

Figure 3.11: The $\mathbf{8}_{20}$ knot.

knot is fibered, the knot complement Lagrangian can be completely shifted off of the zero section S^3, just like the knot conormal Lagrangian. Since the geometry is completely analogous, we expect that the coefficients of F_K for a fibered knot K are polynomials, just like (colored) HOMFLY-PT polynomials are polynomials.

Remark 3.2.15. Based on the principles of topological field theory, it is natural to expect that $F_K(x, q)$ for a fibered knot is a (graded) trace of the monodromy action on the Hilbert space $\mathcal{H}_{\Sigma_{g,1}}$ associated to the fiber surface. It is a very interesting problem to figure out the exact formula for the monodromy representation on $\mathcal{H}_{\Sigma_{g,1}}$ and compare it with $F_K(x, q)$.

3.3 Proof of Theorem 3.2.2

In this section, we will prove Theorem 3.2.2, which is restated in a more precise way below.

Theorem 3.3.1. *For any nice link L, let*

$$F_L := \epsilon(x^{\frac{1}{2}} - x^{-\frac{1}{2}})Z(D, I),$$

where x is the holonomy parameter associated to the open strand, and $\epsilon \in \{\pm 1\}$ is the sign that we explained in the previous section. Then the following is true.

1. *F_L is an invariant of L. That is, it is independent of the choice of the homogeneous braid representative.*

2. *Setting $q = e^{\hbar}$, its $\hbar$-expansion agrees with the Melin-Morton-Rozansky expansion of the colored Jones polynomials.*

3. *F_L is annihilated by the quantum A-polynomial (or quantum A-ideal in case it has multiple components).*

In other words, F_L is the invariant whose existence was conjectured in [GM21].

Proof. For simplicity, let's focus on the case L is a knot. The argument we are about to present can be easily generalized to the case of links. In this case, $\epsilon Z(D, I)$ is an element of $\mathbb{Z}[q, q^{-1}][[x^{-1}]]$. Our goal is to show that the $\hbar$-expansion of this series agrees with the Melvin-Morton-Rozansky expansion of the colored Jones polynomials of L expanded near $x = \infty$, which is part (2) of the Theorem. Before doing that, let's first see how part (1) and (3) immediately follow from part (2). Part (1) follows from part (2) because the Melvin-Morton-Rozansky expansion is an invariant of a knot, and part (2) shows that it can be re-summed into a series in x^{-1} with coefficients in $\mathbb{Z}[q, q^{-1}]$. Since the $\hbar$-series uniquely determines the Laurent polynomial in $q = e^{\hbar}$, F_L itself is an invariant of L, and that proves part (1). Proof of part (3) from (2) is similar. Since the Melvin-Morton-Rozansky expansion is annihilated by the quantum A-polynomial, $\hat{A}_L Z(D, I)$ should vanish when expanded into a series in $\hbar$. Since $\hat{A}_L Z(D, I) \in \mathbb{Z}[q, q^{-1}][[x^{-1}]]$, it follows that each coefficient should vanish, meaning that $\hat{A}_L Z(D, I) = 0$.

Now let's prove part (2). For this, we combine ideas from [LW01] and [Roz98]. Following [Roz98], we define the *parametrized R-matrices* to be

$$\begin{aligned} \mathsf{R}(\alpha, \beta, \gamma)_{i,j}^{i',j'} &= \delta_{i+j,i'+j'} \binom{i}{j'} \alpha^j \beta^{j'} \gamma^{i-j'}, \\ \mathsf{R}^{-1}(\alpha, \beta, \gamma)_{i,j}^{i',j'} &= \delta_{i+j,i'+j'} \binom{j}{i'} \alpha^i \beta^{i'} \gamma^{j-i'}, \end{aligned} \tag{3.10}$$

where $i, j, i', j' \geq 0$. Given an oriented knot diagram with one strand open, we can consider the state sum by replacing each positive crossing with R and negative crossing with R^{-1}. We will use different parameters for each crossing, so there will be $3c$ independent parameters in total, where c is the number of crossings of the knot diagram. It should be noted that the parametrized R-matrices do *not* satisfy either Yang-Baxter relation or unitarity. In particular, R is *not* the inverse matrix of R^{-1};

we are abusing the notation for convenience. The significance of the parametrized R-matrix comes from the fact that they induce an algebra morphism in the following way. Denoting the vector $v^i \otimes v^j$ by a monomial $z_1^i z_2^j$, we see that

$$\begin{aligned}\mathsf{R}(z_1^i z_2^j) &= (\gamma z_1 + \beta z_2)^i (\alpha z_1)^j = \mathsf{R}(z_1)^i \mathsf{R}(z_2)^j,\\ \mathsf{R}^{-1}(z_1^i z_2^j) &= (\alpha z_2)^i (\beta z_1 + \gamma z_2)^j = \mathsf{R}^{-1}(z_1)^i \mathsf{R}^{-1}(z_2)^j.\end{aligned}$$

Put in a slightly different language, this means that the parametrized R-matrices induce a model of random walk of free bosons on the knot diagram. It follows from the theorem of Foata and Zeilberger [FZ99] (see also [LW01] for an exposition of Foata-Zeilberger formula) that the result of this state sum is

$$\mathsf{Z}(\{\alpha\}, \{\beta\}, \{\gamma\}) = \frac{1}{\det(I - \mathcal{B})}, \tag{3.11}$$

where $\mathcal{B}$ is the transition matrix of this model of random walk. That is, $\mathcal{B}$ is the $n \times n$ matrix where n is the number of internal arcs of the knot diagram, and it records the probability (or the weight) of a boson to jump from one arc to another. The weight is determined by the corresponding entry of the matrix R or R^{-1}, with $(i, j) = (0, 1)$ or $(1, 0)$ and $(i', j') = (0, 1)$ or $(1, 0)$. From the definition of the transition matrix, it is easy to see that the denominator, $\det(I - \mathcal{B})$, can be expressed in the following way.

$$\det(I - \mathcal{B}) = \sum_c (-1)^{|c|} W(c), \tag{3.12}$$

where the sum ranges over all simple multi-cycles c, $|c|$ is the number of components of the multi-cycle c, and $W(c)$ denotes the weight of c. Let us clarify some of the terminologies. A *cycle* is a cyclic path (without a starting point or an end point) on the knot diagram as an oriented graph. A *multi-cycle* is an unordered tuple of cycles. We call a multi-cycle *simple* if it uses each arc at most once. Since it counts simple multi-cycles (with weights), $\det(I - \mathcal{B})$ can be obtained as a result of a state sum where the space of spin states is spanned by 0 and 1, instead of all non-negative integers, as long as we keep track of the sign $(-1)^{|c|}$. In this sense, $\det(I - \mathcal{B})$ can be obtained as a state sum in a system of random walk of free fermions.

The argument we are about to present applies to all nice diagrams, but for simplicity of exposition, let's assume that our oriented knot diagram is given by a homogeneous braid diagram. With the canonical inversion datum for this homogeneous braid diagram, each crossing will look like one of the four types in Figure 3.12. The $-$-signed arcs are the ones whose orientations get inverted in the inversion datum. The sign ϵ is given by

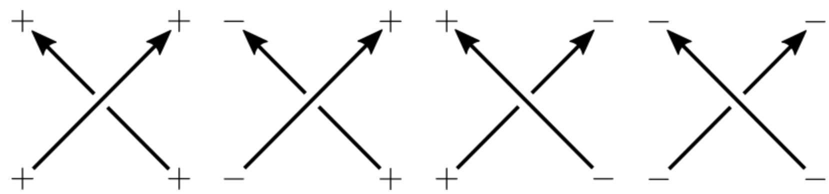

Figure 3.12: Four possible types of crossings

$$\epsilon = (-1)^{(\text{\# of columns with negative crossings})+(\text{\# of }(\check{R}^{-1})^{-,-}_{-,-}\text{ crossings})}.$$

Now let's "invert" this model of random walk. That is, we consider the inverted state sum, but using R and R^{-1} instead $\check{R}$ and $\check{R}^{-1}$. Explicitly, the four types of crossings are given by

$$\begin{aligned}
\mathsf{R}^{+,+}_{+,+} &: \delta_{i+j,i'+j'}\binom{i}{j'}\alpha^j\beta^{j'}\gamma^{i-j'}, \\
\mathsf{R}^{-,+}_{-,+} &: \delta_{i+j,i'+j'}\gamma^{-1}\binom{j'+(-i-1)}{j'}\alpha^j(-\beta)^{j'}\gamma^{-(-i-1)-j'}, \\
(\mathsf{R}^{-1})^{+,-}_{+,-} &: \delta_{i+j,i'+j'}\gamma^{-1}\binom{i'+(-j-1)}{i'}\alpha^i(-\beta)^{i'}\gamma^{-i'-(-j-1)}, \\
(\mathsf{R}^{-1})^{-,-}_{-,-} &: \delta_{i+j,i'+j'}\alpha^{-1}\beta^{-1}\binom{-i'-1}{-j-1}\alpha^{-(-i-1)}\beta^{-(-i'-1)}(-\gamma)^{(-i'-1)-(-j-1)}.
\end{aligned} \tag{3.13}$$

Extracting out the factors γ^{-1} and $\alpha^{-1}\beta^{-1}$ to normalize these "inverted" parametrized R-matrices, we see that this again gives a model of random walk of free bosons. This can be best described with what we call "highway diagrams." Before inversion, the highway diagrams for the positive and the negative crossing look like Figure 3.13. Note the arcs connecting the over-strand with the under-strand. They denote the

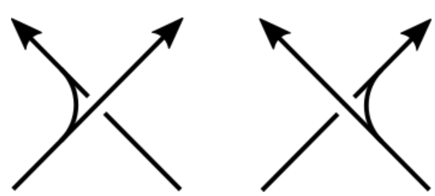

Figure 3.13: Highway diagrams for the positive and the negative crossing.

way the bosons can move; they can move from the over-strand to the under-strand, but not the other way around. After inverting some of the indices according to the four types of crossings as in Figure 3.12, we can make a change of variables to the inverted indices and use $k_{\text{inv}} := -k-1 \in \mathbb{Z}_{\geq 0}$ instead of $k \in \mathbb{Z}_{<0}$ for each inverted index k (i, j, i', or j'). The effect of this change of variables to the diagram is to invert the orientation of the inverted arcs. As a result, the inverted highway diagrams for the four types of crossings look like Figure 3.14. The inverted parametrized

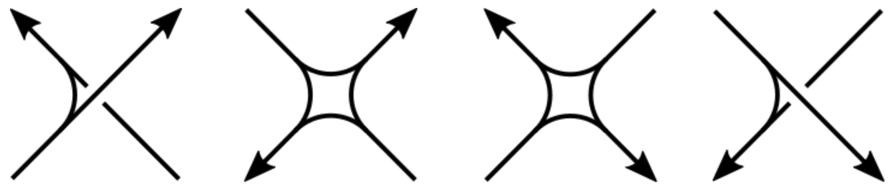

Figure 3.14: Inverted highway diagrams for the four types of crossings.

R-matrices can now be thought of as the maps from the incoming strands to the outgoing strands. After extracting out the pre-factor (γ^{-1} for $\mathsf{R}^{-,+}_{-,+}$ and $(\mathsf{R}^{-1})^{+,-}_{+,-}$, and $\alpha^{-1}\beta^{-1}$ for $(\mathsf{R}^{-1})^{-,-}_{-,-}$), each of these maps induce an algebra morphism in the sense we discussed above. For instance, in case of $\gamma\mathsf{R}^{-,+}_{-,+}$, denoting the vector $w_{i'_{\text{inv}}} \otimes v_j$ by a monomial $z_1^{i'_{\text{inv}}} z_2^j$, we see that

$$\gamma\mathsf{R}(z_1^{i'_{\text{inv}}} z_2^j) = (\gamma^{-1}z_1 - \beta\gamma^{-1}z_2)^{i'_{\text{inv}}}(\alpha\gamma^{-1}z_1 - \alpha\beta\gamma^{-1}z_2)^j = (\gamma\mathsf{R}(z_1))^{i'_{\text{inv}}}(\gamma\mathsf{R}(z_2))^j.$$

It follows that the result of the state sum of this new model of random walk of free bosons is

$$\mathsf{Z}^{\text{inv}}(\{\alpha\},\{\beta\},\{\gamma\}) = \frac{\prod_{c_2}\gamma^{-1}\prod_{c_3}\gamma^{-1}\prod_{c_4}\alpha^{-1}\beta^{-1}}{\det(I - \mathcal{B}_{\text{inv}})}, \tag{3.14}$$

where $\mathcal{B}_{\text{inv}}$ is the transition matrix of this new model of random walk (determined by $\mathsf{R}^{+,+}_{+,+}, \gamma\mathsf{R}^{-,+}_{-,+}, \gamma\mathsf{R}^{+,-}_{+,-}, \alpha\beta\mathsf{R}^{-,-}_{-,-}$), and the term in the numerator denotes the product of γ^{-1} for each crossing of the second and the third type multiplied by the product of $\alpha^{-1}\beta^{-1}$ for each crossing of the fourth type, basically pulling out the pre-factor.

We will prove the following lemma.

Lemma 3.3.2.

$$\mathsf{Z}(\{\alpha\},\{\beta\},\{\gamma\}) = \epsilon\mathsf{Z}^{\text{inv}}(\{\alpha\},\{\beta\},\{\gamma\}). \tag{3.15}$$

To prove the lemma, let's compare the denominators, $\det(I - \mathcal{B})$ and $\det(I - \mathcal{B}_{\text{inv}})$. Recall from (3.12) that each of these determinants can be understood as the weighted sum over all simple multi-cycles. So our strategy is to find a one-to-one correspondence between the set of all simple multi-cycles in the first model of random walk of free fermions and that of the second model. A crucial observation is the following correspondence.

Proposition 3.3.3. *For $i, i', j, j' \in \{0, 1\}$, there is a correspondence between the parametrized R-matrix and its inverted version , as in Figure 3.15.*

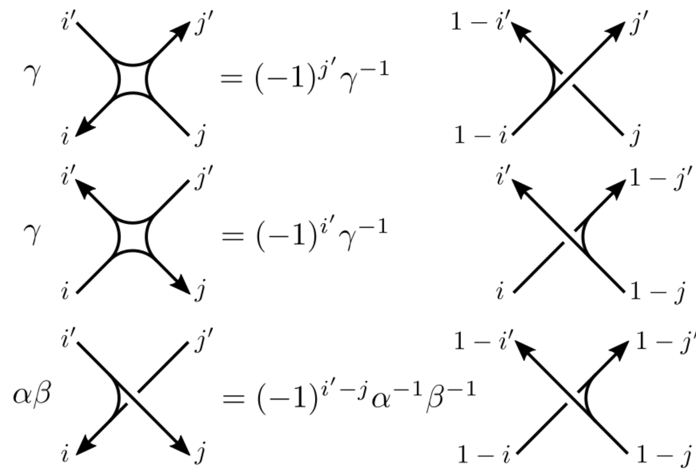

Figure 3.15: The correspondence between the parametrized R-matrix and its inversion.

This can be proved by checking all the cases. There are two cases we need to be a little careful of. Those are when i, j, i', j' are all 1 in the crossing of the type either $\mathsf{R}^{-,+}_{-,+}$ or $\mathsf{R}^{+,-}_{+,-}$. In those cases, the right-hand side of the equations in Figure 3.15 are zero, but naively the inverted parametrized R-matrices (3.13) themselves are non-zero. This is okay, and in fact when we consider the fermionic model that computes $\det(I - \mathcal{B}_{\text{inv}})$ (instead of the bosonic model that computes its inverse), it is more natural to set the value of the matrices $\mathsf{R}^{-,+}_{-,+}$ and $\mathsf{R}^{+,-}_{+,-}$ to be 0 when i, j, i', j' are all 1. This is because in those types of crossing, when i, j, i', j' are all 1, then there are two different ways to make it into a simple multi-cycle. That is, there are two different simple multi-cycles realizing that configuration. For instance, in the case of $\mathsf{R}^{-,+}_{-,+}$, we can either connect i' to j' and j to i, or we can connect i' to i and j to j'. Moreover, one of the two simple multi-cycles have one more component than the other. Since we are counting simple multi-cycles with weight and sign as in 3.12, the contribution of that configuration is 0. Therefore in this fermionic model $\mathsf{R}^{-,+}_{-,+}$ and $\mathsf{R}^{+,-}_{+,-}$ are zero when i, j, i', j' are all 1, and this proves the proposition.

We are now ready to compare $\det(I - \mathcal{B})$ with $\det(I - \mathcal{B}_{\text{inv}})$. Let D and D_{inv} be the highway diagrams for the original knot diagram and its inversion. Any multi-cycles in either D or D_{inv} can be thought of as a configuration of 0's and 1's on the diagram. Moreover, any such configuration that has a non-zero weight uniquely determines the simple multi-cycle. Following the rule as in Figure 3.15, for each simple multi-cycle c in D, there is a corresponding multi-cycle c_{inv} in D_{inv} and vice versa. Even their weights agree, up to a simple factor as given in Figure 3.15. We need to carefully study these extra factors. The factors γ^{-1} and $\alpha^{-1}\beta^{-1}$ give an overall factor of

$\prod_{c_2} \gamma^{-1} \prod_{c_3} \gamma^{-1} \prod_{c_4} \alpha^{-1}\beta^{-1}$, which gets cancelled out with the numerator of (3.14).

Let's take a careful look at the sign factors. We claim that the overall sign factor agrees with $(-1)^{|c|-|c_{\text{inv}}|}\epsilon$. The basic idea is the following. Suppose we have n number of disjoint intervals on a circle, and suppose that the ends of the intervals are connected in a certain way so that they form a collection of cycles. If we change the set of intervals on the circle to their complement, then the resulting number of cycles and the original number of cycles have the same parity if n is odd, and they have the opposite parity if n is even. See Figure 3.16 as an illustration. This is exactly what

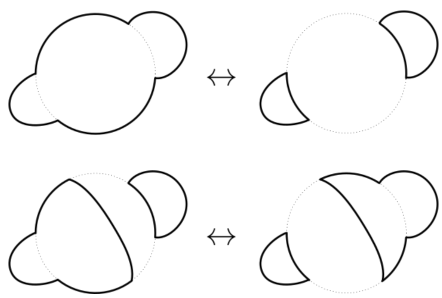

Figure 3.16: The change of parity of the number of components as we invert the circle.

happens when we invert a column of a knot diagram. Under the correspondence in Figure 3.15, 0's and 1's in a column labeled with − signs change place. So, for instance, if we have a column labeled with − signs and if the adjacent columns are labeled with + signs, then a typical picture would be something like Figure 3.17. In the figure, the column we are inverting is highlighted with a green stripe, and this is the one that plays the role of the circle in Figure 3.16. A part of a typical multi-cycle is drawn with red lines. As pointed out above, the change of parity of the number of components of the multi-cycle is determined by the parity of the red intervals in the green stripe. The number of such intervals equals the number of red outgoing strands from the green stripe, which is the sum of i''s for the crossings on the left edge of the stripe plus the sum of j''s for the crossings on the right edge of the stripe.

More generally, there can be some number of columns labeled with − signs that are adjacent to each other. In that case, the number of circles is not just the number of columns that we invert, because some of the circles are connected through crossings of type $(\mathsf{R}^{-1})^{-,-}_{-,-}$ with either $(i,j,i',j') = (1,0,0,1),\ (0,1,1,0)$ or $(1,1,1,1)$. As a result, the parity of the number of circles that we invert has the same parity with the number of columns with − sign plus the number of such crossings. Note that the number of crossings of type $(\mathsf{R}^{-1})^{-,-}_{-,-}$ with either $(i,j,i',j') = (1,0,0,1),\ (0,1,1,0)$

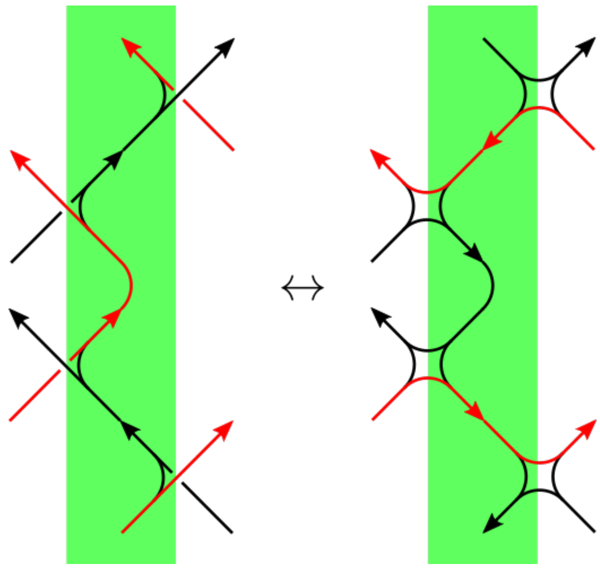

Figure 3.17: Inverting a column labeled with $-$ sign.

or $(1,1,1,1)$ equals the number of all crossings of type $(\mathsf{R}^{-1})^{-,-}_{-,-}$ minus the number of such crossings with $(i,j,i',j')=(0,1,0,1)$ (or $(1,0,1,0)$ after inversion). All in all, we have

$$(-1)^{\text{change of parity in the \# of components}} = (-1)^{\sum_{c_2} j' + \sum_{c_3} i' + \sum_{c_4} (i'-j)}\epsilon,$$

where $\sum_{c_2} j' + \sum_{c_3} i' + \sum_{c_4} (i'-j)$ denotes the sum of j''s for all the crossings of the second type plus the sum of i''s for all the crossings of the third type plus the sum of $(i'-j)$'s for all the crossings of the fourth type. Comparing with Figure 3.15, we see that the overall change of sign in the weight of any multi-cycle is just ϵ. This concludes the proof of Lemma 3.3.2.

In the classical limit, the R-matrices $\check{R}(x)$ and $\check{R}^{-1}(x)$ can be obtained by specializing the parameters of the parametrized R-matrix. More precisely,

$$\begin{aligned} \check{R}(x)^{i',j'}_{i,j}\Big|_{q=1} &= \mathsf{R}(\alpha,\beta,\gamma)^{i',j'}_{i,j}\Big|_{\alpha=x^{-\frac{1}{2}},\beta=x^{-\frac{1}{2}},\gamma=1-x^{-1}}, \\ \check{R}^{-1}(x)^{i',j'}_{i,j}\Big|_{q=1} &= \mathsf{R}^{-1}(\alpha,\beta,\gamma)^{i',j'}_{i,j}\Big|_{\alpha=x^{\frac{1}{2}},\beta=x^{\frac{1}{2}},\gamma=1-x}. \end{aligned} \tag{3.16}$$

This fact, combined with Lemma 3.3.2, immediately proves that the classical limit of $\epsilon Z(D,I)$ agrees with $\frac{1}{\Delta_L(x)}$, where $\Delta_L(x)$ denotes the Alexander polynomial of L. The rest of the proof follows easily from what Rozansky proved in [Roz98]; there exists a differential operator D_n in the parameters $\{\alpha\}, \{\beta\}, \{\gamma\}$ with polynomial coefficients such that the coefficient of $\hbar^n$ in the Melvin-Morton-Rozansky expansion is

$$D_n \,\mathsf{Z}(\{\alpha\},\{\beta\},\{\gamma\})\Big|_{\text{specialize } \{\alpha\},\{\beta\},\{\gamma\} \text{ according to (3.16)}}. \tag{3.17}$$

The way it is proved is by observing that the $\hbar$-expansion of $\check{R}(x)$ can be obtained by acting a certain differential operator in α, β, γ to $\mathsf{R}(\alpha, \beta, \gamma)$ and then specializing these parameters. It is easy to see that the differential operator for the R-matrix remains the same even when we invert some of the indices, and it follows that the operator D_n itself remains the same under inversion. So the corresponding $\hbar^n$-coefficient for the inverted state sum is given by

$$(-1)^s D_n \,\mathsf{Z}^{\mathrm{inv}}(\{\alpha\},\{\beta\},\{\gamma\})\Big|_{\text{specialize } \{\alpha\},\{\beta\},\{\gamma\} \text{ according to (3.16)}}. \tag{3.18}$$

By Lemma 3.3.2, (3.17) and (3.18) are the same as rational functions. This finishes the proof of Theorem 3.3.1. □

Remark 3.3.4. It is important to note that (3.17) is a power series in $(1-x)$ while (3.18) is a power series in x^{-1}. In other words, a state sum and its inversion are typically defined in a different domain; one near $x = 1$ and the other near $x = \infty$ (or $x = 0$ if we had started with the lowest weight Verma module). For this reason, they can't be compared directly. This is why even though a lot is known about the integral form of the Melvin-Morton-Rozansky expansion cyclotomically (see e.g., [Hab02; Hab07; Wil22]), it has been a challenge to find its integral form near $x = 0$ or $x = \infty$ as [GM21] conjectured.

In the above proof, we circumvented the issue of having different domains of convergence by making use of the fact that they can both be expressed as rational functions and showed that the two rational functions are the same.

Remark 3.3.5. The effect of the sign factor on the positive and negative stabilization moves can be summarized as in Figure 3.18.

Remark 3.3.6. When specialized according to (3.16), the equation (3.12) becomes Murakami's state sum expression for the (multi-variable) Alexander polynomial [Mar05]. In Murakami's state sum model, the space of spin states is a 2-dimensional super-vector space $V = \mathrm{span}\{v_0, v_1\}$ where v_0 has even degree and v_1 has odd degree. The trace is replaced by the super-trace, and one of the R-matrix element has an extra $-$ sign. The set of v_1-colored arcs form a simple multi-cycle, and the number of components is counted by the signs coming from the super-trace and the R-matrix element.

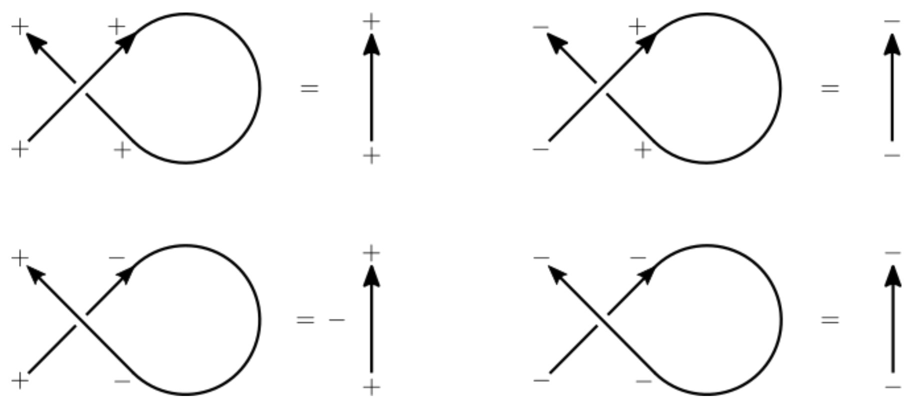

Figure 3.18: Sign factors under stabilizations.

Chapter 4

DEHN SURGERY

In the previous chapter we have studied how to define and compute $\hat{Z}$ for various link complements. In this chapter, we turn our attention to Dehn surgery, in order to glue in solid tori along the boundaries of those link complements.

The most basic form of the surgery formula is (2.5) [GM21, Conjecture 1.7], which we expect to be true for all knots, whenever $-\frac{r}{p}$ is big enough (where $\frac{p}{r}$ is the Dehn surgery coefficient). There is a natural generalization for links.

Conjecture 4.0.1. *Let $S^3_{p_1,\cdots,p_l}(L)$ be the 3-manifold obtained by performing the $(p_1,\cdots,p_l)$-surgery on $L\subset S^3$, and let B be the $l\times l$ linking matrix defined by*

$$B_{ij}=\begin{cases} p_i & \text{if } i=j \\ lk(i,j) & \text{otherwise}\end{cases}. \tag{4.1}$$

Let $\mathcal{L}^b_B$ be the "Laplace transform" defined by

$$\mathcal{L}^b_B : x^u \mapsto \begin{cases} q^{-(u,B^{-1}u)} & \text{if } u\in b+B\mathbb{Z}^l \\ 0 & \text{otherwise}\end{cases}. \tag{4.2}$$

Then [1]

$$\hat{Z}_{S^3_{p_1,\cdots,p_l}(L),b}(q)\cong\mathcal{L}^b_B\left[(x_1^{\frac{1}{2}}-x_1^{-\frac{1}{2}})\cdots(x_l^{\frac{1}{2}}-x_l^{-\frac{1}{2}})F_L(x_1,\cdots,x_l,q)\right], \tag{4.3}$$

whenever the smallest eigenvalue of $-B^{-1}$ is big enough so that the right-hand side converges.

Remark 4.0.2. The range of surgery coefficients for which this Dehn surgery formula is applicable is closely related to the rate of quadratic growth of the order of q (i.e., the minimal q-degree) of the coefficients of $F_K(x,q)$. More precisely, for any knot K, if we define

$$c_K:=\liminf_{n\to\infty}\frac{\mathrm{ord}_q f_n(q)}{n^2},$$

[1] Here, $\cong$ denotes equality up to a sign and a shift in overall q-degree. That is, $f\cong g$ iff $f=\epsilon q^d g$ for some sign $\epsilon\in\{\pm1\}$ and $d\in\mathbb{Q}$.

where $f_n(q)$ is the coefficient of $x^{n+\frac{1}{2}}$ in $F_K(x,q)$, then the right-hand side of the surgery formula converges whenever whenever $-\frac{1}{p/r}+c_K>0$. It would be very interesting to understand how the invariant c_K is related to some other known invariants of knots, such as the boundary slopes of the A-polynomial Newton polygon.

Assuming Conjecture 4.0.1 and its consistency, one can deduce formulas for partial Dehn surgery (i.e., performing Dehn surgery only on some strands of a link). In particular, the following partial small surgery formula is often useful:

Conjecture 4.0.3. *Let L be a link with components $L_0, L_1, \cdots, L_l$, with L_0 being an unknot. Let L' be the link obtained by performing the $-\frac{1}{r}$-surgery on L_0. Then*

$$F_{L'}(x_1,\cdots,x_l,q) \cong \mathcal{L}\left[(x_0^{\frac{1}{2r}}-x_0^{-\frac{1}{2r}})F_L(x_0,\cdots,x_l,q)\right] \tag{4.4}$$

whenever r is big enough so that the right-hand side converges, where

$$\mathcal{L}: x_0^u \mapsto q^{ru^2}\prod_{1\le i\le l} x_i^{lk(L_i,L_0)ru}. \tag{4.5}$$

This partial Dehn surgery formula was used in [Par20b] to reverse-engineer F_L for the Whitehead link and the Borromean rings, from the double twist knots, and the result is consistent with Examples 3.2.7 and 3.2.8.

While the Dehn surgery formulas we have just reviewed are nice, they are limited to the surgeries for which the minus of the inverse of the surgery coefficient is big enough. In the rest of this chapter, we present some hints and ideas toward overcoming this issue. The main observation is that the two-variable series $F_K(x,q)$ can be expanded in a form that we call the *inverted Habiro series*, and that in this form there are some nice q-series identities that allow us to go beyond the range of surgery coefficients that we were limited to.

4.1 Inverted Habiro series

It is a well-known theorem of Habiro [Hab02] that for any knot K, there is a sequence of Laurent polynomials $a_m(K)\in\mathbb{Z}[q,q^{-1}]$ such that the colored Jones polynomials $J_K(V_n)$, colored by the n-dimensional irreducible representation V_n of $\mathfrak{sl}_2$, can be decomposed as

$$J_K(V_n)=\sum_{m=0}^{\infty}a_m(K)\prod_{j=1}^{m}(x+x^{-1}-q^j-q^{-j})\Big|_{x=q^n}.$$

The purpose of this section is to make a curious observation that for some simple knots and links, the sequence $\{a_m(K)\}_{m\geq 0}$ can be naturally extended to negative values of m. The simplest example is the figure-eight knot. In this case we have $a_m(\mathbf{4}_1) = 1$ for any $m \geq 0$, so it is very natural to set $a_m(\mathbf{4}_1) = 1$ for any $m \in \mathbb{Z}$. Once we have such an extension of the sequence $\{a_m(K)\}$, we can "invert" the Habiro series in the following way:

$$\sum_{m=0}^{\infty} a_m(K) \prod_{j=1}^{m} (x + x^{-1} - q^j - q^{-j}) \rightsquigarrow -\sum_{m=1}^{\infty} \frac{a_{-m}(K)}{\prod_{j=0}^{m-1}(x + x^{-1} - q^j - q^{-j})}.$$

The series on the right-hand side is what we will call an *inverted Habiro series*. As we will see through examples, $a_m(K)$ with $m < 0$ are in general not necessarily Laurent polynomials, but rather Laurent power series in q with integer coefficients.

A priori the "inverted Habiro series" is a very different object compared to the original Habiro series. For one thing, the specialization $x = q^n$ doesn't make sense any more for the inverted Habiro series, as it has poles at $q^{\mathbb{Z}}$. For another thing, the inverted Habiro series can be expanded into a power series in x or x^{-1}, which is not possible for the usual Habiro series. The distinction is clearer in the classical limit $q \to 1$ where the usual Habiro series take values in $\mathbb{Z}[[x + x^{-1} - 2]]$ (a completion at a finite place $x + x^{-1} = 2$) whereas the inverted Habiro series take values in $\mathbb{Q}[[\frac{1}{x+x^{-1}-2}]]$ (a completion at an infinite place $x + x^{-1} = \infty$). Morally, this is the same as what we did in the previous section; whether it is a state sum or a Habiro series, we are inverting it to make it convergent near $x + x^{-1} = \infty$.

We conjecture that F_K can be thought of as the inverted Habiro series.

Conjecture 4.1.1. *For any knot K with $\Delta_K(x) \neq 1$, it has an inverted Habiro series, and it agrees with the F_K in the sense that*

$$F_K(x,q) = -(x^{\frac{1}{2}} - x^{-\frac{1}{2}}) \sum_{m=1}^{\infty} \frac{a_{-m}(K)}{\prod_{j=0}^{m-1}(x + x^{-1} - q^j - q^{-j})}$$

when the right-hand side is expanded into a power series in x.

Remark 4.1.2. In this conjecture, we have imposed the condition that $\deg \Delta_K(x) > 0$ to make sure that $\frac{1}{\Delta_K(x)} = O(x)$ as a power series in x.

The following identity allows us to transform a power series in x into an inverted Habiro series and vice versa.

Proposition 4.1.3. *If we write*

$$-(x^{\frac{1}{2}}-x^{-\frac{1}{2}})\sum_{m=1}^{\infty}\frac{a_{-m}(K;q)}{\prod_{k=0}^{m-1}(x+x^{-1}-q^k-q^{-k})}=x^{\frac{1}{2}}\sum_{j\geq 0}f_j(K;q)x^j,$$

then

$$\begin{aligned} f_j(K;q) &= \sum_{i=0}^{j}\begin{bmatrix} j+i \\ 2i \end{bmatrix} a_{-i-1}(K;q), \\ a_{-i-1}(K;q) &= \sum_{j=0}^{i}(-1)^{i+j}\begin{bmatrix} 2i \\ i-j \end{bmatrix}\frac{[2j+1]}{[i+j+1]}f_j(K;q). \end{aligned} \tag{4.6}$$

Proof. The first identity is a direct consequence of Heine's binomial formula

$$\frac{1}{(z)_n}=\sum_{j\geq 0}\begin{bmatrix} n+j-1 \\ j \end{bmatrix}_q z^j.$$

The second identity is the inverse of the first identity and can be verified using qZeil [PR97]. □

It follows from this proposition and Theorem 3.3.1, that for any nice knot K (such as any homogeneous braid knot) that is not an unknot, F_K can be expressed as as an inverted Habiro series.

Remark 4.1.4. Proposition 4.1.3 says that the inverted Habiro series and the power series in x contain the same amount of information. Still, the inverted Habiro series is an especially nice way of presenting F_K, as it is manifestly Weyl-symmetric. What is more, it helps us uncover various surgery formulas, as we we will see in later subsections.

Inverted Habiro series for some simple knots and links

The $a_m(K)$ for the figure-eight and the trefoil knots of both handedness are particularly simple:

$$a_m(\mathbf{4}_1)=1,\quad a_m(\mathbf{3}_1^l)=(-1)^m q^{\frac{m(m+3)}{2}},\quad a_m(\mathbf{3}_1^r)=(-1)^m q^{-\frac{m(m+3)}{2}}.$$

It is straightforward to extend these to negative m. From this, we obtain the inverted Habiro expansions of the corresponding F_K's:

$$F_{\mathbf{4}_1}(x,q)=-(x^{\frac{1}{2}}-x^{-\frac{1}{2}})\sum_{m=1}^{\infty}\frac{1}{\prod_{j=0}^{m-1}(x+x^{-1}-q^j-q^{-j})}, \tag{4.7}$$

$$F_{\mathbf{3}_1^l}(x,q) = -(x^{\frac{1}{2}} - x^{-\frac{1}{2}}) \sum_{m=1}^{\infty} \frac{(-1)^m q^{\frac{m(m-3)}{2}}}{\prod_{j=0}^{m-1}(x + x^{-1} - q^j - q^{-j})} \tag{4.8}$$
$$= q^{-1}(x^{\frac{1}{2}} - x^{-\frac{1}{2}}) \sum_{n\geq 0} \frac{(-1)^n q^{\frac{n(n-1)}{2}}}{\prod_{j=0}^{n}(x + x^{-1} - q^j - q^{-j})},$$

$$F_{\mathbf{3}_1^r}(x,q) = -(x^{\frac{1}{2}} - x^{-\frac{1}{2}}) \sum_{m=1}^{\infty} \frac{(-1)^m q^{-\frac{m(m-3)}{2}}}{\prod_{j=0}^{m-1}(x + x^{-1} - q^j - q^{-j})} \tag{4.9}$$
$$= q(x^{\frac{1}{2}} - x^{-\frac{1}{2}}) \sum_{n\geq 0} \frac{(-1)^n q^{-\frac{n(n-1)}{2}}}{\prod_{j=0}^{n}(x + x^{-1} - q^j - q^{-j})}.$$

Their power series expansions agree with the known results in [GM21].

The Habiro coefficients for the Whitehead link and the Borromean rings are given in [Hab00]. Inverting them, we obtain the following expressions for the corresponding F_K's:

$$F_{\mathbf{Wh}}(x_1,x_2,q) = q^{-\frac{1}{2}}(x_1^{\frac{1}{2}} - x_1^{-\frac{1}{2}})(x_2^{\frac{1}{2}} - x_2^{-\frac{1}{2}}) \sum_{n\geq 0} \frac{(-1)^n q^{-\frac{n(n+1)}{2}}(q^{n+1})_n}{\prod_{j=0}^{n}(x_1 + x_1^{-1} - q^j - q^{-j})(x_2 + x_2^{-1} - q^j - q^{-j})}, \tag{4.10}$$

$$F_{\mathbf{Bor}}(x_1,x_2,x_3,q) = (x_1^{\frac{1}{2}} - x_1^{-\frac{1}{2}})(x_2^{\frac{1}{2}} - x_2^{-\frac{1}{2}})(x_3^{\frac{1}{2}} - x_3^{-\frac{1}{2}}) \sum_{n\geq 0} \frac{(-1)^n q^{-\frac{3n^2+n}{2}}(q^{n+1})_n^2}{\prod_{j=0}^{n}(x_1 + x_1^{-1} - q^j - q^{-j})(x_2 + x_2^{-1} - q^j - q^{-j})(x_3 + x_3^{-1} - q^j - q^{-j})}. \tag{4.11}$$

These formulas agree perfectly with the results from the previous chapter (Examples 3.2.7 and 3.2.8).

+1-surgery

One surprising aspect of inverted Habiro series is that it allows us to uncover some surgery formulas that were not known before.

Proposition 4.1.5. *The following identity holds*

$$\left.\frac{1}{\prod_{j=1}^{n}(x + x^{-1} - q^j - q^{-j})}\right|_{x^u \mapsto q^{u^2}} = \frac{q^{n^2}}{(q^{n+1})_n}, \tag{4.12}$$

where $\left. f(x)\right|_{x^u \mapsto q^{u^2}}$ *is a shorthand notation for "first expand* $f(x)$ *into a power series in* x *and then replace each* x^u *by* q^{u^2}*." In other words,*

$$\sum_{k=0}^{\infty}(q^{(n+k)^2} - q^{(n+k+1)^2}) \begin{bmatrix} 2n+k \\ 2n \end{bmatrix} = \frac{q^{n^2}}{(q^{n+1})_n}.$$

Proof. In Proposition 4.1.14, we will show that $(q)_{2n} \frac{1}{\prod_{j=1}^{n}(x+x^{-1}-q^j-q^{-j})}\Big|_{x^u \mapsto q^{u^2}}$ is a polynomial. Using qZeil [PR97], one can verify that this polynomial is $q^{n^2}(q)_n$. $\square$

Corollary 4.1.6 (−1-surgery formula)**.** *Suppose that*

$$F_K(x,q) = -(x^{\frac{1}{2}} - x^{-\frac{1}{2}}) \sum_{m=1}^{\infty} \frac{a_{-m}(K)}{\prod_{j=0}^{m-1}(x + x^{-1} - q^j - q^{-j})}.$$

Then the -1*-surgery formula of [GM21] can be written as*

$$\hat{Z}_{S^3_{-1}(K)}(q) = -q^{-\frac{1}{2}} \sum_{n \geq 0} a_{-n-1}(K) \frac{q^{n^2}}{(q^{n+1})_n}.$$

Example 4.1.7 (−1-surgery on $\mathbf{4}_1$)**.** Let's take a look at the -1-surgery on the figure-eight knot $\mathbf{4}_1$. Since the inverted Habiro coefficients of $\mathbf{4}_1$ are all 1, we immediately get the following formula

$$\hat{Z}_{-\Sigma(2,3,7)}(q) = \hat{Z}_{S^3_{-1}(\mathbf{4}_1)}(q) = -q^{-\frac{1}{2}} \sum_{n \geq 0} \frac{q^{n^2}}{(q^{n+1})_n}.$$

Up to a prefactor, this is $\mathcal{F}_0(q)$, one of Ramanujan's mock theta functions of order 7.

It is a very useful fact that the right-hand side of (4.12) is a rational function in q. This means that even if we replace q by q^{-1}, the right-hand side will still make sense as a power series in q.

Corollary 4.1.8. *We have the identity*

$$\frac{1}{\prod_{j=1}^{n}(x + x^{-1} - q^j - q^{-j})}\Bigg|_{x^u \mapsto q^{-u^2}} = \frac{(-1)^n q^{\frac{n(n+1)}{2}}}{(q^{n+1})_n}. \tag{4.13}$$

Since the transform $x^u \mapsto q^{-u^2}$ when applied to $(x^{\frac{1}{2}} - x^{-\frac{1}{2}})F_K(x,q)$ is the $+1$-surgery formula given in [GM21], we can make use of this identity to do $+1$-surgery. The result, written in terms of inverted Habiro coefficients, looks like

$$\hat{Z}_{S^3_{+1}(K)}(q) = q^{\frac{1}{2}} \sum_{n \geq 0} a_{-n-1}(K) \frac{(-1)^n q^{\frac{n(n+1)}{2}}}{(q^{n+1})_n}. \tag{4.14}$$

However, one should note the important difference between the $+1$-surgery formula of [GM21] and the above formula. In (4.14), we are making an implicit regularization of the q-series. This is because the left-hand side of (4.13) is a power series in q^{-1}, whereas we are using the right-hand side of (4.13) as a series in q. This is more evident when we write the transform (4.14) in terms of $F_K(x,q) = x^{\frac{1}{2}} \sum_{j \geq 0} f_j(K;q) x^j$ using Proposition 4.1.3.

Proposition 4.1.9. *For any $j \geq 0$,*

$$\sum_{n=j}^{\infty}(-1)^{n+j}\begin{bmatrix}2n\\ n-j\end{bmatrix}\frac{[2j+1]}{[n+j+1]}\frac{(-1)^n q^{\frac{n(n+1)}{2}}}{(q^{n+1})_n}$$
$$= (q^{-j^2}-q^{-(j+1)^2})\left(1-\frac{\sum_{|k|\leq j}(-1)^k q^{\frac{k(3k+1)}{2}}}{(q)_\infty}\right).$$

Proof. The left-hand side can be simplified as

$$(q^{-j^2}-q^{-(j+1)^2})(-1)^{j+1}q^{\frac{j(3j+1)}{2}}\sum_{n=0}^{\infty}q^{n+2j+1}\frac{(q^{n+1})_j}{(q)_{n+2j+1}}.$$

Therefore, it suffices to prove that[2]

$$(-1)^{j+1}q^{\frac{j(3j+1)}{2}}\sum_{n\geq 0}q^{n+2j+1}(q^{n+1})_j(q^{n+2j+2})_\infty \stackrel{?}{=} \sum_{|k|>j}(-1)^k q^{\frac{k(3k+1)}{2}}. \tag{4.15}$$

Firstly, it follows from the q-Vandermonde convolution identity

$$\prod_{0\leq l\leq j-1}(x-q^l y) = \sum_{0\leq i\leq j}(-1)^i q^{\frac{i(i-1)}{2}}\begin{bmatrix}j\\ i\end{bmatrix}_q (q^{-i+1}x)_i(y)_{j-i},$$

that

$$(-1)^{j+1}q^{\frac{j(3j+1)}{2}}(q^{n+1})_j = \sum_{0\leq i\leq j}(-1)^{i+1}q^{\frac{i(i-1)}{2}}\begin{bmatrix}j\\ i\end{bmatrix}_q (q^{n+2j-i+2})_i(q^{j+1})_{j-i}.$$

So, the left-hand side of (4.15) becomes

$$\sum_{n\geq 0}q^{n+2j+1}(q^{n+2j+2})_\infty\sum_{0\leq i\leq j}(-1)^{i+1}q^{\frac{i(i-1)}{2}}\begin{bmatrix}j\\ i\end{bmatrix}_q (q^{n+2j-i+2})_i(q^{j+1})_{j-i}$$
$$= \sum_{n\geq 0}q^{n+2j-i+1}(q^{n+2j-i+2})_\infty\sum_{0\leq i\leq j}(-1)^{i+1}q^{\frac{i(i+1)}{2}}\begin{bmatrix}j\\ i\end{bmatrix}_q (q^{j+1})_{j-i}$$
$$= \sum_{n\geq 0}\Big((q^{n+2j-i+2})_\infty-(q^{n+2j-i+1})_\infty\Big)\sum_{0\leq i\leq j}(-1)^{i+1}q^{\frac{i(i+1)}{2}}\begin{bmatrix}j\\ i\end{bmatrix}_q (q^{j+1})_{j-i}$$
$$= \Big(1-(q^{2j-i+1})_\infty\Big)\sum_{0\leq i\leq j}(-1)^{i+1}q^{\frac{i(i+1)}{2}}\begin{bmatrix}j\\ i\end{bmatrix}_q (q^{j+1})_{j-i}$$
$$= \left(\sum_{0\leq i\leq j}(-1)^{i+1}q^{\frac{i(i+1)}{2}}\begin{bmatrix}j\\ i\end{bmatrix}_q (q^{j+1})_{j-i}\right)-(q^{j+1})_\infty\sum_{0\leq i\leq j}(-1)^{i+1}q^{\frac{i(i+1)}{2}}\begin{bmatrix}j\\ i\end{bmatrix}_q$$
$$= \left(\sum_{0\leq i\leq j}(-1)^{i+1}q^{\frac{i(i+1)}{2}}\begin{bmatrix}j\\ i\end{bmatrix}_q (q^{j+1})_{j-i}\right)+(q)_\infty,$$

[2] I thank Fedor Petrov for providing a proof of this identity.

where we have used the q-binomial identity in the last equality. Euler's pentagonal number theorem says

$$(q)_\infty = \sum_{k\in\mathbb{Z}} (-1)^k q^{\frac{k(3k+1)}{2}},$$

and therefore (4.15) is reduced to the following simple identity:

$$\sum_{0\le i\le j} (-1)^i q^{\frac{i(i+1)}{2}} \begin{bmatrix} j \\ i \end{bmatrix}_q (q^{j+1})_{j-i} \stackrel{?}{=} \sum_{|k|\le j} (-1)^k q^{\frac{k(3k+1)}{2}}.$$

The left-hand side is a polynomial of degree at most

$$\max_{0\le i\le j} \left\{ \frac{i(i+1)}{2} + i(j-i) + \frac{(3j-i+1)(j-i)}{2} \right\} = \frac{j(3j+1)}{2}.$$

On the other hand, we know that

$$\begin{aligned} (q)_\infty - \sum_{0\le i\le j} (-1)^i q^{\frac{i(i+1)}{2}} \begin{bmatrix} j \\ i \end{bmatrix}_q (q^{j+1})_{j-i} &= (-1)^{j+1} q^{\frac{j(3j+1)}{2}} \sum_{n\ge 0} q^{n+2j+1} (q^{n+1})_j (q^{n+2j+2})_\infty \\ &\equiv 0 \mod q^{\frac{j(3j+1)}{2}+2j+1}. \end{aligned}$$

Therefore,

$$\sum_{0\le i\le j} (-1)^i q^{\frac{i(i+1)}{2}} \begin{bmatrix} j \\ i \end{bmatrix}_q (q^{j+1})_{j-i} = (q)_\infty \bmod q^{\frac{j(3j+1)}{2}+2j+1} = \sum_{|k|\le j} (-1)^k q^{\frac{k(3k+1)}{2}}$$

as desired. □

As a result, we can write (4.14) as

$$\hat{Z}_{S^3_{+1}(K)}(q) = q^{\frac{1}{2}} \sum_{j\ge 0} f_j(K;q)(q^{-j^2} - q^{-(j+1)^2}) \left(1 - \frac{\sum_{|k|\le j} (-1)^k q^{\frac{k(3k+1)}{2}}}{(q)_\infty} \right). \tag{4.16}$$

In this form, it is clear what the effect of the implicit regularization (4.13) is; it adds the "regularization factor" of $1 - \frac{\sum_{|k|\le j}(-1)^k q^{\frac{k(3k+1)}{2}}}{(q)_\infty}$. Note that (4.16) can be written in the following form

$$\hat{Z}_{S^3_{+1}(K)}(q) = \frac{q^{\frac{1}{2}}}{(q)_\infty} \sum_{\substack{j\ge 0 \\ |k|>j}} f_j(K;q)(q^{-j^2} - q^{-(j+1)^2})(-1)^k q^{\frac{k(3k+1)}{2}}. \tag{4.17}$$

This expression hints that the +1-surgery formula is related to indefinite theta functions. We study this connection further in Section 4.2.

Conjecture 4.1.10 (Regularized +1-surgery formula)**.** *Suppose F_K can be expressed as an inverted Habiro series. Then $\hat{Z}$ for the $+1$-surgery on K is given by* (4.14)*, or equivalently* (4.17).

We have checked this conjecture through various examples.

Example 4.1.11 (+1-surgery on $\mathbf{4}_1$)**.** Naive application of the +1-surgery formula of [GM21] to $F_{\mathbf{4}_1}$ does not converge. So we need to use our regularization. From (4.14), we immediately get

$$\hat{Z}_{\Sigma(2,3,7)}(q) = \hat{Z}_{S^3_{+1}(\mathbf{4}_1)}(q) = q^{\frac{1}{2}} \sum_{n\geq 0} \frac{(-1)^n q^{\frac{n(n+1)}{2}}}{(q^{n+1})_n},$$

which agrees with the computation from the plumbing description of $\Sigma(2,3,7)$ in [GM21].

Example 4.1.12 (+1-surgery on Whitehead link)**.** Consider the Whitehead link which is obtained by -1-surgery on a component of the Borromean rings (mirror to Example 3.2.7). If we apply the +1-surgery of [GM21], then it stabilizes to $F_{\mathbf{4}_1}$ but does not converge to it. This is because even if we add more and more terms, there are always terms with higher and higher power of q^{-1}. This issue is solved by using the regularized +1-surgery formula; in this way, the result actually converges to $F_{\mathbf{4}_1}$.

Example 4.1.13 (+1-surgery on **L7a1**)**.** As briefly mentioned in Example 3.2.9, the +1-surgery on the x_2-component of **L7a1** is the $\mathbf{6}_2$ knot. Indeed, applying the regularized +1-surgery formula, the result converges to $F_{\mathbf{6}_2}(x_1, q)$.

Other positive integer surgeries

Now we study some other integer surgeries in a similar fashion.

Proposition 4.1.14. *The q-series*

$$\left.\frac{1}{\prod_{j=1}^{n}(x + x^{-1} - q^j - q^{-j})}\right|_{x^u \mapsto \delta_{b,u (mod\ p)} q^{\frac{u^2}{p}}}$$

is a rational function function in q. Here, $f(x)\Big|_{x^u \mapsto \delta_{b,u (mod\ p)} q^{\frac{u^2}{p}}}$ is a shorthand notation for "first expand $f(x)$ into a power series in x and then replace each x^u by $q^{\frac{u^2}{p}}$ whenever $b = u$ (mod p) and by 0 otherwise."

Proof. We start by putting it in a form that is easier to deal with:

$$
\begin{aligned}
&(q)_{2n}\frac{1}{\prod_{j=1}^{n}(x+x^{-1}-q^{j}-q^{-j})}\Bigg|_{x^u\mapsto\delta_{b,u(\mathrm{mod}\ p)}q^{\frac{u^2}{p}}} \\
&= -(q)_{2n}(x^{\frac{1}{2}}-x^{-\frac{1}{2}})\sum_{k\geq 0}x^{n+k+\frac{1}{2}}\begin{bmatrix}2n+k\\2n\end{bmatrix}\Bigg|_{x^u\mapsto\delta_{b,u(\mathrm{mod}\ p)}q^{\frac{u^2}{p}}} \\
&= \sum_{k\geq 0}(x^{n+k}-x^{n+k+1})q^{-nk}(1-q^{k+1})\cdots(1-q^{k+2n})\Bigg|_{x^u\mapsto\delta_{b,u(\mathrm{mod}\ p)}q^{\frac{u^2}{p}}} \\
&= \sum_{\substack{k\geq 0\\ k\equiv b-n \bmod p}} q^{\frac{(n+k)^2}{p}}q^{-nk}(1-q^{k+1})\cdots(1-q^{k+2n}) \\
&\quad - \sum_{\substack{k\geq 0\\ k\equiv b-n-1 \bmod p}} q^{\frac{(n+k+1)^2}{p}}q^{-nk}(1-q^{k+1})\cdots(1-q^{k+2n}).
\end{aligned}
$$

Expanding $(1-q^{k+1})\cdots(1-q^{k+2n})$ on both sides, there are 2^{2n} terms on each side of the summation. There is a natural pairing between the terms on the left side with the terms on the right side, given by the following rule. Any term on the left side can be expressed as a sequence of signs, where the i-th sign would represent whether we choose 1 or $-q^{k+i}$ from $(1-q^{k+i})$. Then we flip all the signs and reverse the order. This new sequence will correspond to a term on the right summation. If we started with a term $q^{\frac{(n+k)^2}{p}+Ak+B}$ from the left summation, then the corresponding term on the right summation is $-q^{\frac{(n+k+1)^2}{p}-Ak+(B-(2n+1)A)}$. Notice that

$$
\begin{aligned}
q^{\frac{(n+k)^2}{p}+Ak+B} &= q^{\frac{1}{p}(n+k)(n+k+pA)+(B-An)}, \\
-q^{\frac{(n+k+1)^2}{p}-Ak+(B-(2n+1)A)} &= -q^{\frac{1}{p}(n+k+1-pA)(n+k+1)+(B-An)}.
\end{aligned}
$$

This means that the summation of these pairs over k telescopes, leaving only finitely many terms. Therefore the expression we started with is a Laurent polynomial in q. ∎

This proposition itself is enough to study positive and negative integer surgeries, but we should remark that, based on experiments, it seems we can say more about the structure of the rational function; it takes the following form:

$$
\frac{1}{\prod_{j=1}^{n}(x+x^{-1}-q^{j}-q^{-j})}\Bigg|_{x^u\mapsto\delta_{b,u(\mathrm{mod}\ p)}q^{\frac{u^2}{p}}} = \frac{q^{n^2}}{(q^{n+1})_n}q^{-\frac{b(p-b)}{p}}P_n^{p,b}(q), \qquad (4.18)
$$

where $P_n^{p,b}(q)\in\mathbb{Z}[q^{-1}]$ is a polynomial with non-negative coefficients of degree at most $p\lfloor\frac{n^2}{4}\rfloor$ whose classical limit (i.e., $q=1$ limit) is p^{n-1} for any $n\geq 1$. In Table 4.1, we list the first few polynomials $P_n^{p,b}$.

n	
0	$P_0^{p,b} = \delta_{b,0}$
1	$P_1^{p,b} = 1$
2	$P_2^{1,0} = 1$
	$P_2^{2,0} = 1 + q^{-2}$
	$P_2^{2,1} = 1 + q^{-1}$
	$P_2^{3,0} = 1 + q^{-2} + q^{-3}$
	$P_2^{3,1} = 1 + q^{-1} + q^{-2}$
3	$P_3^{1,0} = 1$
	$P_3^{2,0} = 1 + q^{-2} + q^{-3} + q^{-4}$
	$P_3^{2,1} = 1 + q^{-1} + q^{-2} + q^{-4}$
	$P_3^{3,0} = 1 + q^{-2} + 2q^{-3} + 2q^{-4} + q^{-5} + 2q^{-6}$
	$P_3^{3,1} = 1 + q^{-1} + 2q^{-2} + q^{-3} + 2q^{-4} + q^{-5} + q^{-6}$

Table 4.1: The first few polynomials $P_n^{p,b}$.

Replacing q with q^{-1}, the right-hand side still makes sense as a power series in q.

Corollary 4.1.15. *We have the identity*

$$\left.\frac{1}{\prod_{j=1}^{n}(x + x^{-1} - q^j - q^{-j})}\right|_{x^u \mapsto \delta_{b,u (mod\ p)} q^{-\frac{u^2}{p}}} = \frac{(-1)^n q^{\frac{n(n+1)}{2}}}{(q^{n+1})_n} q^{\frac{b(p-b)}{p}} P_n^{p,b}(q^{-1}). \tag{4.19}$$

Just like we made use of (4.13) to conjecture a regularized version of the +1-surgery formula, we conjecture that we can use (4.19) to regularize p-surgery.

Example 4.1.16 (+1, +2, +3-surgery on $\mathbf{4}_1$)**.** The +1, +2, +3-surgeries on $\mathbf{4}_1$ are all Seifert manifolds. They are nicely summarized in [GM21, Table 9]. In that table, $\hat{Z}$ for those 3-manifolds were computed from their plumbing descriptions. The surgery formula of [GM21] cannot be applied directly to compute them as +1, +2, +3-surgeries on $\mathbf{4}_1$, as it gives non-convergent results. Instead, we can use the regularized $+p$-surgery formula (4.19), and we find that the results agree perfectly with the computation from plumbing descriptions.

Quantum C-polynomial recursion and positive small surgeries

So far, we have discussed how to use inverted Habiro series to study various integer surgeries, but we haven't discussed much how to compute the inverted Habiro series. Of course, once we know F_K, we can use Proposition 4.1.3 to compute inverted Habiro coefficients, but is there a way to compute the inverted Habiro coefficients just from the Habiro coefficients? Sometimes this is possible by solving the quantum (i.e., non-commutative) C-polynomial recursion, which is the topic of this subsection.

It was shown in [GL05] that the coefficients $\{a_m(K)\}_{m\geq 0}$ of the Habiro series are q-holonomic. The recurrence relation was further studied in [GS06] and was named the *C-polynomial*. A quantum C-polynomial $\hat{C}_K(\hat{E},\hat{Q},q)$ is written in terms of the q-commuting operators $\hat{Q}$ and $\hat{E}$. These operators act on the set of discrete functions by

$$(\hat{Q}f)(m) = q^m f(m), \quad (\hat{E}f)(m) = f(m+1),$$

and they satisfy the following q-commutation relation

$$\hat{E}\hat{Q} = q\hat{Q}\hat{E}.$$

Let E be a variable where $\hat{Q}$ and $\hat{E}$ act by

$$\hat{Q}E^{-m} = q^m E^{-m}, \quad \hat{E}E^{-m} = E^{-(m-1)}.$$

It is useful to combine the Habiro coefficients $\{a_m(K)\}_{m\geq 0}$ into a series

$$\sum_{m\geq 0} a_m(K)E^{-m}.$$

Since $\hat{C}_K(\hat{E},\hat{Q},q)$ defines a recurrence relation for $\{a_m(K)\}_{m\geq 0}$, when we apply $\hat{C}_K$ to the above series, all but finitely many terms will cancel out. However, in general it doesn't vanish completely, because the boundary terms survive. The non-vanishing of $\hat{C}_K(\hat{E},\hat{Q},q)\sum_{m\geq 0} a_m(K)E^{-m}$ is actually very useful for our purpose, because we can take it as the starting point of the recursion and use it to extend the sequence $\{a_m(K)\}_{m\geq 0}$ to negative m. More precisely, we want to extend it into a bilateral sequence $\{a_m(K)\}_{m\in\mathbb{Z}}$ in such a way that

$$\hat{C}_K(\hat{E},\hat{Q},q)\sum_{m\in\mathbb{Z}} a_m(K)E^{-m} = 0. \tag{4.20}$$

Since explicit expressions for the quantum C-polynomials for twist knots are given in [GS06], we will use them and demonstrate how this strategy works.

The simplest cases are the trefoil knot and the figure-eight knot. In those cases, we find that solving the quantum C-polynomial recursion, there is a unique way to extend the series $\sum_{m\geq 0} a_m(K)E^{-m}$ into a bilateral series $\sum_{m\in\mathbb{Z}} a_m(K)E^{-m}$,[3] and the result agrees with what we found in Section 4.1.

[3]More generally, we expect that for any fibered knot K, the quantum C-polynomial uniquely determines the extension into a bilateral series.

Other twist knots are more interesting. Let's focus on the two-twist knot $K_2 = \mathbf{5}_2$ for the moment. In this case, the series $\sum_{m\geq 0} a_m(\mathbf{5}_2)E^{-m}$ looks like

$$1+(-q^2-q^4)E^{-1}+(q^5+q^7+q^8+q^{11})E^{-2}+(-q^9-q^{11}-q^{12}-q^{13}-q^{15}-q^{16}-q^{17}-q^{21})E^{-3}+\cdots,$$

and the quantum C-polynomial is given by

$$\hat{C}_{\mathbf{5}_2}(\hat{E},\hat{Q},q) = \hat{E}^2 + (q^2+q^3)\hat{E}\hat{Q} + (q^6 - q^3\hat{E})\hat{Q}^2 + (-q^7 + q^4\hat{E})\hat{Q}^3.$$

When we try to solve the recursion, we quickly realize that $a_{-1}(\mathbf{5}_2)$ cannot be determined by $\{a_m(\mathbf{5}_2)\}_{m\geq 0}$, but once we know $a_{-1}(\mathbf{5}_2)$ all the other $a_m(\mathbf{5}_2)$ with $m < -1$ are uniquely determined.[4]

So, how do we determine $a_{-1}(\mathbf{5}_2)$? It turns out this can be done by imposing a certain boundary condition on the bilateral sequence. More precisely, we take the ansatz where we express $a_{-1}(K)$ in terms of $\{a_m(K)\}_{m\leq -M}$ and take the limit where M goes to ∞. Explicitly, we have the following sequence of relations coming from the quantum C-polynomial recursion:

$$\begin{aligned}
a_{-1}(\mathbf{5}_2) &= \frac{1}{1+q}\Big(-q^{-1} + (1-q)a_{-2}(\mathbf{5}_2)\Big)\\
a_{-2}(\mathbf{5}_2) &= \frac{1}{1+q^2+q^3+q^4}\Big(q + (1+q-q^2-q^3)a_{-3}(\mathbf{5}_2)\Big)\\
a_{-3}(\mathbf{5}_2) &= \frac{1}{1+q^3+q^4+q^5+q^6+q^7+q^8+q^9}\Big(-q^6 + (1+q^2+q^4-q^5-q^6-q^7)a_{-4}(\mathbf{5}_2)\Big),
\end{aligned}$$

and so on. Starting with the first equation, we can plug in the second equation to express $a_{-1}(\mathbf{5}_2)$ in terms of $a_{-3}(\mathbf{5}_2)$. Plugging in the third equation to that would give an expression of $a_{-1}(\mathbf{5}_2)$ in terms of $a_{-4}(\mathbf{5}_2)$, and we can proceed in the same way indefinitely. Taking the limit, we have the following ansatz for $a_{-1}(\mathbf{5}_2)$:

$$a_{-1}(\mathbf{5}_2) = \frac{-q^{-1}}{1+q}\left(1 + \frac{-(1-q)q^2}{1+q^2+q^3+q^4}\left(1 + \frac{-(1+q-q^2-q^3)q^5}{1+q^3+q^4+q^5+q^6+q^7+q^8+q^9}(\cdots)\right)\right). \tag{4.21}$$

Expanding this into a power series in q, we find

$$a_{-1}(\mathbf{5}_2) = -q^{-1} + 1 - q^2 + q^5 - q^9 + q^{14} - q^{20} + q^{27} - O(q^{35}),$$

which agrees perfectly with $F_{\mathbf{5}_2}(x,q)$ obtained in [Par20b] (our $\mathbf{5}_2$ is the knot that was denoted $m(\mathbf{5}_2)$ in [Par20b]).

[4] This is analogous to how we need to know the first two terms to determine the full power series $F_{\mathbf{5}_2}(x,q)$ if we were to solve it using quantum A-polynomial recursion.

The same type of ansatz seems to work for all twist knots. In general, for the n-twist knot K_n, $a_l(K_n)$ can be expressed in terms of $\{a_{l-k}(K_n)\}_{1\le k\le |n|-1}$. Using these relations, we can always express $a_l(K_n)$ in terms of $\{a_m(K_n)\}_{m\le -M}$ for any M. Sending M to ∞, we get the ansatz.

All these ansatz can be obtained as a limit of a sequence of rational functions in q. As we emphasized in previous subsections, having a rational function is especially useful as it allows us to study the mirror knot and the orientation-reversed 3-manifold. For instance, we can simply replace q by q^{-1} in (4.21) and still expand it as a power series in q. As a result, we get a candidate for $a_{-1}(m(\mathbf{5}_2))$:

$$a_{-1}(m(\mathbf{5}_2)) = -q^2 + q^4 - q^5 + 2q^6 - 2q^7 + q^8 - 3q^{10} + O(q^{11}).$$

By construction, the asymptotic expansion of this series near each root of unity agrees with that of $a_{-1}(\mathbf{5}_2)\big|_{q\to q^{-1}}$. What we are doing here is morally very similar to what we did when we described the regularized versions of positive integer surgery formulas. We are regularizing $a_{-1}(\mathbf{5}_2)\big|_{q\to q^{-1}}$ into a power series in q by using the fact that it can be naturally expressed as the limit of a sequence of rational functions.

In a similar fashion, we get candidates of the inverted Habiro coefficients for all mirror twist knots. For instance, the mirror of

$$\begin{aligned} a_{-1}(\mathbf{7}_2) &= -q^{-1} + 1 - q^4 + q^7 - q^{15} + q^{20} - q^{32} + q^{39} - O(q^{55}),\\ a_{-2}(\mathbf{7}_2) &= q^3 - q^5 - q^6 + q^8 + q^{13} + q^{14} - q^{16} - q^{17} - O(q^{18}) \end{aligned}$$

are

$$\begin{aligned} a_{-1}(m(\mathbf{7}_2)) &= -q^3 + q^5 - q^7 + 2q^8 - 2q^{10} + 2q^{12} + O(q^{13}),\\ a_{-2}(m(\mathbf{7}_2)) &= q^5 - q^8 - q^9 - q^{11} + q^{13} + O(q^{14}). \end{aligned}$$

Since all these twist knots can be obtained from the Whitehead link by doing $\frac{1}{r}$-surgery for various r, we can use these results to reverse-engineer the regularized $\frac{1}{r}$-surgery formula. It turns out, the end result is very simple.

Conjecture 4.1.17 (Regularized $+\frac{1}{r}$-surgery formula)**.** *When the $+\frac{1}{r}$-surgery formula of [GM21] does not converge, we can regularize it in the following way, as long as this regularization converges:*

$$\hat{Z}_{S^3_{+1/r}(K)}(q) = q^{\frac{r+r^{-1}}{4}} \sum_{j\ge 0} f_j(K;q)\left(q^{-r(j+\frac{1}{2}-\frac{1}{2r})^2} - q^{-r(j+\frac{1}{2}+\frac{1}{2r})^2}\right)\left(1 - \frac{\sum_{|k|\le j}(-1)^k q^{\frac{k((2r+1)k+1)}{2}}}{f(-q^r, -q^{r+1})}\right) \tag{4.22}$$

where $F_K(x,q) = x^{\frac{1}{2}} \sum_{j\geq 0} f_j(K;q)x^j$, *and*

$$f(a,b) := \sum_{n\in\mathbb{Z}} a^{\frac{n(n+1)}{2}} b^{\frac{n(n-1)}{2}} = (-a;ab)_\infty(-b,ab)_\infty(ab;ab)_\infty$$

denotes the Ramanujan theta function.

As a small consistency check, we find that the three surgery descriptions $S^3_{\frac{1}{2}}(\mathbf{4}_1) = S^3_{-1}(m(K_2)) = S^3_{+1}(K_{-2})$ of the same manifold give the same result for $\hat{Z}$, which is

$$q^{3/2}(1 - 2q^2 + q^3 - 3q^4 + 4q^5 - q^6 + q^7 + 5q^8 + O(q^9)).$$

Remark 4.1.18. We have to warn the readers though, that this last conjecture is far more speculative compared to any other conjectures presented in this thesis. We are not entirely sure yet, for instance, if the candidate q-series for $a_{-1}(m(\mathbf{5}_2))$ is the correct one. In fact, there is another candidate, coming from the following q-series identity (found from an inverted state sum model for $F_{\mathbf{5}_2}(x,q)$):

$$\sum_{n\geq 0}(-1)^n q^{\frac{n(n+1)}{2}} = \sum_{m,n\geq 0} \frac{(-1)^{m+n} q^{\frac{m(m+1)+n(n+1)}{2}}}{(q)_m(q)_n(1-q^{m+n+1})}.$$

While the left-hand side of this identity only makes sense inside the unit disk $|q| < 1$, the right-hand side of this identity can be expanded into a power series in q^{-1} as well. Since $a_{-1}(\mathbf{5}_2) = -q^{-1}\sum_{n\geq 0}(-1)^n q^{\frac{n(n+1)}{2}}$, substituting q by q^{-1} in the identity above, we get the following candidate for q-series for $a_{-1}(m(\mathbf{5}_2))$:

$$a_{-1}(m(\mathbf{5}_2)) \stackrel{?}{=} q^2 + 3q^3 + 6q^4 + 13q^5 + 23q^6 + 44q^7 + 74q^8 + O(q^9).$$

Figuring out the correct expression for $F_{m(\mathbf{5}_2)}(x,q)$ is the next important step that will take us even closer toward a full definition of $\hat{Z}$.

Inverted Habiro series in higher rank

When we restrict our attention to symmetric representations, the higher rank analogue of the Habiro's cyclotomic expansion is known. See [Ito+12; MMM13] and references therein. The q-holonomicity of these cyclotomic coefficients follows from the q-holonomicity of the colored HOMFLY-PT polynomials. The corresponding higher rank analogue of the quantum C-polynomial was studied in [MM95]. Thanks to these known results, it is straightforward to extend our analysis in this section to the higher rank case, by solving the higher rank quantum C-polynomial recursions. For example, in case of the figure-eight knot, the reduced version of $F_{\mathbf{4}_1}^{\mathfrak{sl}_N,sym}(x,q)$ is given by

$$F_{\mathbf{4}_1}^{\mathfrak{sl}_N,sym,red}(x,q) = -\sum_{n\geq 0} \frac{\frac{[-n][-n+1]\cdots[-n+N-3]}{[N-2]!}}{\prod_{j=0}^{n}(x^{\frac{1}{2}}q^{\frac{j}{2}} - x^{-\frac{1}{2}}q^{-\frac{j}{2}})(x^{\frac{1}{2}}q^{\frac{(N-2)-j}{2}} - x^{-\frac{1}{2}}q^{\frac{j-(N-2)}{2}})}$$

Note that in this form the Weyl symmetry $F_K^{\mathfrak{sl}_N}(x,q) = F_K^{\mathfrak{sl}_N}(q^{2-N}x^{-1},q)$ is manifest. We will encounter this Weyl symmetry again in (5.35).

4.2 Connection to indefinite theta functions

While the definition of $\hat{Z}$ for negative definite plumbed 3-manifolds was given in [Guk+20] (Definition 2.2.2), it has been a challenge to extend it to indefinite plumbings. This is mainly because the formula gives a non-convergent result when applied naively to a plumbed 3-manifold that is not negative definite. One approach to overcome this issue suggested by Cheng, Ferrari, and Sgroi [CFS20] is to use indefinite theta functions with a regularization factor. Only one example, $-\Sigma(2,3,7)$, was given in their paper. Starting from the plumbing formula of Gukov-Pei-Putrov-Vafa naively applied to a plumbing description of $-\Sigma(2,3,7)$, they multiplied both the numerator and the denominator by $(q)_\infty$. The factor $(q)_\infty = \sum_{k\in\mathbb{Z}}(-1)^k q^{\frac{k(3k+1)}{2}}$ in the numerator is then interpreted as a part of an indefinite theta function. Then they inserted a regularization factor (denoted by $\rho(\mathbf{v})$ in their paper), and the resulting formula somewhat magically gives the correct $\hat{Z}_{-\Sigma(2,3,7)}(q)$.

In this section, we explore this connection to indefinite theta functions based on our observation from the previous section that the regularization factors appearing in the regularized positive surgery formulas look very much like the regularization factors we can use for indefinite theta functions. We will work out a number of explicit examples, hoping that they will eventually shed light on figuring out a formula for $\hat{Z}$ for general plumbed 3-manifolds.

Example 4.2.1 ($-\Sigma(2,3,7)$)**.** The 3-manifold $-\Sigma(2,3,7)$ has various descriptions, for instance,

$$-\Sigma(2,3,7) = M(1;-\frac{1}{2},-\frac{1}{3},-\frac{1}{7}) = S^3_{+1}(\mathbf{3}_1^l) = S^3_{-1}(\mathbf{4}_1).$$

For our purpose, the description as the +1-surgery on the left-handed trefoil knot is the most useful one. The naive plumbing formula [Guk+20] applied to $-\Sigma(2,3,7)$

gives the following expression

$$\hat{Z}_{-\Sigma(2,3,7)}(q)\text{“} \cong \text{”} \oint \frac{dx_1}{2\pi i x_1}\frac{dx_2}{2\pi i x_2}\frac{dx_3}{2\pi i x_3}\frac{dx_7}{2\pi i x_7}\frac{(x_2^{\frac{1}{2}}-x_2^{-\frac{1}{2}})(x_3^{\frac{1}{2}}-x_3^{-\frac{1}{2}})(x_7^{\frac{1}{2}}-x_7^{-\frac{1}{2}})}{x_1^{\frac{1}{2}}-x_1^{-\frac{1}{2}}}$$
$$\times \sum_{\vec{\ell}\in M\mathbb{Z}^4+\frac{1}{2}\vec{1}} q^{-(\vec{\ell},M^{-1}\vec{\ell})}\vec{x}^{\vec{\ell}},$$

where

$$M=\begin{pmatrix}1&1&1&1\\1&2&0&0\\1&0&3&0\\1&0&0&7\end{pmatrix},\quad M^{-1}=\begin{pmatrix}42&-21&-14&-6\\-21&11&7&3\\-14&7&5&2\\-6&3&2&1\end{pmatrix}.$$

The symbol $\cong$ denotes equality up to an overall sign and a power of q, and we wrote it in quote, because the right-hand side does not converge. Integrating out x_2, x_3, x_7, we get

$$\hat{Z}_{-\Sigma(2,3,7)}(q)\text{“} \cong \text{”} \oint \frac{dx_1}{2\pi i x_1}\frac{1}{x_1^{\frac{1}{2}}-x_1^{-\frac{1}{2}}}\sum_{\epsilon_2,\epsilon_3,\epsilon_7=\pm 1}\sum_{\ell_1\in\mathbb{Z}+\frac{1}{2}}\epsilon_2\epsilon_3\epsilon_7\, q^{-42(\ell_1-\frac{1}{2}(\frac{1}{2}\epsilon_2+\frac{1}{3}\epsilon_3+\frac{1}{7}\epsilon_7))^2+\frac{1}{168}}x_1^{\ell_1}. \tag{4.23}$$

Now recall that from the plumbing description of the left-handed trefoil, we have

$$F_{3_1^l}(x,q) \cong \oint \frac{dx_1}{2\pi i x_1}\frac{dx_2}{2\pi i x_2}\frac{dx_3}{2\pi i x_3}\frac{(x_2^{\frac{1}{2}}-x_2^{-\frac{1}{2}})(x_3^{\frac{1}{2}}-x_3^{-\frac{1}{2}})}{x_1^{\frac{1}{2}}-x_1^{-\frac{1}{2}}}\sum_{\vec{n}\in\mathbb{Z}^3\times\{0\}} q^{-(\vec{n},M'\vec{n})-(\vec{n},\vec{1})}\vec{x}^{M'\vec{n}+\frac{1}{2}\vec{1}},$$

where

$$M'=\begin{pmatrix}1&1&1&1\\1&2&0&0\\1&0&3&0\\1&0&0&6\end{pmatrix}.$$

So the power of $x = x_6$ is $n_1 + \frac{1}{2}$. We have seen previously that the regularized +1 surgery formula can be written as

$$x^{m+\frac{1}{2}} \mapsto (q^{-m^2}-q^{-(m+1)^2})\frac{\sum_{\substack{k\in\mathbb{Z}\\|k|>|m+\frac{1}{2}|}}(-1)^k q^{\frac{k(3k-1)}{2}}}{(q)_\infty}.$$

Therefore,

$$
\begin{aligned}
&\hat{Z}_{-\Sigma(2,3,7)}(q) \\
&\cong \oint \frac{dx_1}{2\pi i x_1}\frac{dx_2}{2\pi i x_2}\frac{dx_3}{2\pi i x_3}\frac{(x_2^{\frac{1}{2}}-x_2^{-\frac{1}{2}})(x_3^{\frac{1}{2}}-x_3^{-\frac{1}{2}})}{x_1^{\frac{1}{2}}-x_1^{-\frac{1}{2}}} \\
&\quad \times \sum_{\vec{n}\in\mathbb{Z}^3\times\{0\}} q^{-(\vec{n},M'\vec{n})-(\vec{n},\vec{1})} x_1^{n_1+n_2+n_3+\frac{1}{2}} x_2^{n_1+2n_2+\frac{1}{2}} x_3^{n_1+3n_3+\frac{1}{2}} (q^{-n_1^2}-q^{-(n_1+1)^2}) \frac{\sum_{\substack{k\in\mathbb{Z}\\ |k|>|n_1+\frac{1}{2}|}} (-1)^k q^{\frac{k(3k-1)}{2}}}{(q)_\infty} \\
&\cong \oint \frac{dx_1}{2\pi i x_1}\frac{dx_2}{2\pi i x_2}\frac{dx_3}{2\pi i x_3}\frac{dx_7}{2\pi i x_7}\frac{(x_2^{\frac{1}{2}}-x_2^{-\frac{1}{2}})(x_3^{\frac{1}{2}}-x_3^{-\frac{1}{2}})(x_7^{\frac{1}{2}}-x_7^{-\frac{1}{2}})}{x_1^{\frac{1}{2}}-x_1^{-\frac{1}{2}}} \\
&\quad \times \sum_{\vec{n}\in\mathbb{Z}^3\times\mathbb{Z}} q^{-(\vec{n},M'\vec{n})-n_7^2-(\vec{n},\vec{1})} x_1^{n_1+n_2+n_3+\frac{1}{2}} x_2^{n_1+2n_2+\frac{1}{2}} x_3^{n_1+3n_3+\frac{1}{2}} x_7^{n_1+n_7+\frac{1}{2}} \frac{\sum_{\substack{k\in\mathbb{Z}\\ |k|>|n_1+\frac{1}{2}|}} (-1)^k q^{\frac{k(3k-1)}{2}}}{(q)_\infty} \\
&= \oint \frac{dx_1}{2\pi i x_1}\frac{dx_2}{2\pi i x_2}\frac{dx_3}{2\pi i x_3}\frac{dx_7}{2\pi i x_7}\frac{(x_2^{\frac{1}{2}}-x_2^{-\frac{1}{2}})(x_3^{\frac{1}{2}}-x_3^{-\frac{1}{2}})(x_7^{\frac{1}{2}}-x_7^{-\frac{1}{2}})}{x_1^{\frac{1}{2}}-x_1^{-\frac{1}{2}}} \sum_{\vec{n}\in\mathbb{Z}^3\times\mathbb{Z}} q^{-(\vec{n},M\vec{n})-(\vec{n},\vec{1})} x^{M\vec{n}+\frac{1}{2}\vec{1}} \frac{\sum_{\substack{k\in\mathbb{Z}\\ |k|>|n_1+6n_7+\frac{1}{2}|}} (-1)^k q^{\frac{k(3k-1)}{2}}}{(q)_\infty} \\
&= \oint \frac{dx_1}{2\pi i x_1}\frac{dx_2}{2\pi i x_2}\frac{dx_3}{2\pi i x_3}\frac{dx_7}{2\pi i x_7}\frac{(x_2^{\frac{1}{2}}-x_2^{-\frac{1}{2}})(x_3^{\frac{1}{2}}-x_3^{-\frac{1}{2}})(x_7^{\frac{1}{2}}-x_7^{-\frac{1}{2}})}{x_1^{\frac{1}{2}}-x_1^{-\frac{1}{2}}} \sum_{\vec{\ell}\in M\mathbb{Z}^4+\frac{1}{2}\vec{1}} q^{-(\vec{\ell},M^{-1}\vec{\ell})} \vec{x}^{\vec{\ell}} \frac{\sum_{\substack{k\in\mathbb{Z}\\ |k|>|((6,-3,-2,0),\vec{\ell})|}} (-1)^k q^{\frac{k(3k-1)}{2}}}{(q)_\infty} \\
&\cong \oint \frac{dx_1}{2\pi i x_1}\frac{1}{x_1^{\frac{1}{2}}-x_1^{-\frac{1}{2}}} \sum_{\epsilon_2,\epsilon_3,\epsilon_7=\pm 1}\sum_{\ell_1\in\mathbb{Z}+\frac{1}{2}} \epsilon_2\epsilon_3\epsilon_7\, q^{-42\ell_1^2+(21\epsilon_2+14\epsilon_3+6\epsilon_7)\ell_1-\frac{1}{2}(7\epsilon_2\epsilon_3+3\epsilon_2\epsilon_7+2\epsilon_3\epsilon_7)} x_1^{\ell_1} \frac{\sum_{\substack{k\in\mathbb{Z}\\ |k|>6|\ell_1-\frac{1}{2}(\frac{1}{2}\epsilon_2+\frac{1}{3}\epsilon_3)|}} (-1)^k q^{\frac{k(3k-1)}{2}}}{(q)_\infty} \\
&\cong \oint \frac{dx_1}{2\pi i x_1}\frac{1}{x_1^{\frac{1}{2}}-x_1^{-\frac{1}{2}}} \sum_{\epsilon_2,\epsilon_3,\epsilon_7=\pm 1}\sum_{\ell_1\in\mathbb{Z}+\frac{1}{2}} \epsilon_2\epsilon_3\epsilon_7\, q^{-42(\ell_1-\frac{1}{2}(\frac{1}{2}\epsilon_2+\frac{1}{3}\epsilon_3+\frac{1}{7}\epsilon_7))^2+\frac{1}{168}} x_1^{\ell_1} \frac{\sum_{\substack{k\in\mathbb{Z}\\ |k|>6|\ell_1-\frac{1}{2}(\frac{1}{2}\epsilon_2+\frac{1}{3}\epsilon_3+\frac{1}{7}\epsilon_7)|}} (-1)^k q^{\frac{3}{2}(k-\frac{1}{6})^2-\frac{1}{24}}}{(q)_\infty} \\
&= \oint \frac{dx_1}{2\pi i x_1}\frac{1}{x_1^{\frac{1}{2}}-x_1^{-\frac{1}{2}}} \sum_{\epsilon_2,\epsilon_3,\epsilon_7=\pm 1}\sum_{\ell_1\in\mathbb{Z}+\frac{1}{2}} \epsilon_2\epsilon_3\epsilon_7\, q^{-42(\ell_1-\frac{1}{2}(\frac{1}{2}\epsilon_2+\frac{1}{3}\epsilon_3+\frac{1}{7}\epsilon_7))^2+\frac{1}{168}} x_1^{\ell_1} \\
&\quad \times \frac{\sum_{\substack{k\in\mathbb{Z}\\ |k-\frac{1}{6}|>6|\ell_1-\frac{1}{2}(\frac{1}{2}\epsilon_2+\frac{1}{3}\epsilon_3+\frac{1}{7}\epsilon_7)|}} (-1)^k q^{\frac{3}{2}(k-\frac{1}{6})^2-\frac{1}{24}}}{(q)_\infty}.
\end{aligned}
$$

Comparing this last expression with (4.23), we see that a regularization factor has been added to the naive non-convergent expression. What this regularization factor is doing is clear: it first multiplies $(q)_\infty$ to both the numerator and the denominator, and then restricts the range of summation from the rank 2 indefinite lattice $(\ell_1, k) \in (\mathbb{Z}+\frac{1}{2})\times\mathbb{Z}$ to a double cone $|k-\frac{1}{6}| > 6|\ell_1 - \frac{1}{2}(\frac{1}{2}\epsilon_2 + \frac{1}{3}\epsilon_3 + \frac{1}{7}\epsilon_7)|$ where the lattice is positive definite.

Remark 4.2.2. While our expression of $\hat{Z}_{-\Sigma(2,3,7)}(q)$ is very similar to that of [CFS20], there is an important difference between the two. While we regularized the indefinite theta function by restricting it to a double cone, the authors of [CFS20] regularized it by restricting it to a one-sided cone $k - \frac{1}{6} > \frac{16}{3}|\ell_1 - \frac{1}{2}(\frac{1}{2}\epsilon_2 + \frac{1}{3}\epsilon_3 + \frac{1}{7}\epsilon_7)|$. The one-sided cone is slightly wider than the double cone, and they give the same answer. See Figure 4.1. We believe it is more natural to use a double cone instead of

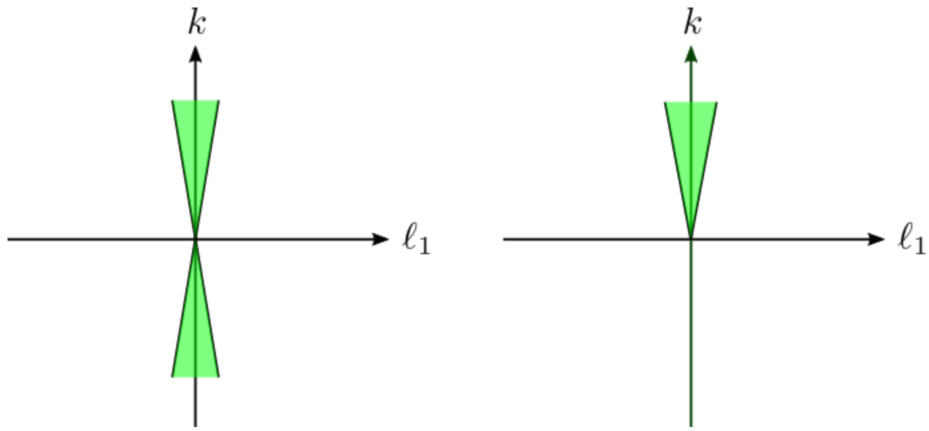

Figure 4.1: Double cone vs one-sided cone.

a one-sided cone since it comes naturally from the regularized surgery formula.

Example 4.2.3 $(-\Sigma(2,3,5))$**.** The 3-manifold $-\Sigma(2,3,5)$ has various descriptions, such as

$$-\Sigma(2,3,5) = M(-1; \frac{1}{2}, \frac{1}{3}, \frac{1}{5}) = S^3_{+1}(\mathbf{3}^r_1).$$

For us, the description as the $+1$-surgery on the right-handed trefoil is the most useful one. The naive plumbing formula gives

$$\hat{Z}_{-\Sigma(2,3,5)}(q) \text{``} \cong \text{''} \oint \frac{dx_1}{2\pi i x_1} \frac{dx_2}{2\pi i x_2} \frac{dx_3}{2\pi i x_3} \frac{dx_5}{2\pi i x_5} \frac{(x_2^{\frac{1}{2}} - x_2^{-\frac{1}{2}})(x_3^{\frac{1}{2}} - x_3^{-\frac{1}{2}})(x_5^{\frac{1}{2}} - x_5^{-\frac{1}{2}})}{x_1^{\frac{1}{2}} - x_1^{-\frac{1}{2}}}$$
$$\times \sum_{\vec{\ell} \in M\mathbb{Z}^4 + \frac{1}{2}\vec{1}} q^{-(\vec{\ell}, M^{-1}\vec{\ell})} \vec{x}^{\vec{\ell}},$$

where

$$M = \begin{pmatrix} -1 & 1 & 1 & 1 \\ 1 & -2 & 0 & 0 \\ 1 & 0 & -3 & 0 \\ 1 & 0 & 0 & -5 \end{pmatrix}.$$

Integrating out x_2, x_3, x_5, we get

$$\hat{Z}_{-\Sigma(2,3,5)}(q) \text{``} \cong \text{''} \oint \frac{dx_1}{2\pi i x_1} \frac{1}{x_1^{\frac{1}{2}} - x_1^{-\frac{1}{2}}} \sum_{\epsilon_2, \epsilon_3, \epsilon_5 = \pm 1} \sum_{\ell_1 \in \mathbb{Z} + \frac{1}{2}} \epsilon_2\epsilon_3\epsilon_5 \, q^{-30(\ell_1 - \frac{1}{2}(\frac{1}{2}\epsilon_2 + \frac{1}{3}\epsilon_3 + \frac{1}{5}\epsilon_5))^2 + \frac{1}{120}} x_1^{\ell_1}.$$

From the plumbing description of the right-handed trefoil knot, we have

$$F_{\mathbf{3}_1^r}(x,q) \cong \oint \frac{dx_1}{2\pi i x_1}\frac{dx_2}{2\pi i x_2}\frac{dx_3}{2\pi i x_3}\frac{(x_2^{\frac{1}{2}}-x_2^{-\frac{1}{2}})(x_3^{\frac{1}{2}}-x_3^{-\frac{1}{2}})}{x_1^{\frac{1}{2}}-x_1^{-\frac{1}{2}}}\sum_{\vec{n}\in\mathbb{Z}^3\times\{0\}} q^{-(\vec{n},M'\vec{n})-(\vec{n},\vec{1})}\vec{x}^{M'\vec{n}+\frac{1}{2}\vec{1}},$$

where

$$M' = \begin{pmatrix} -1 & 1 & 1 & 1 \\ 1 & -2 & 0 & 0 \\ 1 & 0 & -3 & 0 \\ 1 & 0 & 0 & -6 \end{pmatrix}.$$

Using the regularized $+1$-surgery formula, we can deduce an expression for $\hat{Z}(-\Sigma(2,3,5))$ in terms of a indefinite theta function, just like the way we obtained such an expression for $\hat{Z}_{-\Sigma(2,3,7)}(q)$. The result looks like

$$\hat{Z}_{-\Sigma(2,3,5)}(q) \cong \oint \frac{dx_1}{2\pi i x_1}\frac{1}{x_1^{\frac{1}{2}}-x_1^{-\frac{1}{2}}}\sum_{\epsilon_2,\epsilon_3,\epsilon_5=\pm1}\sum_{\ell_1\in\mathbb{Z}+\frac{1}{2}}\epsilon_2\epsilon_3\epsilon_5\, q^{-30(\ell_1-\frac{1}{2}(\frac{1}{2}\epsilon_2+\frac{1}{3}\epsilon_3+\frac{1}{5}\epsilon_5))^2+\frac{1}{120}}x_1^{\ell_1}$$
$$\times \frac{\sum_{\substack{k\in\mathbb{Z} \\ |k-\frac{1}{6}|>6|\ell_1-\frac{1}{2}(\frac{1}{2}\epsilon_2+\frac{1}{3}\epsilon_3+\frac{1}{5}\epsilon_5)|}}(-1)^k q^{\frac{3}{2}(k-\frac{1}{6})^2-\frac{1}{24}}}{(q)_\infty}.$$

Again, we see that the indefinite theta function is regularized by restricting the range of summation to a double cone $|k-\frac{1}{6}| > 6|(\ell_1-\frac{1}{2}(\frac{1}{2}\epsilon_2+\frac{1}{3}\epsilon_3+\frac{1}{5}\epsilon_5))|$.

Example 4.2.4 ($S^3_{-2}(\mathbf{4}_1)$)**.** The -2-surgery on the figure-eight knot is a Seifert manifold

$$S^3_{-2}(\mathbf{4}_1) = M(1;-\frac{1}{2},-\frac{1}{4},-\frac{1}{5}).$$

As a plumbed 3-manifold, the plumbing graph has the linking matrix

$$M = \begin{pmatrix} 1 & 1 & 1 & 1 \\ 1 & 2 & 0 & 0 \\ 1 & 0 & 4 & 0 \\ 1 & 0 & 0 & 5 \end{pmatrix}.$$

We have experimentally found the double cone, and the resulting expression for $\hat{Z}_{S^3_{-2}(\mathbf{4}_1)}(q)$ is given by

$$\hat{Z}_{S^3_{-2}(\mathbf{4}_1)}(q) \cong \oint \frac{dx_1}{2\pi i x_1}\frac{1}{x_1^{\frac{1}{2}}-x_1^{-\frac{1}{2}}}\sum_{\epsilon_2,\epsilon_4,\epsilon_5=\pm1}\sum_{\ell_1\in\mathbb{Z}+\frac{1}{2}}\epsilon_2\epsilon_4\epsilon_5\, q^{-\frac{40}{2}(\ell_1-\frac{1}{2}(\frac{1}{2}\epsilon_2+\frac{1}{4}\epsilon_4+\frac{1}{5}\epsilon_5))^2+\frac{1}{80}}x_1^{\ell_1}$$
$$\times \frac{\sum_{\substack{k\in\mathbb{Z} \\ |k-\frac{1}{6}|>4|\ell_1-\frac{1}{2}(\frac{1}{2}\epsilon_2+\frac{1}{4}\epsilon_4+\frac{1}{5}\epsilon_5)|}}(-1)^k q^{\frac{3}{2}(k-\frac{1}{6})^2-\frac{1}{24}}}{(q)_\infty}.$$

To separate the contribution of each b, we just need to add the characteristic function for the following condition:

$$\begin{pmatrix} \ell_1 \\ \epsilon_2 \\ \epsilon_4 \\ \epsilon_5 \end{pmatrix} \in M\mathbb{Z}^4 + b.$$

Example 4.2.5 ($S^3_{-3}(\mathbf{4}_1)$)**.** The -3-surgery on the figure-eight knot is a Seifert manifold

$$S^3_{-3}(\mathbf{4}_1) = M(1; -\frac{1}{3}, -\frac{1}{3}, -\frac{1}{4}).$$

As a plumbed 3-manifold, the plumbing graph has the linking matrix

$$M = \begin{pmatrix} 1 & 1 & 1 & 1 \\ 1 & 3 & 0 & 0 \\ 1 & 0 & 3 & 0 \\ 1 & 0 & 0 & 4 \end{pmatrix}.$$

We have experimentally found the double cone, and the resulting expression for $\hat{Z}_{S^3_{-3}(\mathbf{4}_1)}(q)$ is given by

$$\hat{Z}_{S^3_{-3}(\mathbf{4}_1)}(q) \cong \oint \frac{dx_1}{2\pi i x_1} \frac{1}{x_1^{\frac{1}{2}} - x_1^{-\frac{1}{2}}} \sum_{\epsilon_{3a}, \epsilon_{3b}, \epsilon_4 = \pm 1} \sum_{\ell_1 \in \mathbb{Z} + \frac{1}{2}} \epsilon_{3a}\epsilon_{3b}\epsilon_4 \, q^{-\frac{36}{3}(\ell_1 - \frac{1}{2}(\frac{1}{3}\epsilon_{3a} + \frac{1}{3}\epsilon_{3b} + \frac{1}{4}\epsilon_4))^2 + \frac{1}{48}} x_1^{\ell_1}$$
$$\times \frac{\sum_{\substack{k \in \mathbb{Z} \\ |k - \frac{1}{6}| > 3|\ell_1 - \frac{1}{2}(\frac{1}{3}\epsilon_{3a} + \frac{1}{3}\epsilon_{3b} + \frac{1}{4}\epsilon_4)|}} (-1)^k q^{\frac{3}{2}(k - \frac{1}{6})^2 - \frac{1}{24}}}{(q)_\infty}.$$

To separate the contribution of each b, we just need to add the characteristic function for the following condition:

$$\begin{pmatrix} \ell_1 \\ \epsilon_{3a} \\ \epsilon_{3b} \\ \epsilon_4 \end{pmatrix} \in M\mathbb{Z}^4 + b.$$

Example 4.2.6 ($-\Sigma(2,3,7)$ with another degree 3 node)**.** As our last example, let's see what happens to the regularization factor if we create a new degree 3 node to the plumbing graph of $-\Sigma(2,3,7)$ by applying Neumann moves twice. The linking matrix of the resulting plumbing graph is

$$M = \begin{pmatrix} 1 & 1 & 1 & 1 & 0 & 0 \\ 1 & 2 & 0 & 0 & 0 & 0 \\ 1 & 0 & 3 & 0 & 0 & 0 \\ 1 & 0 & 0 & 5 & 1 & 1 \\ 0 & 0 & 0 & 1 & -1 & 0 \\ 0 & 0 & 0 & 1 & 0 & -1 \end{pmatrix}.$$

As a result, after multiplying $(q)_\infty$ in both the numerator and the denominator, the indefinite theta function is of signature $+, -, -$. With a bit of experimenting, we found an appropriate double cone, and the resulting expression is given below

$$\begin{aligned}\hat{Z}_{-\Sigma(2,3,7)}(q) \cong \oint \frac{dx_1}{2\pi i x_1}\frac{dx_5}{2\pi i x_5}\frac{1}{x_1^{\frac{1}{2}} - x_1^{-\frac{1}{2}}}\frac{1}{x_5^{\frac{1}{2}} - x_5^{-\frac{1}{2}}} \sum_{\epsilon_2,\epsilon_3,\epsilon_{-1a},\epsilon_{-1b}=\pm 1} \sum_{\ell_1,\ell_5\in\mathbb{Z}+\frac{1}{2}} \epsilon_2\epsilon_3\epsilon_{-1a}\epsilon_{-1b} \\ \times q^{(\ell_1-\frac{1}{2}(\frac{1}{2}\epsilon_2+\frac{1}{3}\epsilon_3),\ell_5-\frac{1}{2}(-\epsilon_{-1a}-\epsilon_{-1b}))\cdot\begin{pmatrix}-42 & 6\\ 6 & -1\end{pmatrix}\cdot(\ell_1-\frac{1}{2}(\frac{1}{2}\epsilon_2+\frac{1}{3}\epsilon_3),\ell_5-\frac{1}{2}(-\epsilon_{-1a}-\epsilon_{-1b}))^t+\frac{1}{24}} \\ \times x_1^{\ell_1}x_5^{\ell_5}\frac{\sum_{\substack{k\in\mathbb{Z} \\ |k-\frac{1}{6}|>6|\ell_1-\frac{1}{2}(\frac{1}{2}\epsilon_2+\frac{1}{3}\epsilon_3)| \\ |k-\frac{1}{6}|>|\ell_5-\frac{1}{2}(-\epsilon_{-1a}-\epsilon_{-1b})|}} (-1)^k q^{\frac{3}{2}(k-\frac{1}{6})-\frac{1}{24}}}{(q)_\infty}.\end{aligned}$$

That is, the double cone is determined by the two inequalities $|k-\frac{1}{6}| > 6|\ell_1 - \frac{1}{2}(\frac{1}{2}\epsilon_2 + \frac{1}{3}\epsilon_3)|$ and $|k - \frac{1}{6}| > |\ell_5 - \frac{1}{2}(-\epsilon_{-1a} - \epsilon_{-1b})|$. Compare this with Example 4.2.1. It is a very interesting problem to study how the double cone behaves under Neumann moves in general.

Chapter 5

HIGHER RANK

The $\hat{Z}$ we considered in the previous chapters was implicitly $\hat{Z}^{\mathfrak{g}}$ for $\mathfrak{g} = \mathfrak{sl}_2$. In this chapter, which is based on [Par20a], we study the dependence of $\hat{Z}$ on the choice of Lie algebra $\mathfrak{g}$ by studying $\hat{Z}^{\mathfrak{g}}$ for general Lie algebra. In particular, we will give explicit formulas for $\hat{Z}^{\mathfrak{g}}$ for negative definite plumbed 3-manifolds and $F_K^{\mathfrak{g}}$ for torus knot complements.

As we will see, $F_K^{\mathfrak{sl}_N}(x,q)$ behaves regularly under change of N, which suggests that there should be a three-variable series $F_K(x,a,q)$ that interpolates all the $F_K^{\mathfrak{sl}_N}(x,q)$'s, analogously to how the HOMFLY-PT polynomial interpolates all the $SU(N)$ Jones polynomials. This three-variable series has a natural interpretation in terms of topological strings, which is the topic of the next chapter.

Notations

Throughout this chapter, $\mathfrak{g}$ is a complex semisimple Lie algebra with the root system $\Delta \subset \mathfrak{h}^*$, $Q \subset \mathfrak{h}^*$ is the root lattice, $Q^\vee \subset \mathfrak{h}$ is the coroot lattice, $P \subset \mathfrak{h}^*$ is the weight lattice, W is the Weyl group, Δ^+ is the set of positive roots, ρ denotes the Weyl vector (half-sum of positive roots), and the letters α and ω will be reserved for roots and fundamental weights. The inner product $(\cdot,\cdot)$ on $\mathfrak{h}^*$ is the standard one normalized such that $(\alpha,\alpha) = 2$ for short roots α. The length of a Weyl group element $w \in W$ will be denoted by $l(w)$. We use the letter B for the linking matrix of a plumbed 3-manifold, and $\sigma = \sigma(B)$ and $\pi = \pi(B)$ denote the signature and the number of positive eigenvalues of B, respectively. For a multi-index monomial, we use the following notation for any $\beta \in P$:

$$x^\beta := \prod_{1\leq j\leq r} x_j^{(\beta,\omega_j)},$$

where $r = \operatorname{rank} \mathfrak{g}$. When it comes to q-series, often we do not bother to fix the overall power of q, and just use the notation $\cong$ for equivalence up to sign and overall power of q.

5.1 Higher rank $\hat{Z}$

The set of labels $\mathcal{B}$

Before getting into the definition of $\hat{Z}_b^{\mathfrak{g}}$ for negative definite plumbings, we have to first describe what the labels b are. Recall that, in case of $\mathfrak{g} = \mathfrak{sl}_2$, these labels b were Spin^c-structures, at least for plumbings on trees, as clarified by [GM21]. Likewise, for a general Lie algebra $\mathfrak{g}$, $\hat{Z}^{\mathfrak{g}}$ will be an invariant of 3-manifolds decorated by structures analogous to Spin^c-structures.

Definition 5.1.1. For a plumbed 3-manifold $Y = Y(\Gamma)$, define

$$\mathcal{B}^{\mathfrak{g}}(Y) := (Q^V + \delta)/BQ^V, \tag{5.1}$$

where $V = V(\Gamma)$ is the set of vertices, and $\delta_v = (2 - \deg v)\rho$.

This is essentially a generalization of Spin^c-structures, in a sense that $\mathcal{B}^{\mathfrak{sl}_2}(Y) \cong \mathrm{Spin}^c(Y)$ canonically. Recall that $\mathrm{Spin}^c(Y)$ is affinely isomorphic to $H^2(Y)$ and admits a $\mathbb{Z}_2$ action by conjugation. Similarly, two of the main features of $\mathcal{B}^{\mathfrak{g}}(Y)$ are that it is affinely isomorphic to $H^2(Y; Q)$ and that it admits an action by the Weyl group W (and hence carries an action by $H^2(Y; Q) \rtimes W$).

Higher rank $\hat{Z}$ for negative definite plumbings

We present here a formula for $\hat{Z}$ for negative definite plumbed 3-manifolds, for arbitrary semisimple Lie algebra $\mathfrak{g}$.

Definition 5.1.2 ([Par20a])**.** For a negative definite plumbed 3-manifold $Y = Y(\Gamma)$ and a choice of $b \in \mathcal{B}^{\mathfrak{g}}(Y)$, define

$$\hat{Z}^{\mathfrak{g}}_{Y,b}(q) := q^{-\frac{3s+\sum_v m_v}{2}(\rho,\rho)} \oint \prod_{\substack{v\in V\\ 1\le j\le r}} \frac{dx_{vj}}{2\pi i x_{vj}} \left(\sum_{w\in W} (-1)^{l(w)} x_v^{w(\rho)}\right)^{2-\deg v} \Theta_b^{-B}(x,q), \tag{5.2}$$

where

$$\Theta_b^{-B}(x,q) := \sum_{\ell\in BQ^V+b} q^{-\frac{1}{2}(\ell, B^{-1}\ell)} \prod_{v\in V} x_v^{-\ell_v}. \tag{5.3}$$

In particular, in case $\mathfrak{g} = \mathfrak{sl}_N$, this takes the following simple form:

$$\hat{Z}^{\mathfrak{sl}_N}_{Y,b}(q) = q^{-\frac{3s+\sum_v m_v}{2}\frac{N^3-N}{12}} \oint \prod_{\substack{v\in V\\ 1\le j\le N-1}} \frac{dx_{vj}}{2\pi i x_{vj}} F_{3d}(x)\Theta^b_{2d}(x,q) \tag{5.4}$$

with

$$F_{3d}(x) := \prod_{v\in V}\left(\sum_{w\in W}(-1)^{l(w)}\prod_{1\le j\le N-1} x_{vj}^{(\omega_j,w(\rho))}\right)^{2-\deg v}$$

$$= \prod_{v\in V}\left(\prod_{1\le j<k\le N}(y_{vj}^{1/2}y_{vk}^{-1/2} - y_{vj}^{-1/2}y_{vk}^{1/2})\right)^{2-\deg v}, \tag{5.5}$$

$$\Theta_{2d}^{b}(x,q) := \sum_{\ell\in BQ^V+b} q^{-\frac{1}{2}(\ell,B^{-1}\ell)}\prod_{v\in V}\prod_{1\le j\le N-1} x_{vj}^{-(\omega_j,\ell_v)}, \tag{5.6}$$

where $x_j = \frac{y_j}{y_{j+1}}$.

Here the contour integral is the principal value integral. That is, taking the average over W number of deformed contours, each corresponding to a Weyl chamber. For instance, for $\mathfrak{g} = \mathfrak{sl}_N$, the deformed contour corresponding to a permutation $\sigma \in W = S_N$ is given by

$$|y_{\sigma(1)}| < |y_{\sigma(2)}| < \cdots < |y_{\sigma(N)}|. \tag{5.7}$$

In practice, this means that there are W number of ways to expand the integrand into power series, and the contour integral simply picks out the constant term in the average of these power series.

Theorem 5.1.3. *The q-series $\hat{Z}^{\mathfrak{g}}_{Y,b}$ defined above is invariant under Neumann moves, and therefore it is a well-defined invariant for negative definite plumbed 3-manifolds.*

Proof. For negative definite plumbed 3-manifolds, there are two types of Neumann moves we need to consider: Type A move, which is the first move in Figure 2.4 with minus signs, and Type B move, which is the second move in Figure 2.4 with minus signs.

Consider the Type A move. Under this move $-3s - \sum_v m_v$ remains unchanged. The contribution of the vector $\ell = (\vec{\ell}_l, 0, \vec{\ell}_r)$ for the top graph to the theta function is the same as the contribution of the vector $\ell' = (\vec{\ell}_l, \vec{\ell}_r)$ for the bottom graph. That is,

$$(\ell, B^{-1}\ell) = (\ell', B'^{-1}\ell'). \tag{5.8}$$

Hence $\hat{Z}^{\mathfrak{g}}$ is invariant under the Type A Neumann move.

Consider the Type B move. Under this move, $-3s - \sum_v m_v$ increases by 1. The contribution of the vector $\ell = (\vec{\ell}_l, \ell_0, w(\rho))$ for the top graph is related to that of the vector $\ell' = (\vec{\ell}_l, \ell_0 + w(\rho))$ for the bottom graph via

$$(\ell, B^{-1}\ell) = (\ell', B'^{-1}\ell') - (\rho, \rho).$$

The extra factor of $q^{-\frac{(\rho,\rho)}{2}}$ due to this change is cancelled out by the change in $q^{-\frac{3s+\sum_v m_v}{2}(\rho,\rho)}$. Hence $\hat{Z}^{\mathfrak{g}}$ is invariant under the Type B Neumann move as well. □

Some examples and higher rank false theta functions

It turns out, in many examples, $\hat{Z}^{\mathfrak{g}}$ can be written in terms of higher rank false theta functions.

Definition 5.1.4. For $p \in \mathbb{Z}_{>0}$ and $\beta \in P$, define the corresponding *higher rank false theta function* to be

$$\chi^{\mathfrak{g}}_{p,\beta}(q) := \sum_{\ell \in P_+ \cap (Q+\rho)} N_\ell \sum_{w \in W} (-1)^{l(w)} q^{\frac{1}{2}||\sqrt{p}\ell - \frac{1}{\sqrt{p}} w(\beta)||^2}, \tag{5.9}$$

where

$$N_\ell := \sum_{w \in W} (-1)^{l(w)} K(w(\ell)), \tag{5.10}$$

and $K(\beta)$ denotes the Kostant partition function.[1]

When $\mathfrak{g} = \mathfrak{sl}_2$, this becomes

$$\chi^{\mathfrak{sl}_2}_{p,n\rho}(q) = \Psi_{p,p-n}(q), \text{ for } n = 1, \cdots, p-1, \tag{5.11}$$

where

$$\Psi_{p,r}(q) := \sum_{\substack{\ell \in \mathbb{Z} \\ \ell = r \bmod 2p}} \operatorname{sign}(\ell)\, q^{\ell^2/4p} \tag{5.12}$$

is the usual false theta function, and in this sense $\chi^{\mathfrak{g}}_{p,\beta}$ is the higher rank generalization of the false theta functions.

$Y = S^3_0(K_n)$

The 0-surgery on twist knots are probably the simplest examples. They admit simple plumbing diagrams given in Figure 5.1.[2] For instance,

[1] For example, N_ℓ is $\operatorname{sgn}((\ell, \alpha_1))$ for $\mathfrak{sl}_2$, and $\operatorname{sgn}(\prod_{\alpha \in \Delta_+}(\ell, \alpha)) \min\{|(\ell, \alpha_1)|, |(\ell, \alpha_2)|\}$ for $\mathfrak{sl}_3$.

[2] Although we have assumed for simplicity in Definition 5.1.2 that the plumbing graph is a tree, we can extend this definition to plumbings with loops, as in [Chu+20].

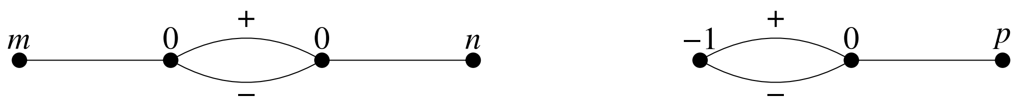

Figure 5.1: Plumbing diagrams for the 0-surgery on $K_{m,n}$ and $K_p = K_{1,p}$.

$\mathfrak{g}$	$\hat{Z}_{S^3_0(\mathbf{5}_2)}(q) \cong$
$\mathfrak{sl}_2$	$\frac{1}{2!}(1 - q + q^3 - q^6 + q^{10} - q^{15} + q^{21} - q^{28} + q^{36} - q^{45} + q^{55} - q^{66} + q^{78} - \cdots)$
$\mathfrak{sl}_3$	$\frac{1}{3!}(1 - 2q + 2q^3 + q^4 - 4q^6 + 2q^9 + 2q^{10} + q^{12} - 2q^{13} - 4q^{15} + 2q^{18} + 2q^{19} + \cdots)$
$\mathfrak{sl}_4$	$\frac{1}{4!}(1 - 3q + q^2 + 4q^3 - 2q^4 + q^5 - 5q^6 - 2q^7 + 3q^8 + 2q^9 + 9q^{10} - 2q^{11} - \cdots)$
$\mathfrak{sl}_5$	$\frac{1}{5!}(1 - 4q + 3q^2 + 6q^3 - 7q^4 - 2q^5 + 2q^7 - 2q^8 + 6q^9 + 15q^{10} - 12q^{11} - 23q^{12} + \cdots)$

Indeed, for every positive twist knot K_p the following is easy to deduce from (5.2).

Proposition 5.1.5. *For the* 0*-surgery on the twist knot* K_p*, its* $\hat{Z}^{\mathfrak{g}}$ *is given by*

$$\hat{Z}^{\mathfrak{g}}_{S^3_0(K_p)}(q) \cong \frac{1}{|W|}\chi_{p,\rho} = \frac{1}{|W|}\sum_{\ell \in P_+ \cap (Q+\rho)} N_\ell \sum_{w\in W} (-1)^{l(w)} q^{\frac{1}{2}||\sqrt{p}\ell - \frac{1}{\sqrt{p}}w(\rho)||^2}. \quad (5.13)$$

Note that $\chi_{p,\rho}$ is exactly the higher rank false theta function (a character of the log-VOA $W^0(p)_Q$) given in [BM17, equation (1.2)]! Similarly for double twist knots $K_{m,n}$ with $m, n > 0$,[3]

$$\hat{Z}^{\mathfrak{g}}_{S^3_0(K_{m,n})}(q) \cong \frac{1}{|W|}\chi_{m,\rho}\chi_{n,\rho}. \quad (5.14)$$

Proof of Proposition 5.1.5. The 0-surgery on K_p has a simple plumbing description as shown in Figure 5.1. The linking matrix and its inverse are

$$B = \begin{pmatrix} -1 & 0 & 0 \\ 0 & 0 & 1 \\ 0 & 1 & p \end{pmatrix} \quad , \quad B^{-1} = \begin{pmatrix} -1 & 0 & 0 \\ 0 & -p & 1 \\ 0 & 1 & 0 \end{pmatrix}.$$

There is a single trivalent vertex with 0 framing. This contributes the following factor in $F_{3d}(x)$:

$$\left(\sum_{w\in W} (-1)^{l(w)} x_0^{w(\rho)}\right)^{-1} = \frac{1}{|W|}\sum_{\ell_0 \in P_+ \cap (Q+\rho)} N_{\ell_0} \sum_{w \in W} (-1)^{l(w)} x_0^{w(\ell_0)}.$$

For $\ell = (0, \ell_0, \ell_p)^t$,

$$q^{-\frac{1}{2}(\ell, B^{-1}\ell)} = q^{\frac{1}{2}||\sqrt{p}\ell_0 - \frac{1}{\sqrt{p}}\ell_p||^2 - \frac{1}{2p}||\ell_p||^2}.$$

[3]In our notation, $K_{m,n}$ denotes the double twist knot with m and n full twists.

Applying (5.2), it is straightforward to get (5.13).

Using a plumbing description of the 0-surgery on $K_{m,n}$ (Figure 5.1), it is easy to derive (5.14) as well. □

$Y = \Sigma(p_1, p_2, p_3)$

Proposition 5.1.6. *For the Brieskorn sphere $Y = \Sigma(p_1, p_2, p_3)$ with $0 < p_1 < p_2 < p_3$ pairwise relatively prime, we have*

$$\hat{Z}^{\mathfrak{g}}_{\Sigma(p_1,p_2,p_3)}(q) \cong \sum_{(w_1,w_2)\in W^2} (-1)^{l(w_1 w_2)} \chi_{p_1p_2p_3, p_2p_3\rho + p_1p_3 w_1(\rho) + p_1p_2 w_2(\rho)}. \tag{5.15}$$

That is, it is a sum of $|W|^2$ number of higher rank false theta functions.[4]

Proof. The proof is analogous to that of [GM21, Proposition 4.8]. □

Note that we did not have to treat $\Sigma(2, 3, 5)$ separately. In this sense, using $\chi_{p,\beta}$ as false theta functions is more natural than using $\Psi_{p,n}$.

$Y = M(a_0; \frac{a_1}{b_1}, \frac{a_2}{b_2}, \frac{a_3}{b_3})$

Let $b_1, b_2, b_3 > 0$ and assume that Y has negative orbifold number; i.e.,

$$e = a_0 + \sum_{j=1}^{3} \frac{a_j}{b_j} < 0. \tag{5.16}$$

Assume further that the central meridian is trivial in homology; i.e.,

$$e \operatorname{lcm}(b_1, b_2, b_3) = -1. \tag{5.17}$$

Then their $\hat{Z}_b$'s can be expressed as signed sum of higher rank false theta functions:

Proposition 5.1.7. *Under the assumptions as above, $\hat{Z}^{\mathfrak{g}}$ for $Y = M(a_0; \frac{a_1}{b_1}, \frac{a_2}{b_2}, \frac{a_3}{b_3})$ is given by*

$$\hat{Z}^{\mathfrak{g}}_{M(a_0;\frac{a_1}{b_1},\frac{a_2}{b_2},\frac{a_3}{b_3}),b}(q) \cong \sum_{(w_1,w_2)\in W^2} \mathbf{1}_b(w_1,w_2)(-1)^{l(w_1w_2)} \chi_{\frac{b_1b_2b_3}{|H_1|}, \frac{b_2b_3}{|H_1|}\rho + \frac{b_1b_3}{|H_1|}w_1(\rho) + \frac{b_1b_2}{|H_1|}w_2(\rho)}, \tag{5.18}$$

where

$$\mathbf{1}_b(w_1, w_2) := \begin{cases} 1 & \text{if } \ell(\rho, \rho, w_1(\rho), w_2(\rho)) \in BQ^V + b, \\ 0 & \text{otherwise.} \end{cases} \tag{5.19}$$

[4] That $\hat{Z}$'s for Brieskorn spheres should be expressed as sums of higher rank false theta functions was envisaged earlier in [Che+19].

Observe that Proposition 5.1.7 is a slight generalization of Proposition 5.1.6.

Proof. Since Y is a Seifert manifold with 3 singular fibers, it can be described as a star-shaped plumbing with 3 legs. The only vertices whose degree is not 2 are the central vertex and the terminal vertices. Denote by $\ell(\ell_0, \ell_1, \ell_2, \ell_3)$ an element $\ell \in BQ^V + b$ such that

$$\ell_v = \begin{cases} \ell_0 & v \text{ is the central vertex,} \\ \ell_1, \ell_2, \ell_3 & v \text{ is the corresponding terminal vertex,} \\ 0 & \text{otherwise.} \end{cases}$$

Then for any ℓ with $\ell_1, \ell_2, \ell_3 \in W(\rho)$,

$$q^{-\frac{1}{2}(\ell, B^{-1}\ell)} = q^{\frac{1}{2|H_1|}||\sqrt{b_1 b_2 b_3}\ell_0 - \frac{1}{\sqrt{b_1 b_2 b_3}}(b_2 b_3 \ell_1 + b_3 b_1 \ell_2 + b_1 b_2 \ell_3)||^2 + C}$$

for some constant C independent of ℓ. Applying (5.2), it is straightforward to obtain (5.18). Note that the assumption $e \operatorname{lcm}(b_1, b_2, b_3) = -1$ was introduced so that

$$\ell(\rho, \rho, w_1(\rho), w_2(\rho)) \in BQ^V + b \Leftrightarrow \ell(\rho + Q, \rho, w_1(\rho), w_2(\rho)) \in BQ^V + b.$$

□

Remark 5.1.8. It is possible to drop the assumption on the Euler number. Then we get up to $|W|^3$ false theta functions with modulus $e \operatorname{lcm}(b_1, b_2, b_3)^2$.[5]

5.2 Higher rank F_K

Higher rank F_K

Let us study the higher rank generalization of $F_K(x, q)$. As a natural generalization of Conjecture 2.2.11, we make the following conjecture.

Conjecture 5.2.1. *For any knot K and a choice of a semisimple Lie algebra $\mathfrak{g}$, there exists a series*

$$F_K^{\mathfrak{g}}(\mathbf{x}, q) = \frac{1}{|W|} \sum_{\beta \in P_+ \cap (Q+\rho)} f_\beta^{\mathfrak{g}}(q) \sum_{w \in W} (-1)^{l(w)} x^{w(\beta)}. \tag{5.20}$$

where $\mathbf{x} = (x_1, \cdots, x_r)$ and the coefficients $f_\beta^{\mathfrak{g}}(q)$ are Laurent series with integer coefficients, such that its asymptotic expansion agrees with the higher rank Melvin-Morton-Rozansky expansion for the higher rank colored Jones polynomials:

$$F_K^{\mathfrak{g}}(\mathbf{x}, e^\hbar) = \prod_{\alpha \in \Delta^+} (x^{\frac{\alpha}{2}} - x^{-\frac{\alpha}{2}}) \sum_{j \geq 0} \frac{P_j(\mathbf{x})}{\prod_{\alpha \in \Delta^+} \Delta_K(x^\alpha)^{2j+1}} \frac{\hbar^j}{j!} \tag{5.21}$$

[5] I thank Josef Svoboda for pointing this out.

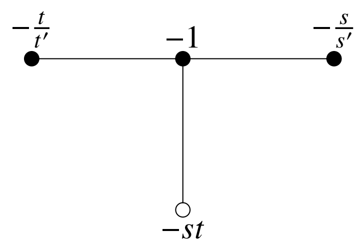

Figure 5.2: Plumbing diagram of the complement of $T_{s,t}$.

where $P_j(\mathbf{x}) \in \mathbb{Z}[x_1, x_1^{-1}, \cdots, x_r, x_r^{-1}]$ *and* $P_0 = 1$. *In particular, in the classical limit we should have*

$$\lim_{q\to 1} F_K^{\mathfrak{g}}(\mathbf{x}, q) = \prod_{\alpha\in\Delta^+} \frac{x^{\frac{\alpha}{2}} - x^{-\frac{\alpha}{2}}}{\Delta_K(x^\alpha)}. \tag{5.22}$$

Moreover, this series should be annihilated by the (higher rank) quantum A-polynomial:

$$\hat{A}_K(\hat{x}_1, \hat{y}_1, \cdots, \hat{x}_r, \hat{y}_r) F_K^{\mathfrak{g}}(\mathbf{x}, q) = 0. \tag{5.23}$$

Our main result in this section is an explicit expression for $F_K^{\mathfrak{g}}(\mathbf{x}, q)$ for torus knots.

Theorem 5.2.2 ([Par20a])**.** *For* $K = T_{s,t}$, $f_\beta^{\mathfrak{g}}(q)$ *is a monomial of degree* $\frac{(\beta,\beta)}{2st}$, *up to an overall* q*-power. More precisely,*

$$\begin{aligned} F_{T_{s,t}}^{\mathfrak{g}} \cong \frac{1}{|W|} & \sum_{\beta\in P_+\cap(Q+\rho)} \sum_{w\in W} (-1)^{l(w)} x^{w(\beta)} \\ & \times \sum_{(w_1,w_2)\in W^2} (-1)^{l(w_1w_2)} \mathbf{1}(\beta, w_1, w_2) N_{\frac{1}{st}(\beta+tw_1(\rho)+sw_2(\rho))} q^{\frac{(\beta,\beta)}{2st}}, \end{aligned} \tag{5.24}$$

where

$$\mathbf{1}(\beta, w_1, w_2) := \begin{cases} 1 & \text{if } \frac{1}{st}(\beta + tw_1(\rho) + sw_2(\rho)) \in P_+ \cap (Q+\rho), \\ 0 & \text{otherwise.} \end{cases} \tag{5.25}$$

Proof. This can be derived either directly from (5.2) by using plumbing description or by reverse-engineering using the higher rank surgery formula that we discuss below. Here we present a direct derivation. Recall from [GM21] that the complement of $T_{s,t}$ has a plumbing description as in Figure 5.2, where $0 < t' < t$, $0 < s' < s$ are chosen such that $st' \equiv -1 (\mathrm{mod}\ t)$ and $ts' \equiv -1 (\mathrm{mod}\ s)$. The linking matrix is

$$B = \begin{pmatrix} -st & 1 & 0 & 0 \\ 1 & -1 & 1 & 1 \\ 0 & 1 & (-\frac{t}{t'}) & 0 \\ 0 & 1 & 0 & (-\frac{s}{s'}) \end{pmatrix},$$

where $(-\frac{t}{t'})$ and $(-\frac{s}{s'})$ should be understood as block matrices corresponding to the continued fractions. To compute the integral (5.2) with x_{-st} left unintegrated, we just have to replace the theta function $\Theta^{-B}(x^{-1},q)$ with

$$\Theta^{-B'}(x^{-1},q) \cong \sum_{\alpha\in Q^{V'}} q^{-\frac{1}{2}(\alpha,B'\alpha)-(\alpha,\delta)} \prod_{v\in V'} x_v^{-(B'\alpha+\delta)} \cdot x_{-st}^{-\alpha_{-1}-\rho},$$

where $V' = V \setminus \{v_{-st}\}$ and B' is the corresponding sub-linking matrix. Set $\beta = -\alpha_{-1}-\rho$. We need to multiply $\Theta^{-B'}(x^{-1},q)$ with

$$\prod_{v\in V'} \left(\sum_{w\in W} (-1)^{l(w)} x_v^{w(\rho)} \right)^{2-\deg v}$$

and take the constant term with respect to variables x_v, $v \in V'$. As $2-\deg v$ is non-zero for only 3 vertices (the central vertex v_{-1} and the 2 terminal vertices) it is pretty easy to compute. The only contributions come from those α's such that $B'\alpha+\delta$ takes values $w_1(\rho), w_2(\rho)$ on the terminal vertices for some $w_1, w_2 \in W$, a value in $Q+\rho$ in the central vertex, and 0 on all the other vertices. Using simple linear algebra, it is easy to check that for those α's,

$$q^{-\frac{1}{2}(\alpha,B'\alpha)-(\alpha,\delta)} = q^{\frac{(\beta,\beta)}{2st}+C}$$

for some constant C independent of α, and that $\frac{1}{st}(\beta+tw_1(\rho)+sw_2(\rho))$ is the value of $B'\alpha+\delta$ on the central vertex. This proves (5.24). □

Example 5.2.3. Right-handed trefoil with $G = \mathfrak{sl}_3$. The first few $f_\beta^{\mathfrak{sl}_3}$ are (up to overall sign and q-power)

$$\begin{aligned} &f_{(1,1)} = -q, \quad f_{(4,1)} = -q^2, \quad f_{(5,2)} = -2q^3, \quad f_{(7,1)} = -q^4, \quad f_{(5,5)} = q^5, \\ &f_{(7,4)} = 2q^6, \quad f_{(10,1)} = -q^7, \quad f_{(8,5)} = q^8, \quad f_{(11,2)} = -2q^9, \quad f_{(7,7)} = -q^9, \\ &f_{(13,1)} = -q^{11}, \quad f_{(11,5)} = q^{12}, \quad \cdots, \end{aligned} \tag{5.26}$$

where we have written β in the fundamental weights basis. (Because $f_{(m,n)} = f_{(n,m)}$, we have only written those terms with $m \geq n$.) The q-power of this f_β is, up to overall constant,

$$\frac{(\beta,\beta)}{12}. \tag{5.27}$$

In the $q \to 1$ limit we have, as expected,

$$F^{\mathfrak{sl}_3}_{\mathbf{3}_1^r}(x_1,x_2,1) = \frac{x_1^{1/2}-x_1^{-1/2}}{x_1+x_1^{-1}-1}\frac{x_2^{1/2}-x_2^{-1/2}}{x_2+x_2^{-1}-1}\frac{x_1^{1/2}x_2^{1/2}-x_1^{-1/2}x_2^{-1/2}}{x_1x_2+x_1^{-1}x_2^{-1}-1}. \tag{5.28}$$

We conjecture the following surgery formula analogous to [GM21, Conjecture 1.7] relating $F_K^{\mathfrak{g}}$ to $\hat{Z}^{\mathfrak{g}}_{S^3_{p/r}(K),b}(q)$:

Conjecture 5.2.4 (Higher rank surgery formula)**.** *Let $K \subset S^3$ be a knot. Then*

$$\hat{Z}^{\mathfrak{g}}_{S^3_{p/r}(K),b}(q) \cong \mathcal{L}^{(b)}_{p/r}\left[\prod_{\alpha\in\Delta^+}(x^{\frac{\alpha}{2r}} - x^{-\frac{\alpha}{2r}})F_K^{\mathfrak{g}}(\mathbf{x},q)\right] \tag{5.29}$$

whenever $-\frac{r}{p}$ is big enough so that the right-hand side converges.

This is a theorem for knots and 3-manifolds represented by negative-definite plumbings, as a straightforward generalization of Theorem 1.2 of [GM21]. For instance, surgery on $\mathbf{3}_1^r$ gives us the following $\hat{Z}^{\mathfrak{sl}_3}$'s:

r	$S^3_{-1/r}(\mathbf{3}_1^r)$	$\hat{Z}^{\mathfrak{sl}_3}_{S^3_{-1/r}(\mathbf{3}_1^r)}(q)$
1	$\Sigma(2,3,7)$	$1-2q+2q^3+q^4-2q^5-2q^8+4q^9+2q^{10}-4q^{11}+2q^{13}-6q^{14}+\cdots$
2	$\Sigma(2,3,13)$	$1-2q+2q^3-q^4+2q^{10}-2q^{11}-2q^{14}+2q^{16}+2q^{19}-2q^{20}+4q^{21}-\cdots$
3	$\Sigma(2,3,19)$	$1-2q+2q^3-q^4+2q^{16}-2q^{17}-2q^{20}+2q^{22}+2q^{25}-2q^{26}+4q^{33}-\cdots$
4	$\Sigma(2,3,25)$	$1-2q+2q^3-q^4+2q^{22}-2q^{23}-2q^{26}+2q^{28}+2q^{31}-2q^{32}+4q^{45}-\cdots$
5	$\Sigma(2,3,31)$	$1-2q+2q^3-q^4+2q^{28}-2q^{29}-2q^{32}+2q^{34}+2q^{37}-2q^{38}+4q^{57}-\cdots$
r	$\Sigma(2,3,6r+1)$	$\sum_{(w_1,w_2)\in W^2}(-1)^{l(w_1w_2)}\chi_{36r+6,3(6r+1)w_1(\rho)+2(6r+1)w_2(\rho)+6\rho}$

In fact it is easy to check that for $K = T_{s,t}$,

$$\begin{aligned}
&\mathcal{L}_{-1/r}\left[\prod_{\alpha\in\Delta^+}(x^{\frac{\alpha}{2r}} - x^{-\frac{\alpha}{2r}})F_K(\mathbf{x},q)\right]\\
&\cong \sum_{(w_1,w_2)\in W^2}(-1)^{l(w_1w_2)}\chi_{st(rst+1),t(rst+1)w_1(\rho)+s(rst+1)w_2(\rho)+st\rho}(q)\\
&\cong \hat{Z}^{\mathfrak{g}}_{\Sigma(s,t,rst+1)}(q),
\end{aligned}$$

which is consistent with what we have seen in Proposition 5.1.6.

5.3 Symmetric representations and large N

Specialization to symmetric representations

In this section we study a specialization of $F_K^{\mathfrak{g}}(\mathbf{x},q)$ to symmetric representations. We restrict our attention to $\mathfrak{g} = \mathfrak{sl}_N$. We start from the reduced version of F_K:

$$F_K^{\mathrm{red}}(\mathbf{x},q) := \frac{1}{|W|}\sum_{\beta\in P_+\cap(Q+\rho)} f_\beta(q)\frac{\sum_{w\in W}(-1)^{l(w)}x^{w(\beta)}}{\sum_{w\in W}(-1)^{l(w)}x^{w(\rho)}}. \tag{5.30}$$

Then the (reduced) symmetrically colored F_K corresponds to the following specialization:

$$F_K^{\mathrm{sym}}(x,q) := F_K^{\mathrm{red}}((x,q,\cdots,q),q). \tag{5.31}$$

That is, we set $x_1 = x$ and $x_2 = \cdots = x_{N-1} = q$. A version of quantum volume conjecture [FGS13] states that this should be annihilated by the symmetrically colored quantum A-polynomial:

$$\hat{A}_K(\hat{x},\hat{y},a=q^N,q)F_K^{\mathfrak{sl}_N,\mathrm{sym}}(x,q) = 0. \tag{5.32}$$

Example 5.3.1. Right-handed trefoil. For the right-handed trefoil, $F_{\mathbf{3}_1^r}^{\mathfrak{sl}_N,\mathrm{sym}}(x,q)$ for the first few values of N look like the following:

- For $\mathfrak{sl}_2$,

$$\begin{aligned} F_{\mathbf{3}_1^r}^{\mathfrak{sl}_2,\mathrm{sym}}(x,q) \cong \frac{1}{2}\big[&(-q+q^2+q^3-q^6-q^8+q^{13}+q^{16}-\cdots)\\ &+(x+x^{-1})(q^2+q^3-q^6-q^8+q^{13}+q^{16}-\cdots)\\ &+(x^2+x^{-2})(q^2+q^3-q^6-q^8+q^{13}+q^{16}-\cdots)\\ &+(x^3+x^{-3})(q^3-q^6-q^8+q^{13}+q^{16}-\cdots)\\ &+(x^4+x^{-4})(-q^6-q^8+q^{13}+q^{16}-\cdots)\\ &+\cdots\big]; \end{aligned}$$

- For $\mathfrak{sl}_3$,

$$\begin{aligned} F_{\mathbf{3}_1^r}^{\mathfrak{sl}_3,\mathrm{sym}}(x,q) \cong \frac{1}{2}\big[&(-2q-2q^2+2q^4+4q^5+4q^6+4q^7+2q^8-2q^{10}-4q^{11}-\cdots)\\ &+(q^{1/2}x+q^{-1/2}x^{-1})q^{1/2}(-1-2q-q^2+q^3+3q^4+4q^5+4q^6+\cdots)\\ &+(qx^2+q^{-1}x^{-2})(-q-q^2+2q^4+3q^5+4q^6+3q^7+2q^8-2q^{10}+\cdots)\\ &+(q^{3/2}x^3+q^{-3/2}x^{-3})q^{1/2}(q^3+2q^4+3q^5+3q^6+2q^7+q^8+\cdots)\\ &+(q^2x^4+q^{-2}x^{-4})(q^3+q^4+2q^5+2q^6+2q^7+q^8+\cdots)\\ &+\cdots\big]; \end{aligned}$$

- For $\mathfrak{sl}_4$,

$$
\begin{aligned}
F^{\mathfrak{sl}_4,\mathrm{sym}}_{\mathbf{3}_1^r}(x,q) \cong \frac{1}{2}\big[&(q^{-2}+q^{-1}-2-4q-8q^2-7q^3-7q^4+\cdots)\\
&+(qx+q^{-1}x^{-1})(q^{-2}-1-5q-6q^2-8q^3-5q^4-2q^5+\cdots)\\
&+(q^2x^2+q^{-2}x^{-2})(-2-3q-6q^2-5q^3-5q^4+4q^6+\cdots)\\
&+(q^3x^3+q^{-3}x^{-3})(-q^{-1}-1-3q-3q^2-4q^3-2q^4+5q^6+9q^7+\cdots)\\
&+(q^4x^4+q^{-4}x^{-4})(-1-q-2q^2-q^3-q^4+2q^5+4q^6+8q^7+\cdots)\\
&+\cdots\big].
\end{aligned}
$$

Note that the overall factor is $\frac{1}{2}$ instead of $\frac{1}{N!}$. This is due to reduction of the Weyl symmetry to $\mathbb{Z}_2$ as we specialize to symmetric representations.

It is easy to experimentally check (5.32) term by term in this case, using the a-deformed quantum A-polynomial for the right-handed trefoil

$$\hat{A}_{\mathbf{3}_1^r}(\hat{x},\hat{y},a,q) = a_0 + a_1\hat{y} + a_2\hat{y}^2,$$

where

$$
\begin{aligned}
a_0 &= -\frac{(-1+\hat{x})(-1+aq\hat{x}^2)}{a\hat{x}^3(-1+a\hat{x})(-q+a\hat{x}^2)},\\
a_1 &= \frac{(-1+a\hat{x}^2)(-a^2\hat{x}^2+aq^3\hat{x}^2+aq\hat{x}(1+\hat{x}+a(-1+\hat{x})\hat{x})-q^2(1+a^2\hat{x}^4))}{a^2q\hat{x}^3(-1+a\hat{x})(-q+a\hat{x}^2)},\\
a_2 &= 1
\end{aligned}
$$

with a specialized to q^N.

Large-N
From (5.32), we are naturally led to the following conjecture:

Conjecture 5.3.2 ([Par20a])**.** *For each knot K, there exists a function $F_K(x,a,q)$ such that*

$$\hat{A}_K(\hat{x},\hat{y},a,q)F_K(x,a,q) = 0 \tag{5.33}$$

and

$$F_K(x,q^N,q) = F_K^{\mathfrak{sl}_N,sym}(x,q) \tag{5.34}$$

for any N. Moreover, this function should have the following Weyl symmetry:

$$F_K(x^{-1},a,q) = F_K(a^{-1}q^2x,a,q). \tag{5.35}$$

In particular, (5.34) implies

$$\lim_{q\to 1} F_K(x, q^N, q) = \Delta_K(x)^{1-N}. \tag{5.36}$$

The study of this HOMFLY-PT analogue (i.e., a-deformation) of F_K is the subject of next chapter.

Remark 5.3.3. This conjecture has been checked for various knots [Ekh+; Ekh+22], by either solving the quantum A-polynomial equation, or by using the R-matrix state sum and then using the knots-quivers correspondence to find the a-deformation.

Chapter 6

TOPOLOGICAL STRINGS

At the end of the previous chapter, we presented a conjecture on the existence of a three-variable series $F_K(x, a, q)$ that interpolates F_K's for $\mathfrak{sl}_N$. In this chapter, following [Ekh+; Ekh+22], we explain how this three-variable series can be interpreted as a topological string partition function. As we will see, this will lead to several concrete mathematical predictions.

6.1 Topological strings and F_K

HOMFLY-PT polynomials

For a knot $K \subset S^3$, its *HOMFLY-PT polynomial* is a topological invariant [Hos+85; PT87] which can be defined by the skein relation

$$a^{1/2}P_{\times}(a,q) - a^{-1/2}P_{\times}(a,q) = (q^{1/2} - q^{-1/2})P_{)(}(a,q)$$

with a normalization condition $P_{0_1}(a, q) = 1$ for the unknot. The HOMFLY-PT polynomial interpolates all the $\mathfrak{sl}_N$ Jones polynomials $J_K^{\mathfrak{sl}_N}(q)$ in the sense that

$$P_K(a = q^N, q) \;=\; J_K^{\mathfrak{sl}_N}(q).$$

More generally, the *colored HOMFLY-PT polynomials* $P_{K,R}(a, q)$ are polynomial knot invariants generalizing the HOMFLY-PT polynomial, which also depends on a representation (a Young diagram) R. The colored HOMFLY-PT polynomial $P_{K,R}(a, q)$ interpolates the colored $\mathfrak{sl}_N$ Jones polynomials in the sense that

$$P_{K,R}(a = q^N, q) \;=\; J_{K,R}^{\mathfrak{sl}_N}(q).$$

The original HOMFLY-PT polynomial corresponds to the case of defining representation $R = \square$. We will be interested mainly in the HOMFLY-PT polynomials colored by the totally symmetric representations

$$R = S^r = \underbrace{\square \cdots \square}_{r}$$

with r boxes in a row in the Young diagram. In order to simplify the notation, we will denote them by $P_{K,r}(a, q)$ and call them simply the HOMFLY-PT polynomials.

There is also a t-deformation of the HOMFLY-PT polynomials [DGR06; GS12a]. The *superpolynomial* $\mathcal{P}_{K,r}(a,q,t)$ is defined as the Poincaré polynomial of the triply-graded homology that categorifies the HOMFLY-PT polynomial:

$$\begin{aligned} P_{K,r}(a,q) &= \sum_{i,j,k} (-1)^k a^i q^j \dim \mathcal{H}^{S^r}_{i,j,k}(K), \\ \mathcal{P}_{K,r}(a,q,t) &= \sum_{i,j,k} a^i q^j t^k \dim \mathcal{H}^{S^r}_{i,j,k}(K). \end{aligned} \tag{6.1}$$

The superpolynomial reduces to the HOMFLY-PT polynomial when $t=-1$:

$$\mathcal{P}_{K,r}(a,q,t=-1) \;=\; P_{K,r}(a,q).$$

A-polynomials

The *A-polynomial* $A_K(x,y)$ is a polynomial knot invariant defining the algebraic curve $\{(x,y)\in(\mathbb{C}^*)^2 \mid A_K(x,y)=0\}$, which is the projection of the character variety of the the knot complement to the boundary torus [Coo+94]. According to the volume conjecture, it also captures the asymptotics of the colored Jones polynomials $J_{K,r}(q)$ for large colors r. The quantization of the A-polynomial encodes information about all colors, not only large ones. Namely, it gives the recurrence relations satisfied by the colored Jones polynomials $J_r(K;q)$:

$$\hat{A}_K(\hat{x},\hat{y},q)J_{K,r}(q)=0,$$

where $\hat{x}$ and $\hat{y}$ act by

$$\hat{x}J_{K,r}(q)=q^r J_{K,r}(q), \qquad \hat{y}J_{K,r}(q)=J_{K,r+1}(q),$$

and satisfy the q-commutation relation $\hat{y}\hat{x}=q\hat{x}\hat{y}$. The q-difference operator $\hat{A}_K(\hat{x},\hat{y},q)$, which we have already seen many times in previous chapters, is called the *quantum A-polynomial*; in the classical limit $q=1$ it becomes the usual A-polynomial $A_K(x,y)$. The existence of the quantum A-polynomial was conjectured independently in the context of quantization of the Chern-Simons theory [Guk05] and in parallel mathematics developments [Gar04].

The A-polynomial can be generalized further for the colored HOMFLY-PT polynomials [AV12] and colored superpolynomials [Awa+12; FGS13], which we briefly introduced in (6.1). In these cases the objects mentioned in the previous paragraph become a- and t-dependent. In particular, the asymptotics of colored superpolynomials $\mathcal{P}_r(K;a,q,t)$ for large r is captured by an algebraic curve $A_K(x,y,a,t)=0$ defined by the *super-A-polynomial*. When $t=-1$ it becomes the a-deformed

A-polynomial, and upon setting in addition $a = 1$, it gets reduced further to the original A-polynomial (as a factor). For brevity, all these objects are often referred to as A-polynomials. The quantization of the super-A-polynomial gives rise to quantum super-A-polynomial $\hat{A}_K(\hat{x}, \hat{y}, a, q, t)$, which is a q-difference operator that encodes the recurrence relations for the colored superpolynomials:

$$\hat{A}_K(\hat{x}, \hat{y}, a, q, t)\mathcal{P}_*(K; a, q, t) = 0.$$

A universal framework that enables us to determine a quantum A-polynomial from an underlying classical curve $A(x, y) = 0$ was proposed in [GS12b] (irrespective of extra parameters these curves depend on, and also beyond examples related to knots).

Large-N transition

In this subsection we explain the physical background in order to motivate the conjectures that we will present in later sections. The mathematically inclined readers may skip this subsection.

The physical system we are interested in[1] can be represented by the system of N fivebranes supported on $\mathbb{R}^2 \times S^1 \times Y$, where Y is embedded as the zero-section inside the Calabi-Yau 3-fold T^*Y and $\mathbb{R}^2 \times S^1 \subset \mathbb{R}^4 \times S^1$:

$$\begin{array}{rl} \text{spacetime}: & \mathbb{R}^4 \times S^1 \times T^*Y \\ & \quad \cup \qquad\quad \cup \\ N \text{ M5-branes}: & \mathbb{R}^2 \times S^1 \times Y. \end{array} \tag{6.2}$$

Finding the large-N limit of this system for general 3-manifold Y is highly nontrivial (see [GPV17, sec.7] and [ES19, Remark 2.4]). However, when Y is a knot complement $M_K := S^3 \backslash K$, there is an equivalent description for which the study of large-N behavior can be reduced to the celebrated "large-N transition" [GV98; OV00].

We consider first a description without transition. From the viewpoint of 3d/3d correspondence, N fivebranes on $Y = M_K$ produce a 4d $\mathcal{N} = 4$ theory — which is a close cousin of (but is *not*) 4d $\mathcal{N} = 4$ super-Yang-Mills — on a half-space $\mathbb{R}^3 \times \mathbb{R}_+$ coupled to 3d $\mathcal{N} = 2$ theory $T[M_K]$ on the boundary. Indeed, near the boundary $T^2 = \Lambda_K = \partial M_K$, the compactification of N fivebranes produces a 4d $\mathcal{N} = 4$ theory which has moduli space of vacua $\mathrm{Sym}^N(\mathbb{C}^2 \times \mathbb{C}^*)$ [Chu+20]. (The moduli space of vacua in 4d $\mathcal{N} = 4$ SYM is $\mathrm{Sym}^N(\mathbb{C}^3)$.) The $SU(N)$ gauge symmetry of this theory appears as a global symmetry of the 3d boundary theory $T[M_K]$. In particular, the

[1] We have already reviewed this briefly in Section 2.2.

variables $x_i \in \mathbb{C}^*$ are complexified fugacities for this global ("flavor") symmetry. For $G = SU(2)$, the moduli space of vacua of the knot complement theory $T_{\mathfrak{sl}_2}[M_K]$ gives precisely the A-polynomial of K. Similarly, for $G = SU(N)$, $G_{\mathbb{C}}$ character varieties of M_K are realized as spaces of vacua in $T_{\mathfrak{sl}_N}[M_K]$ [FGS13; Fuj+13].

We next give another equivalent description of the physical system (6.2) with $Y = M_K$, where the large-N behavior is easier to analyze:

$$\begin{aligned}
\text{spacetime}: \quad & \mathbb{R}^4 \times S^1 \times T^*S^3 \\
& \quad\ \cup \qquad\quad \cup \\
N \text{ M5-branes}: \quad & \mathbb{R}^2 \times S^1 \times S^3 \\
\rho \text{ M5}'\text{-branes}: \quad & \mathbb{R}^2 \times S^1 \times L_K.
\end{aligned} \tag{6.3}$$

This brane configuration is basically a variant of (6.2) with $Y = S^3$ and ρ extra M5-branes supported on $\mathbb{R}^2 \times S^1 \times L_K$, where $L_K \subset T^*S^3$ is the conormal bundle of the knot $K \subset S^3$ (often called the *knot conormal Lagrangian*). There is, however, a crucial difference between fivebranes on S^3 and L_K. Since the latter are non-compact in two directions orthogonal to K, they carry no dynamical degrees of freedom away from K. One can path integrate those degrees of freedom along K, which effectively removes K from S^3 and puts the corresponding boundary conditions on the boundary $T^2 = \partial M_K$. The resulting system is precisely (6.2) with $Y = M_K$. Equivalently, one can use the topological invariance along S^3 to move the tubular neighbourhood of $K \subset S^3$ to "infinity." This creates a long neck isomorphic to $\mathbb{R} \times T^2$, as in the above discussion. Either way, we end up with a system of N fivebranes on the knot complement and no extra branes on L_K, so that the choice of $GL(\rho, \mathbb{C})$ flat connection on L_K is now encoded in the boundary condition for $SL(N, \mathbb{C})$ connection[2] on $T^2 = \partial M_K$. In particular, the latter has at most ρ nontrivial parameters $x_i \in \mathbb{C}^*$, $i = 1, \ldots, \rho$.

We will consider the simplest case of $\rho = 1$. Then we can use the geometric transition of [GV98], upon which there is one brane on L_K and N fivebranes on the zero-section of T^*S^3 disappear. The Calabi-Yau space T^*S^3 undergoes a topology changing transition to a new Calabi-Yau space X, the so-called "resolved conifold", which is the total space of $\mathcal{O}(-1) \oplus \mathcal{O}(-1) \to \mathbb{CP}^1$, and only the Ooguri-Vafa fivebranes

[2] To be more precise, it is a $GL(N, \mathbb{C})$ connection, but the dynamics of the $GL(1, \mathbb{C})$ sector is different from that of the $SL(N, \mathbb{C})$ sector and can be decoupled.

supported on the conormal bundle L_K remain:

$$\begin{array}{rl} \text{spacetime}: & \mathbb{R}^4 \times S^1 \times X \\ & \quad \cup \qquad \cup \\ \rho\ \text{M5}'\text{-branes}: & \mathbb{R}^2 \times S^1 \times L_K. \end{array} \tag{6.4}$$

Note that on the resolved conifold side, i.e., after the geometric transition, $\log a = \mathrm{Vol}(\mathbb{CP}^1) + i\int B = N\hbar$ is the complexified Kähler parameter which enters the generating function of enumerative invariants.

To summarize, a system of N fivebranes on a knot complement (6.2) is equivalent to a brane configuration (6.4), with a suitable map that relates the boundary conditions in the two cases. There is another system closely related to (6.4) that one can obtain from (6.3) by first reconnecting ρ branes on L_K with ρ branes on S^3. This give ρ branes on M_K (that go off to infinity just like L_K does) plus $N - \rho$ branes on S^3. Assuming that $\rho \sim O(1)$ as $N \to \infty$ (e.g. $\rho = 1$ in the context of this paper), after the geometric transition we end up with a system like (6.4), except L_K is replaced by M_K and $\mathrm{Vol}(\mathbb{CP}^1) + i\int B = (N - \rho)\hbar$. Both of these systems on the resolved side compute the HOMFLY-PT polynomials of K colored by Young diagrams with at most ρ rows.

F_K as the count of open holomorphic curves

From the mathematical point of view, what the above physical picture tells us is that $F_K(x, a, q)$ is the count of open topological strings in the resolved conifold X, with the knot complement Lagrangian $M_K \subset X$.

Mathematically, the large-N transition (going from T^*S^3 to the resolved conifold) corresponds to the *Symplectic Field Theory (SFT)-stretching* [ES19]. With enough stretching, all the curves leave a neighborhood of S^3, so one can effectively replace T^*S^3 with the resolved conifold. In order for the SFT-stretching to work nicely, we should be able to shift the Lagrangian completely off of the zero section S^3. With M_K, that would be exactly when K is fibered. When M_K is non-fibered, it cannot be completely shifted off of the zero section. Instead, there will be finitely many intersection points where M_K looks like the cotangent fiber. In this case, even after SFT-stretching, the curves can end on Reeb chords ending on those intersection points, which complicates the story.

Before moving onto the next topic, let us point out one implication of this interpretation. Write

$$F_K(x, a, q = e^{g_s}) = e^{\frac{1}{g_s}U_K(x,a) + U_K^0(x,a) + g_s U_K^1(x,a) + g_s^2 U_K^2(x,a) + \cdots}.$$

The U_K's are the open Gromov-Witten invariants in our setup (with knot complement Lagrangian M_K). Then, if $\hat{b}$ is the operator such that

$$\hat{b} : N \mapsto N+1 \quad (\text{i.e., } a \mapsto qa),$$

then its expectation value is

$$\langle \hat{b} \rangle|_{(y,a)=(1,1)} = \lim_{q\to 1} \frac{F_K(x,qa,q)}{F_K(x,a,q)}\bigg|_{(y,a)=(1,1)} = \Delta_K(x)^{-1} \tag{6.5}$$

since, according to Conjecture 5.3.2,

$$\lim_{q\to 1} F_K^{\mathfrak{sl}_N,sym}(x,q) = \Delta_K(x)^{1-N}.$$

But also,

$$\begin{aligned}
\langle \hat{b} \rangle|_{(y,a)=(1,1)} &= \exp\left(\frac{\partial U_K(x,a)}{\partial \log a}\bigg|_{(y,a)=(1,1)}\right) \\
&= \exp\left(\int \frac{\partial \log y(x,a)}{\partial \log a}\bigg|_{(y,a)=(1,1)} d\log x\right) \\
&= \exp\left(\int -\frac{\partial_{\log a} A_K}{\partial_{\log y} A_K}\bigg|_{(y,a)=(1,1)} d\log x\right).
\end{aligned}$$

So we have a formula for $\Delta_K(x)$ in terms of the a-deformed A-polynomial $A_K(x,y,a)$. This was confirmed recently by Diogo and Ekholm.

Theorem 6.1.1 ([DE20])**.** *The Alexander polynomial can be computed from the augmentation polynomial*[3] $\mathrm{Aug}_K(x,y,a)$ *near the abelian branch:*

$$\Delta_K(x) = (1-x)\exp\left(\int \frac{\partial_{\log a}\mathrm{Aug}_K}{\partial_{\log y}\mathrm{Aug}_K}\bigg|_{(y,a)=(1,1)} d\log x\right).$$

6.2 Branches

The variables x and y of the A-polynomial correspond to the holonomy eigenvalues of the meridian and longitude of the knot. Since there are always abelian $SL_2(\mathbb{C})$ connections regardless of the choice of knot, the A-polynomial $A_K(x,y)$ always have a factor of $(y-1)$. By *branches*, we mean the solutions y of $A_K(x,y)=0$ as a function of x. So, there are as many branches as $\deg_y A_K(x,y)$. The canonical

[3] The augmentation polynomial in knot contact homology is essentially the same as the a-deformed A-polynomial (also known as the Q-deformed A-polynomial). See [Aga+14; AV12].

solution $y = 1$ is called the *abelian branch*. Similarly in the a-deformed setting, we call the branch $y^{(\alpha)}(x, a)$ abelian branch if $y^{(\alpha)}(x, a = 1) = 1$.

All of our discussions so far have been on the abelian branch. This is because for $F_K(x, q)$, the expectation value of the $\hat{y}$ operator is always 1:

$$\langle \hat{y} \rangle = \lim_{q \to 1} \frac{F_K(qx, q)}{F_K(x, q)} = 1.$$

As briefly mentioned in the previous section, a choice of branch corresponds to a choice of vacuum in the 3d theory $T[M_K]$. Therefore, it is natural to expect that there are invariants analogous to $F_K(x, a, q)$ associated to other branches of the A-polynomial.

Conjecture 6.2.1 ([Ekh+22])**.** *Given a knot K, let $y^{(\alpha)}(x, a)$ be a branch of y near $x = 0$ (or $x = \infty$) of the a-deformed A-polynomial of K, $A_K(x, y, a)$. Then, there exists a wave function $F_K^{(\alpha)}(x, a, q)$ associated to this branch in a sense that*

$$\langle \hat{y} \rangle := \lim_{q \to 1} \frac{F_K^{(\alpha)}(qx, a, q)}{F_K^{(\alpha)}(x, a, q)} = y^{(\alpha)}(x, a),$$

and this wave function is annihilated by the quantum a-deformed A-polynomial $\hat{A}_K(\hat{x}, \hat{y}, a, q)$ (which is the same for all branches $y^{(\alpha)}(x, a)$):

$$\hat{A}_K(\hat{x}, \hat{y}, a, q) F_K^{(\alpha)}(x, a, q) = 0.$$

This conjecture has been checked in numerous examples in [Ekh+22]. In fact, in many cases, we can obtain $F_K^{(\alpha)}(x, a, q)$ by solving the q-difference equation given by the quantum A-polynomial. If $y^{(\alpha)}(x) \sim x^d$ asymptotically near $x = 0$, for some $d \in \mathbb{Q}$, then we can use it as the initial condition and find a solution of the form

$$F_K^{(\alpha)}(x, a, q) = e^{d \frac{(\log x)^2}{2 \log q}} \cdot (\text{some Puiseux series in } x),$$

up to an overall factor independent of x. Possible values of d correspond exactly to the boundary slopes of the A-polynomial Newton polygon. More precisely, $-\frac{1}{d}$ should be a boundary slope of the Newton polygon, with x- and y-axis representing the x- and y-degree of the monomials. The abelian branch always corresponds to the slope ∞ (or equivalently $d = 0$), and that's why the two-variable series $F_K(x, q)$ we considered in previous chapters do not have the exponential prefactor $e^{d \frac{(\log x)^2}{2 \log q}}$. For non-abelian branches, however, $F_K^{(\alpha)}(x, q)$ in general involve such a prefactor.

Example 6.2.2 (Figure-eight knot $\mathbf{4}_1$)**.** For simplicity, let's consider the $\mathfrak{sl}_2$ case (i.e., $a = q^2$). The A-polynomial of the figure-eight knot is of y-degree 3, so it has 3 branches. One of them is the abelian branch, and there are two non-abelian branches of boundary slope $\pm\frac{1}{2}$ which are conjugate to each other. Let's denote the non-abelian branches by $\alpha_{\pm 1/2}$, according to their boundary slopes.

Using the quantum A-polynomial, we can solve for $F_{\mathbf{4}_1}^{(\alpha_{\pm 1/2})}(x,q)$ term by term. It turns out, they have nice expressions similar to the inverted Habiro series! Explicitly, they are given by

$$F_{\mathbf{4}_1}^{(\alpha_{-1/2})}(x,q) = e^{\frac{(\log x)^2}{\log q}} \sum_{n\geq 0} \frac{\frac{(-1)^n q^{-\frac{n(n-1)}{2}}}{(q)_n}}{\prod_{0\leq j\leq n}(x + x^{-1} - q^j - q^{-j})},$$

and

$$F_{\mathbf{4}_1}^{(\alpha_{1/2})}(x,q) = e^{-\frac{(\log x)^2}{\log q}} \sum_{n\geq 0} \frac{\frac{q^{n^2}}{(q)_n}}{\prod_{0\leq j\leq n}(x + x^{-1} - q^j - q^{-j})}.$$

Remark 6.2.3. The abelian branch $F_K(x,q)$, as we have reviewed extensively in previous chapters, was part of a bigger story that involves closed 3-manifolds. On the other hand, it is not clear at the moment if the non-abelian branch $F_K^{(\alpha)}(x,q)$'s can be extended to closed 3-manifolds. Given that there seems to be some correlation between the window of good surgery coefficients (Remark 4.0.2) and the boundary slope of the A-polynomial Newton polygon, it is not too far-fetched to speculate that perhaps these non-abelian branch F_K's might play some role to get a full understanding of $\hat{Z}$.

6.3 Holomorphic Lagrangian subvarieties

Consider the $\hat{b}$ operator that we introduced earlier. It is the operator that substitutes a by qa. We have seen that in the abelian branch the expectation value of the $\hat{b}$ operator provides an a-deformation of the inverse Alexander polynomial. On other branches $y^{(\alpha)}(x,a)$, the expectation value of the $\hat{b}$ operator will be some other functions; let's define

$$b^{(\alpha)}(x,a) := \lim_{q\to 1} \frac{F_K^{(\alpha)}(x,qa,q)}{F_K^{(\alpha)}(x,a,q)}.$$

It turns out, the functions $b^{(\alpha)}(x,a)$ describe branches of the equation $B_K(a,b,x) = 0$ defined by a polynomial $B_K(a,b,x)$ that we call the *B-polynomial* in [Ekh+22]. The B-polynomial is uniquely determined by the A-polynomial, thanks to the equation

$$\frac{\partial \log b^{(\alpha)}(x,a)}{\partial \log x} = \frac{\partial \log y^{(\alpha)}(x,a)}{\partial \log a}.$$

We summarize the B-polynomials for some simple knots in Table 6.1.

K	$B_K(a,b,x)$
0_1	$1-b$
3_1	$1-x^{-1}(2-(1+x)a+x^2a^2)b+x^{-2}(1-a)(1-xa)b^2$
4_1	$1+a^{-1}x^{-1}(2-(1+3x+x^2)a+2x^2a^2)b$ $+a^{-2}x^{-2}(1-a)(1-xa)(1-2x(1+x)a+x^3a^2)b^2$ $-a^{-2}x^{-1}(1-a)(1-a)(1-xa)(1-xa)b^3$
5_1	$1-x^{-2}(3-2(1+x)a+x(1+2x)a^2-x^2(1+x)a^3+x^4a^4)b$ $+x^{-4}(1-a)(1-xa)(3-(1+x)a+2x^2a^2)b^2$ $-x^{-6}(1-a)(1-a)(1-xa)(1-xa)b^3$
5_2	$1-x^{-2}\left(2a^2x^3+a^2x^2-4ax^2-ax-a+3x+1\right)b$ $-x^{-3}(a-1)(ax-1)\left(a^3x^4-3a^2x^3-2a^2x^2+5ax^2+ax+a-3x-3\right)b^2$ $-x^{-4}(a-1)^2(ax-1)^2\left(a^2x^3-2ax^2-ax+x+3\right)b^3$ $+x^{-5}(a-1)^3(ax-1)^3b^4$

Table 6.1: Classical B-polynomials for some simple knots.

One important feature of the B-polynomial is that it takes the following simple form in the $a=1$ limit, which can be seen from equation (6.5):

$$B_K(a=1,b,x)=1-\Delta_K(x)b.$$

The B-polynomial shares many features similar to the A-polynomial. For instance, the b-degree of the B-polynomial equals the y-degree of the A-polynomial (since there is a one-to-one correspondence between the branches). Moreover, $B_K(a,b,x=1)$ always has a factor of $b-1$, just like $A_K(x,y,a=1)$ always has a factor of $y-1$.

Just like A-polynomials can be quantized to q-difference equations, so do B-polynomials. We summarize the quantum B-polynomials for some simple knots in Table 6.2.

In fact, there is a better way to think of A- and B-polynomials. This is by lifting them to the same holomorphic Lagrangian in $(\mathbb{C}^*)^4$ parametrized by x, y, a, b. Physically, this holomorphic Lagrangian corresponds to the Coulomb branch of a 3d-5d coupled system, which should have a quantization. Therefore, we propose the following conjecture.

K	$\hat{B}_K(\hat{a},\hat{b},x,q)$
0_1	$1-\hat{b}$
3_1	$1-q^{-1}x^{-1}(1+q-(1+qx)\hat{a}+qx^2\hat{a}^2)\hat{b}+q^{-1}x^{-2}(1-\hat{a})(1-qx\hat{a})\hat{b}^2$
4_1	$1+q^{-1}x^{-1}\hat{a}^{-1}(1+q-(1+3qx+q^2x^2)\hat{a}+qx^2(1+q)\hat{a}^2)\hat{b}$ $+q^{-2}x^{-2}\hat{a}^{-2}(1-\hat{a})(1-qx\hat{a})(1-2qx(1+qx)\hat{a}+q^3x^3\hat{a}^2)\hat{b}^2$ $-q^{-2}x^{-1}\hat{a}^{-2}(1-\hat{a})(1-q\hat{a})(1-qx\hat{a})(1-q^2x\hat{a})\hat{b}^3$
5_1	$1-q^{-2}x^{-2}\big(1+q+q^2-(1+q)(1+qx)\hat{a}+qx(1+x+qx)\hat{a}^2-qx^2(1+qx)\hat{a}^3+q^2x^4\hat{a}^4\big)\hat{b}$ $+q^{-3}x^{-4}(1-\hat{a})(1-qx\hat{a})(1+q+q^2-q(1+qx)\hat{a}+q^2x^2(1+q)\hat{a}^2)\hat{b}^2$ $-q^{-3}x^{-6}(1-\hat{a})(1-q\hat{a})(1-qx\hat{a})(1-q^2x\hat{a})\hat{b}^3$

Table 6.2: Quantum B-polynomials for some simple knots.

Conjecture 6.3.1 ([Ekh+22]). *Let us endow $(\mathbb{C}^*)^4$ with the holomorphic symplectic form*

$$\Omega := d\log x \wedge d\log y + d\log a \wedge d\log b, \quad x,y,a,b \in \mathbb{C}^*.$$

For every knot K, there is a holomorphic Lagrangian subvariety $\Gamma_K \subset (\mathbb{C}^*)^4$ with the following properties:

1. *This holomorphic Lagrangian is preserved under the Weyl symmetry*

$$x \mapsto a^{-1}x^{-1}, \quad y \mapsto y^{-1}, \quad a \mapsto a, \quad b \mapsto y^{-1}b.$$

2. *The projection of Γ_K on $(\mathbb{C}^*)^3_{x,y,a}$ is the zero set of the a-deformed A-polynomial of K.*

3. *Moreover, if $\hat{x},\hat{y},\hat{a},\hat{b}$ are operators such that*

$$\hat{y}\hat{x} = q\hat{x}\hat{y}, \quad \hat{b}\hat{a} = q\hat{a}\hat{b},$$

and all the other pairs commute, then the ideal defining Γ_K can be quantized to a left ideal $\hat{\Gamma}_K \subset \mathbb{C}[\hat{x}^{\pm1},\hat{y}^{\pm1},\hat{a}^{\pm1},\hat{b}^{\pm1}]$ that annihilates $F_K(x,a,q)$.

This conjecture can be generalized even further, by introducing the t-variable and its conjugate which we denote by u.

Conjecture 6.3.2 ([Ekh+22]). *Let us endow $(\mathbb{C}^*)^6$ with the holomorphic symplectic form*

$$\Omega' := d\log x \wedge d\log y + d\log a \wedge d\log b + d\log t \wedge d\log u, \quad x,y,a,b,t,u \in \mathbb{C}^*.$$

For every knot K, there is a holomorphic Lagrangian subvariety $\Gamma'_K \subset (\mathbb{C}^*)^6$ with the following properties:

1. *This holomorphic Lagrangian is preserved under the Weyl symmetry*

$$x \mapsto (-t)^3 a^{-1} x^{-1}, \quad y \mapsto t^s y^{-1}, \quad a \mapsto a, \quad b \mapsto (-t)^{\frac{s}{2}} y^{-1} b,$$

$$t \mapsto t, \quad u \mapsto x^{-s} y^{-3} a^{-\frac{s}{2}} u,$$

where s is a version of s-invariant of the knot K.

2. *The projection of Γ'_K on $(\mathbb{C}^*)^4_{x,y,a,t}$ is the zero set of the super-A-polynomial of K.*

3. *Moreover, if $\hat{x}, \hat{y}, \hat{a}, \hat{b}, \hat{t}, \hat{u}$ are operators such that*

$$\hat{y}\hat{x} = q\hat{x}\hat{y}, \quad \hat{b}\hat{a} = q\hat{a}\hat{b}, \quad \hat{u}\hat{t} = q\hat{t}\hat{u},$$

and all the other pairs commute, then the ideal defining Γ'_K can be quantized to a left ideal $\hat{\Gamma}'_K \subset \mathbb{C}[\hat{x}^{\pm 1}, \hat{y}^{\pm 1}, \hat{a}^{\pm 1}, \hat{b}^{\pm 1}, \hat{t}^{\pm 1}, \hat{u}^{\pm 1}]$ that annihilates $F_K(x, a, q, t)$.[4]

6.4 Knots-quivers correspondence

In this final section, we briefly review the knots-quivers correspondence for colored HOMFLY-PT polynomials, and then conjecture that $F_K^{(\alpha)}(x, a, q)$ also has a quiver form.

Quivers and their representations

A quiver Q is an oriented graph, i.e., a pair (Q_0, Q_1) where Q_0 is a finite set of vertices and Q_1 is a finite set of arrows between them. We number the vertices by $1, 2, ..., m = |Q_0|$. An adjacency matrix of Q is the $m \times m$ integer matrix with entries C_{ij} equal to the number of arrows from i to j. If $C_{ij} = C_{ji}$, we call the quiver symmetric.

A quiver representation with a dimension vector $\mathbf{d} = (d_1, ..., d_m)$ is an assignment of a vector space of dimension d_i to the node $i \in Q_0$ and a linear map $\gamma_{ij} : \mathbb{C}^{d_i} \to \mathbb{C}^{d_j}$ to each arrow from vertex i to vertex j. Quiver representation theory studies moduli spaces of quiver representations. While explicit expressions for invariants describing those spaces are difficult to find in general, they are quite well understood in the case of symmetric quivers [KS08; KS11; Efi12; MR19; FR18]. Important information about the moduli space of representations of a symmetric quiver is encoded in the

[4] While we haven't discussed much about t-deformation of $F_K(x, a, q)$ in this thesis, since there are quantum super A-polynomials that involves both a and t variables, solving the q-difference equations we naturally obtain a t-deformation of F_K.

motivic generating series defined as

$$P_Q(\mathbf{x},q)=\sum_{\mathbf{d}\geq 0}(-q^{1/2})^{\mathbf{d}\cdot\mathbf{C}\cdot\mathbf{d}}\frac{\mathbf{x}^{\mathbf{d}}}{(q)_{\mathbf{d}}}=\sum_{d_1,\ldots,d_m\geq 0}(-q^{1/2})^{\sum_{i,j}C_{ij}d_id_j}\prod_{i=1}^{m}\frac{x_i^{d_i}}{(q)_{d_i}}. \tag{6.6}$$

Let us define the *plethystic exponential* of $f=\sum_n a_n t^n$, $a_0=0$ in the following way:

$$\mathrm{Exp}\big(f\big)(t)=\exp\left(\sum_k \tfrac{1}{k}f(t^k)\right)=\prod_n (1-t^n)^{a_n}.$$

Then we can write

$$\begin{aligned}P_Q(\mathbf{x},q)&=\mathrm{Exp}\left(\frac{\Omega(\mathbf{x},q)}{1-q}\right),\\ \Omega(\mathbf{x},q)&=\sum_{\mathbf{d},s}\Omega_{\mathbf{d},s}\mathbf{x}^{\mathbf{d}}q^{s/2}=\sum_{\mathbf{d},s}\Omega_{(d_1,\ldots,d_m),s}\left(\prod_i x_i^{d_i}\right)q^{s/2},\end{aligned} \tag{6.7}$$

where $\Omega_{\mathbf{d},s}$ are motivic Donaldson-Thomas (DT) invariants [KS08; KS11]. The DT invariants have two geometric interpretations, either as the intersection homology Betti numbers of the moduli space of all semi-simple representations of Q of dimension vector $\mathbf{d}$, or as the Chow-Betti numbers of the moduli space of all simple representations of Q of dimension vector $\mathbf{d}$; see [MR19; FR18]. [Efi12] provides a proof of integrality of DT invariants for the symmetric quivers.

Knots-quivers correspondence for knot conormals

In the context of the knots-quivers correspondence, we combine $P_{K,r}(a,q)$ into the HOMFLY-PT generating series:

$$P_K(y,a,q)=\sum_{r=0}^{\infty}\frac{y^{-r}}{(q)_r}P_{K,r}(a,q).$$

Using this expression we can encode the Labastida-Mariño-Ooguri-Vafa (LMOV) invariants [OV00; LM01; LMV00] in the following way:

$$P_K(y,a,q)=\mathrm{Exp}\left(\frac{N(y,a,q)}{1-q}\right),\qquad N(y,a,q)=\sum_{r,i,j}N_{r,i,j}y^{-r}a^{i/2}q^{j/2}. \tag{6.8}$$

According to the LMOV conjecture [OV00; LM01; LMV00], $N_{r,i,j}$ are integer numbers counting BPS states in the effective 3d $\mathcal{N}=2$ theories described in subsection 6.1.

The knots-quivers correspondence for the knot conormals [Kuc+17; Kuc+19] is an assignment of a symmetric quiver Q (with adjacency matrix C), vector

$\mathbf{n} = (n_1, \ldots, n_m)$ with integer entries, and vectors $\mathbf{a} = (a_1, \ldots, a_m)$, $\mathbf{l} = (l_1, \ldots, l_m)$ with half-integer entries to a given knot K in such a way that

$$P_K(y, a, q) = \sum_{\mathbf{d}\geq 0} (-q^{1/2})^{\mathbf{d}\cdot\mathbf{C}\cdot\mathbf{d}} \frac{y^{\mathbf{n}\cdot\mathbf{d}} a^{\mathbf{a}\cdot\mathbf{d}} q^{\mathbf{l}\cdot\mathbf{d}}}{(q)_{\mathbf{d}}} = P_Q(\mathbf{x}, q)\big|_{x_i = y^{n_i} a^{a_i} q^{l_i}} . \tag{6.9}$$

The possibility of such assignment was proven for all 2-bridge knots in [SW19] and for all arborescent knots in [SW21]. Some exotic cases with $n_i < -1$ (the simplest examples are $\mathbf{9}_{42}$ and $\mathbf{10}_{132}$) require a generalization of the correspondence, for more details see [EKL21].

Equation (6.9) can be rewritten as

$$N(y, a, q) = \Omega(\mathbf{x}, q)\big|_{x_i = y^{n_i} a^{a_i} q^{l_i}} , \tag{6.10}$$

which ties the knots-quivers correspondence with LMOV conjecture using the fact that DT invariants of symmetric quivers are integer.

Knots-quivers correspondence for knot complements

The knots-quivers correspondence can be generalized to knot complements, as proposed in [Kuc20] and studied extensively in [Ekh+22]. Then it is an assignment of a symmetric quiver Q, an integer n_i, and half-integers, a_i, l_i, $i \in Q_0$ to a given knot complement $M_K = S^3 \backslash K$ in such a way that

$$F_K(x, a, q) = \sum_{\mathbf{d}\geq 0} (-q^{1/2})^{\mathbf{d}\cdot\mathbf{C}\cdot\mathbf{d}} \frac{x^{\mathbf{n}\cdot\mathbf{d}} a^{\mathbf{a}\cdot\mathbf{d}} q^{\mathbf{l}\cdot\mathbf{d}}}{(q)_{\mathbf{d}}} = P_Q(\mathbf{x}, q)\big|_{x_i = x^{n_i} a^{a_i} q^{l_i}} . \tag{6.11}$$

In fact, we conjecture a version of knots-quivers correspondence not just for the abelian branch but for any branch:

Conjecture 6.4.1 ([Ekh+22])**.** *The wave function $F_K^{(\alpha)}(x, a, q)$ has a quiver form.*

This conjecture has been checked in a number of examples. We list a couple of simple examples below. See [Ekh+22] for more examples.

Example 6.4.2 ($\mathbf{3}_1$ knot)**.** For the abelian branch of the $\mathbf{3}_1$ knot, we have

$$F_{\mathbf{3}_1^r}(x, a, q) = e^{\frac{\log x \log a}{\log q}} x^{-1} \sum_{d_1, d_2, d_3, d_4 \geq 0} (-q^{\frac{1}{2}})^{\sum_{1\leq i,j\leq 4} C_{ij} d_i d_j} \prod_{i=1}^{4} \frac{x_i^{d_i}}{(q)_{d_i}}$$

with

$$C = \begin{pmatrix} 0 & 1 & 0 & 0 \\ 1 & 0 & 1 & 0 \\ 0 & 1 & 1 & 0 \\ 0 & 0 & 0 & 1 \end{pmatrix}, \quad \begin{pmatrix} x_1 \\ x_2 \\ x_3 \\ x_4 \end{pmatrix} = \begin{pmatrix} qx \\ ax \\ q^{-\frac{1}{2}} ax \\ q^{-\frac{1}{2}} ax \end{pmatrix}.$$

Example 6.4.3 (**4**$_1$ knot)**.** For the abelian branch of the **4**$_1$ knot, we have

$$F_{\mathbf{4}_1}(x,a,q) = e^{\frac{\log x \log a}{\log q}} x^{-1} \sum_{d_1,\cdots,d_6 \geq 0} (-q^{\frac{1}{2}})^{\sum_{1\leq i,j\leq 6} C_{ij} d_i d_j} \prod_{i=1}^{6} \frac{x_i^{d_i}}{(q)_{d_i}}$$

with

$$C = \begin{pmatrix} 0 & 0 & 0 & 0 & 0 & 0 \\ 0 & 0 & -1 & -1 & 0 & 0 \\ 0 & -1 & 0 & 0 & 1 & 0 \\ 0 & -1 & 0 & 1 & 1 & 0 \\ 0 & 0 & 1 & 1 & 1 & 0 \\ 0 & 0 & 0 & 0 & 0 & 1 \end{pmatrix}, \quad \begin{pmatrix} x_1 \\ x_2 \\ x_3 \\ x_4 \\ x_5 \\ x_6 \end{pmatrix} = \begin{pmatrix} qx \\ qx \\ qx \\ q^{-\frac{1}{2}}ax \\ q^{-\frac{1}{2}}ax \\ q^{-\frac{1}{2}}ax \end{pmatrix}.$$

Remark 6.4.4. Conjecture 6.4.1 imposes a strong condition on the structure of the series $F_K^{(\alpha)}(x,a,q)$. In many cases, it allows us to find the a-deformation, even when only $F_K^{(\alpha)}(x,q)$ for $\mathfrak{sl}_2$ is available.

Remark 6.4.5. Having a quiver form is very useful in finding the holomorphic Lagrangian Γ_K which we discussed in the previous section. This is because any quiver form satisfies a set of q-difference equations known as *quantum quiver A-polynomials*. The holomorphic Lagrangian Γ_K can be found by eliminating variables (e.g. using Gröbner basis) from the classical quiver A-polynomials, according to the knots-quivers change of variables.

Remark 6.4.6. For a fixed knot K, the quivers for $F_K^{(\alpha)}(x,a,q)$ for different branches α will look different, but they should be closely related because, for instance, the same holomorphic Lagrangian Γ_K can be deduced from those quivers. It is an interesting problem to understand given a quiver for one branch how to obtain a quiver for another branch of the same knot.

BIBLIOGRAPHY

[Aga+14] Mina Aganagic, Tobias Ekholm, Lenhard Ng, and Cumrun Vafa. "Topological Strings, D-Model, and Knot Contact Homology". In: *Adv.Theor.Math.Phys* 18.4 (2014). arXiv:1304.5778, pp. 827–956.

[AJK21] Rostislav Akhmechet, Peter K. Johnson, and Vyacheslav Krushkal. *Lattice cohomology and q-series invariants of 3-manifolds*. 2021. DOI: 10.48550/ARXIV.2109.14139. URL: https://arxiv.org/abs/2109.14139.

[AM22] Jørgen Ellegaard Andersen and William Elbæk Mistegård. "Resurgence analysis of quantum invariants of Seifert fibered homology spheres". In: *J. Lond. Math. Soc. (2)* 105.2 (2022), pp. 709–764. ISSN: 0024-6107. DOI: 10.1112/jlms.12506. URL: https://doi.org/10.1112/jlms.12506.

[Ati88] Michael Atiyah. "Topological quantum field theories". In: *Inst. Hautes Études Sci. Publ. Math.* 68 (1988), 175–186 (1989). ISSN: 0073-8301. URL: http://www.numdam.org/item?id=PMIHES_1988__68__175_0.

[Ati90] Michael Atiyah. *The geometry and physics of knots*. Lezioni Lincee. [Lincei Lectures]. Cambridge University Press, Cambridge, 1990, pp. x+78. ISBN: 0-521-39521-6. DOI: 10.1017/CBO9780511623868. URL: https://doi.org/10.1017/CBO9780511623868.

[Atl] The Knot Atlas. *The Knot Atlas*. http://katlas.org/. URL: http://katlas.org/.

[AV12] Mina Aganagic and Cumrun Vafa. *Large N Duality, Mirror Symmetry, and a Q-deformed A-polynomial for Knots*. arXiv:1204.4709. 2012.

[Awa+12] Hidetoshi Awata, Sergei Gukov, Piotr Sulkowski, and Hiroyuki Fuji. "Volume Conjecture: Refined and Categorified". In: *Adv. Theor. Math. Phys.* 16.6 (2012). arXiv:1203.2182, pp. 1669–1777. DOI: 10.4310/ATMP.2012.v16.n6.a3.

[BG96] Dror Bar-Natan and Stavros Garoufalidis. "On the Melvin-Morton-Rozansky conjecture". In: *Invent. Math.* 125.1 (1996), pp. 103–133. ISSN: 0020-9910. DOI: 10.1007/s002220050070. URL: https://doi.org/10.1007/s002220050070.

[BK01] Bojko Bakalov and Alexander Kirillov Jr. *Lectures on tensor categories and modular functors*. Vol. 21. University Lecture Series. American Mathematical Society, Providence, RI, 2001, pp. x+221. ISBN: 0-8218-2686-7.

[BM17] Kathrin Bringmann and Antun Milas. “W-algebras, higher rank false theta functions, and quantum dimensions”. In: *Selecta Math. (N.S.)* 23.2 (2017), pp. 1249–1278. ISSN: 1022-1824. DOI: 10.1007/s00029-016-0289-z. URL: https://doi.org/10.1007/s00029-016-0289-z.

[BMM20a] Kathrin Bringmann, Karl Mahlburg, and Antun Milas. “Higher depth quantum modular forms and plumbed 3-manifolds”. In: *Lett. Math. Phys.* 110.10 (2020), pp. 2675–2702. ISSN: 0377-9017. DOI: 10.1007/s11005-020-01310-z. URL: https://doi.org/10.1007/s11005-020-01310-z.

[BMM20b] Kathrin Bringmann, Karl Mahlburg, and Antun Milas. “Quantum modular forms and plumbing graphs of 3-manifolds”. In: *J. Combin. Theory Ser. A* 170 (2020), pp. 105145, 32. ISSN: 0097-3165. DOI: 10.1016/j.jcta.2019.105145. URL: https://doi.org/10.1016/j.jcta.2019.105145.

[Bri+21] Kathrin Bringmann, Jonas Kaszian, Antun Milas, and Caner Nazaroglu. *Higher Depth False Modular Forms*. 2021. DOI: 10.48550/ARXIV.2109.00394. URL: https://arxiv.org/abs/2109.00394.

[CFS20] Miranda C. N. Cheng, Francesca Ferrari, and Gabriele Sgroi. “Three-manifold quantum invariants and mock theta functions”. In: *Philos. Trans. Roy. Soc. A* 378.2163 (2020). arXiv:1912.07997, pp. 20180439, 15. ISSN: 1364-503X.

[Che+19] Miranda C. N. Cheng, Sungbong Chun, Francesca Ferrari, Sergei Gukov, and Sarah M. Harrison. “3d modularity”. In: *Journal of High Energy Physics* 2019.10, 10 (Oct. 2019), p. 10. DOI: 10.1007/JHEP10(2019)010. arXiv: 1809.10148 [hep-th].

[Chu+20] Sungbong Chun, Sergei Gukov, Sunghyuk Park, and Nikita Sopenko. “3d-3d correspondence for mapping tori”. In: *J. High Energy Phys.* 9 (2020), pp. 152, 59. ISSN: 1126-6708. DOI: 10.1007/jhep09(2020)152. URL: https://doi.org/10.1007/jhep09(2020)152.

[Chu20] Hee-Joong Chung. “BPS invariants for Seifert manifolds”. In: *J. High Energy Phys.* 3 (2020), pp. 113, 66. ISSN: 1126-6708. DOI: 10.1007/jhep03(2020)113. URL: https://doi.org/10.1007/jhep03(2020)113.

[Coo+94] D. Cooper, M. Culler, H. Gillet, D. D. Long, and P. B. Shalen. “Plane curves associated to character varieties of 3-manifolds”. In: *Invent. Math.* 118.1 (1994), pp. 47–84. ISSN: 0020-9910. DOI: 10.1007/BF01231526.

[DE20] Luis Diogo and Tobias Ekholm. *Augmentations, Annuli, and Alexander polynomials*. arXiv:2005.09733. 2020.

[DGR06] Nathan M. Dunfield, Sergei Gukov, and Jacob Rasmussen. "The superpolynomial for knot homologies". In: *Experiment. Math.* 15.2 (2006), pp. 129–159. ISSN: 1058-6458. URL: http://projecteuclid.org/euclid.em/1175789736.

[Efi12] Alexander I. Efimov. "Cohomological Hall algebra of a symmetric quiver". In: *Compos. Math.* 148.4 (2012). arXiv:1103.2736, pp. 1133–1146. arXiv: 1103.2736 [math.AG].

[Ekh+] Tobias Ekholm, Angus Gruen, Sergei Gukov, Piotr Kucharski, Sunghyuk Park, and Piotr Sulkowski. *$\widehat{Z}$ at large N: from curve counts to quantum modularity*. eprint: 2005.13349.

[Ekh+22] Tobias Ekholm, Angus Gruen, Sergei Gukov, Piotr Kucharski, Sunghyuk Park, Marko Stošić, and Piotr Sułkowski. "Branches, quivers, and ideals for knot complements". In: *Journal of Geometry and Physics* 177 (2022), p. 104520. ISSN: 0393-0440. DOI: 10.1016/j.geomphys.2022.104520.

[EKL21] Tobias Ekholm, Piotr Kucharski, and Pietro Longhi. *Knot homologies and generalized quiver partition functions*. arXiv:2108.12645. 2021.

[Eli+89] Shmuel Elitzur, Gregory Moore, Adam Schwimmer, and Nathan Seiberg. "Remarks on the canonical quantization of the Chern-Simons-Witten theory". In: *Nuclear Phys. B* 326.1 (1989), pp. 108–134. ISSN: 0550-3213. DOI: 10.1016/0550-3213(89)90436-7. URL: https://doi.org/10.1016/0550-3213(89)90436-7.

[ES19] Tobias Ekholm and Vivek Shende. *Skeins on Branes*. arXiv:1901.08027. 2019. arXiv: 1901.08027 [math.SG].

[FGS13] Hiroyuki Fuji, Sergei Gukov, and Piotr Sułkowski. "Super-A-polynomial for knots and BPS states". In: *Nuclear Phys. B* 867.2 (2013), pp. 506–546. ISSN: 0550-3213. DOI: 10.1016/j.nuclphysb.2012.10.005. URL: https://doi.org/10.1016/j.nuclphysb.2012.10.005.

[FP20] Francesca Ferrari and Pavel Putrov. *Supergroups, q-series and 3-manifolds*. 2020. DOI: 10.48550/ARXIV.2009.14196. URL: https://arxiv.org/abs/2009.14196.

[FR18] Hans Franzen and Markus Reineke. "Semi-Stable Chow-Hall Algebras of Quivers and Quantized Donaldson-Thomas Invariants". In: *Alg. Number Th.* 12.5 (2018). arXiv:1512.03748, pp. 1001–1025. ISSN: 1937-0652. DOI: 10.2140/ant.2018.12.1001. arXiv: 1512.03748 [math.RT].

[Fuj+13] Hiroyuki Fuji, Sergei Gukov, Piotr Sulkowski, and Marko Stosic. "3d analogs of Argyres-Douglas theories and knot homologies". In: *JHEP* 01 (2013). arXiv:1209.1416, p. 175.

[Fuj+21] Hiroyuki Fuji, Kohei Iwaki, Hitoshi Murakami, and Yuji Terashima. "Witten–Reshetikhin–Turaev Function for a Knot in Seifert Manifolds". In: *Communications in Mathematical Physics* 386.1 (Mar. 2021), pp. 225–251. DOI: 10.1007/s00220-021-03953-y. URL: https://doi.org/10.1007%2Fs00220-021-03953-y.

[FZ99] Dominique Foata and Doron Zeilberger. "A combinatorial proof of Bass's evaluations of the Ihara-Selberg zeta function for graphs". In: *Trans. Amer. Math. Soc.* 351.6 (1999), pp. 2257–2274. ISSN: 0002-9947. DOI: 10.1090/S0002-9947-99-02234-5. URL: https://doi.org/10.1090/S0002-9947-99-02234-5.

[Gar04] Stavros Garoufalidis. "On the Charactersitic and deformation varieties of a knot". In: *Geometry and Topology Monographs* 7 (2004). math/0306230, pp. 291–304.

[GL05] Stavros Garoufalidis and Thang T. Q. Lê. "The colored Jones function is q-holonomic". In: *Geom. Topol.* 9 (2005), pp. 1253–1293. ISSN: 1465-3060. DOI: 10.2140/gt.2005.9.1253. URL: https://doi.org/10.2140/gt.2005.9.1253.

[GM21] Sergei Gukov and Ciprian Manolescu. "A two-variable series for knot complements". In: *Quantum Topol.* 12.1 (2021). arXiv:1904.06057, pp. 1–109. ISSN: 1663-487X. DOI: 10.4171/qt/145. URL: https://doi.org/10.4171/qt/145.

[GMP16] Sergei Gukov, Marcos Marino, and Pavel Putrov. *Resurgence in complex Chern-Simons theory*. 2016. DOI: 10.48550/ARXIV.1605.07615. URL: https://arxiv.org/abs/1605.07615.

[GPP21] Sergei Gukov, Sunghyuk Park, and Pavel Putrov. "Cobordism invariants from BPS q-series". In: *Ann. Henri Poincaré* 22.12 (2021), pp. 4173–4203. ISSN: 1424-0637. DOI: 10.1007/s00023-021-01089-2. URL: https://doi.org/10.1007/s00023-021-01089-2.

[GPV17] Sergei Gukov, Pavel Putrov, and Cumrun Vafa. "Fivebranes and 3-manifold homology". In: *J. High Energy Phys.* 7 (2017), 071, front matter+80. ISSN: 1126-6708. DOI: 10.1007/JHEP07(2017)071. URL: https://doi.org/10.1007/JHEP07(2017)071.

[GS06] Stavros Garoufalidis and Xinyu Sun. "The C-polynomial of a knot". In: *Algebr. Geom. Topol.* 6 (2006), pp. 1623–1653. ISSN: 1472-2747. DOI: 10.2140/agt.2006.6.1623. URL: https://doi.org/10.2140/agt.2006.6.1623.

[GS12a] Sergei Gukov and Marko Stosic. "Homological algebra of knots and BPS states". In: *Geom. Topol. Monographs* 18 (2012). arXiv:1112.0030, pp. 309–367.

[GS12b] Sergei Gukov and Piotr Sulkowski. "A-polynomial, B-model, and Quantization". In: *JHEP* 02 (2012). arXiv:1108.0002, p. 070. DOI: 10.1007/JHEP02(2012)070.

[Guk+20] Sergei Gukov, Du Pei, Pavel Putrov, and Cumrun Vafa. "BPS spectra and 3-manifold invariants". In: *J. Knot Theory Ramifications* 29.2 (2020). arXiv:1701.06567, pp. 2040003, 85. ISSN: 0218-2165. DOI: 10.1142/S0218216520400039. URL: https://doi.org/10.1142/S0218216520400039.

[Guk05] Sergei Gukov. "Three-dimensional quantum gravity, Chern-Simons theory, and the A-polynomial". In: *Commun. Math. Phys.* 255 (2005). hep-th/0306165, pp. 577–627. DOI: 10.1007/s00220-005-1312-y.

[GV98] Rajesh Gopakumar and Cumrun Vafa. *M-theory and topological strings–II*. hep-th/9812127. 1998.

[Hab00] Kazuo Habiro. "On the colored Jones polynomials of some simple links". In: 1172. Recent progress towards the volume conjecture (Japanese) (Kyoto, 2000). 2000, pp. 34–43.

[Hab02] Kazuo Habiro. "On the quantum sl_2 invariants of knots and integral homology spheres". In: *Invariants of knots and 3-manifolds (Kyoto, 2001)*. Vol. 4. Geom. Topol. Monogr. Geom. Topol. Publ., Coventry, 2002, pp. 55–68. DOI: 10.2140/gtm.2002.4.55. URL: https://doi.org/10.2140/gtm.2002.4.55.

[Hab07] Kazuo Habiro. "An integral form of the quantized enveloping algebra of sl_2 and its completions". In: *J. Pure Appl. Algebra* 211.1 (2007), pp. 265–292. ISSN: 0022-4049. DOI: 10.1016/j.jpaa.2007.01.011. URL: https://doi.org/10.1016/j.jpaa.2007.01.011.

[Hik05a] Kazuhiro Hikami. "On the quantum invariant for the Brieskorn homology spheres". In: *Internat. J. Math.* 16.6 (2005), pp. 661–685. ISSN: 0129-167X. DOI: 10.1142/S0129167X05003004. URL: https://doi.org/10.1142/S0129167X05003004.

[Hik05b] Kazuhiro Hikami. "Quantum invariant, modular form, and lattice points". In: *Int. Math. Res. Not.* 3 (2005), pp. 121–154. ISSN: 1073-7928. DOI: 10.1155/IMRN.2005.121. URL: https://doi.org/10.1155/IMRN.2005.121.

[Hik06a] Kazuhiro Hikami. "On the quantum invariants for the spherical Seifert manifolds". In: *Comm. Math. Phys.* 268.2 (2006), pp. 285–319. ISSN: 0010-3616. DOI: 10.1007/s00220-006-0094-1. URL: https://doi.org/10.1007/s00220-006-0094-1.

[Hik06b] Kazuhiro Hikami. "Quantum invariants, modular forms, and lattice points. II". In: *J. Math. Phys.* 47.10 (2006), pp. 102301, 32. ISSN: 0022-2488. DOI: 10.1063/1.2349484. URL: https://doi.org/10.1063/1.2349484.

[Hos+85] Jim Hoste, Adrian Ocneanu, Kenneth Millett, Peter J. Freyd, W. B. R. Lickorish, and David N. Yetter. "A new polynomial invariant of knots and links". In: *Bull. Am. Math. Soc.* 12.2 (1985), pp. 239–246.

[Ito+12] H. Itoyama, A. Mironov, A. Morozov, and And. Morozov. "HOMFLY and superpolynomials for figure eight knot in all symmetric and antisymmetric representations". In: *Journal of High Energy Physics* 2012.7 (July 2012). arXiv:1203.5978. ISSN: 1029-8479. DOI: 10.1007/jhep07(2012)131. URL: http://dx.doi.org/10.1007/JHEP07(2012)131.

[Jon85] Vaughan F. R. Jones. "A polynomial invariant for knots via von Neumann algebras". In: *Bull. Amer. Math. Soc. (N.S.)* 12.1 (1985), pp. 103–111. ISSN: 0273-0979. DOI: 10.1090/S0273-0979-1985-15304-2. URL: https://doi.org/10.1090/S0273-0979-1985-15304-2.

[Kho00] Mikhail Khovanov. "A categorification of the Jones polynomial". In: *Duke Math. J.* 101.3 (2000), pp. 359–426. ISSN: 0012-7094. DOI: 10.1215/S0012-7094-00-10131-7. URL: https://doi.org/10.1215/S0012-7094-00-10131-7.

[Kir78] Robion Kirby. "A calculus for framed links in S^3". In: *Invent. Math.* 45.1 (1978), pp. 35–56. ISSN: 0020-9910. DOI: 10.1007/BF01406222. URL: https://doi.org/10.1007/BF01406222.

[KM91] Robion Kirby and Paul Melvin. "The 3-manifold invariants of Witten and Reshetikhin-Turaev for $\mathrm{sl}(2, \mathbf{C})$". In: *Invent. Math.* 105.3 (1991), pp. 473–545. ISSN: 0020-9910. DOI: 10.1007/BF01232277. URL: https://doi.org/10.1007/BF01232277.

[Koh02] Toshitake Kohno. *Conformal field theory and topology*. Vol. 210. Translations of Mathematical Monographs. Translated from the 1998 Japanese original by the author, Iwanami Series in Modern Mathematics. American Mathematical Society, Providence, RI, 2002, pp. x+172. ISBN: 0-8218-2130-X. DOI: 10.1090/mmono/210. URL: https://doi.org/10.1090/mmono/210.

[KS08] Maxim Kontsevich and Yan Soibelman. *Stability structures, motivic Donaldson-Thomas invariants and cluster transformations*. arXiv:0811.2435. 2008. arXiv: 0811.2435 [math.AG].

[KS11] Maxim Kontsevich and Yan Soibelman. "Cohomological Hall algebra, exponential Hodge structures and motivic Donaldson-Thomas invariants". In: *Commun.Num.Theor.Phys.* 5 (2011). arXiv:1006.2706, pp. 231–352. arXiv: 1006.2706 [math.AG].

[Kuc+17] Piotr Kucharski, Markus Reineke, Marko Stosic, and Piotr Sulkowski. "BPS states, knots and quivers". In: *Phys. Rev.* D96.12 (2017). arXiv:1707.02991,

p. 121902. DOI: 10.1103/PhysRevD.96.121902. arXiv: 1707.02991 [hep-th].

[Kuc+19] Piotr Kucharski, Markus Reineke, Marko Stosic, and Piotr Sulkowski. "Knots-quivers correspondence". In: *Adv. Theor. Math. Phys.* 23.7 (2019). arXiv:1707.04017, pp. 1849–1902. arXiv: 1707.04017 [hep-th].

[Kuc20] Piotr Kucharski. "Quivers for 3-manifolds: the correspondence, BPS states, and 3d $\mathcal{N} = 2$ theories". In: *JHEP* 09 (2020). arXiv:2005.13394, p. 075. DOI: 10.1007/JHEP09(2020)075. arXiv: 2005.13394 [hep-th].

[Lic62] W. B. R. Lickorish. "A representation of orientable combinatorial 3-manifolds". In: *Ann. of Math. (2)* 76 (1962), pp. 531–540. ISSN: 0003-486X. DOI: 10.2307/1970373. URL: https://doi.org/10.2307/1970373.

[Lic63] W. B. R. Lickorish. "Homeomorphisms of non-orientable two-manifolds". In: *Proc. Cambridge Philos. Soc.* 59 (1963), pp. 307–317. ISSN: 0008-1981. DOI: 10.1017/s0305004100036926. URL: https://doi.org/10.1017/s0305004100036926.

[LM] C. Livingston and A. H. Moore. *KnotInfo: Table of Knot Invariants*. http://www.indiana.edu/ knotinfo. URL: http://www.indiana.edu/~knotinfo.

[LM01] J. M. F. Labastida and Marcos Marino. "Polynomial invariants for torus knots and topological strings". In: *Comm. Math. Phys.* 217.2 (2001). arXiv:hep-th/0004196, pp. 423–449.

[LMV00] Jose M. F. Labastida, Marcos Marino, and Cumrun Vafa. "Knots, links and branes at large N". In: *JHEP* 11 (2000). arXiv:hep-th/0010102, p. 007.

[LW01] Xiao-Song Lin and Zhenghan Wang. "Random walk on knot diagrams, colored Jones polynomial and Ihara-Selberg zeta function". In: *Knots, braids, and mapping class groups—papers dedicated to Joan S. Birman (New York, 1998)*. Vol. 24. AMS/IP Stud. Adv. Math. Amer. Math. Soc., Providence, RI, 2001, pp. 107–121.

[LZ99] Ruth Lawrence and Don Zagier. "Modular forms and quantum invariants of 3-manifolds". In: vol. 3. 1. Sir Michael Atiyah: a great mathematician of the twentieth century. 1999, pp. 93–107. DOI: 10.4310/AJM.1999.v3.n1.a5. URL: https://doi.org/10.4310/AJM.1999.v3.n1.a5.

[Mar05] Marcos Mariño. "Chern-Simons theory, matrix integrals, and perturbative three-manifold invariants". In: *Comm. Math. Phys.* 253.1 (2005), pp. 25–49. ISSN: 0010-3616. DOI: 10.1007/s00220-004-1194-4. URL: https://doi.org/10.1007/s00220-004-1194-4.

[MM21] Akihito Mori and Yuya Murakami. *Witten-Reshetikhin-Turaev invariants, homological blocks, and quantum modular forms*. 2021. DOI: 10.48550/ARXIV.2110.10958. URL: https://arxiv.org/abs/2110.10958.

[MM95] P. M. Melvin and H. R. Morton. "The coloured Jones function". In: *Comm. Math. Phys.* 169.3 (1995), pp. 501–520. ISSN: 0010-3616. URL: http://projecteuclid.org/euclid.cmp/1104272852.

[MMM13] A. Mironov, A. Morozov, and And. Morozov. "Evolution method and "differential hierarchy" of colored knot polynomials". In: (2013). arXiv:1306.3197. DOI: 10.1063/1.4828688. URL: http://dx.doi.org/10.1063/1.4828688.

[MR19] Sven Meinhardt and Markus Reineke. "Donaldson-Thomas invariants versus intersection cohomology of quiver moduli". In: *J. Reine Angew. Math.* 754 (2019). arXiv:1411.4062, pp. 143–178. ISSN: 0075-4102. DOI: 10.1515/crelle-2017-0010. URL: https://doi.org/10.1515/crelle-2017-0010.

[Neu81] Walter D. Neumann. "A calculus for plumbing applied to the topology of complex surface singularities and degenerating complex curves". In: *Trans. Amer. Math. Soc.* 268.2 (1981), pp. 299–344. ISSN: 0002-9947. DOI: 10.2307/1999331. URL: https://doi.org/10.2307/1999331.

[OV00] Hirosi Ooguri and Cumrun Vafa. "Knot invariants and topological strings". In: *Nucl. Phys.* B577 (2000). hep-th/9912123, pp. 419–438.

[Par] Sunghyuk Park. *Inverted state sums, inverted Habiro series, and indefinite theta functions*. eprint: 2106.03942.

[Par20a] Sunghyuk Park. "Higher rank $\hat{Z}$ and F_K". In: *SIGMA Symmetry Integrability Geom. Methods Appl.* 16 (2020), Paper No. 044, 17. DOI: 10.3842/SIGMA.2020.044.

[Par20b] Sunghyuk Park. "Large color R-matrix for knot complements and strange identities". In: *J. Knot Theory Ramifications* 29.14 (2020), pp. 2050097, 32. ISSN: 0218-2165. DOI: 10.1142/S0218216520500972.

[PR97] Peter Paule and Axel Riese. "A Mathematica q-analogue of Zeilberger's algorithm based on an algebraically motivated approach to q-hypergeometric telescoping". In: *Special functions, q-series and related topics (Toronto, ON, 1995)*. Vol. 14. Fields Inst. Commun. Amer. Math. Soc., Providence, RI, 1997, pp. 179–210.

[PT87] Jozef Przytycki and Pawel Traczyk. "Invariants of links of Conway type". In: *Kobe J. Math.* 4 (1987), pp. 115–139.

[Ras10] Jacob Rasmussen. "Khovanov homology and the slice genus". In: *Invent. Math.* 182.2 (2010), pp. 419–447. ISSN: 0020-9910. DOI: 10.1007/s00222-010-0275-6. URL: https://doi.org/10.1007/s00222-010-0275-6.

[Roz97] L. Rozansky. "Higher order terms in the Melvin-Morton expansion of the colored Jones polynomial". In: *Comm. Math. Phys.* 183.2 (1997), pp. 291–306. ISSN: 0010-3616. DOI: 10.1007/BF02506408. URL: https://doi.org/10.1007/BF02506408.

[Roz98] L. Rozansky. "The universal R-matrix, Burau representation, and the Melvin-Morton expansion of the colored Jones polynomial". In: *Adv. Math.* 134.1 (1998), pp. 1–31. ISSN: 0001-8708. DOI: 10.1006/aima.1997.1661. URL: https://doi.org/10.1006/aima.1997.1661.

[RT91] N. Reshetikhin and V. G. Turaev. "Invariants of 3-manifolds via link polynomials and quantum groups". In: *Invent. Math.* 103.3 (1991), pp. 547–597. ISSN: 0020-9910. DOI: 10.1007/BF01239527. URL: https://doi.org/10.1007/BF01239527.

[Sta78] John R. Stallings. "Constructions of fibred knots and links". In: *Algebraic and geometric topology (Proc. Sympos. Pure Math., Stanford Univ., Stanford, Calif., 1976), Part 2*. Proc. Sympos. Pure Math., XXXII. Amer. Math. Soc., Providence, R.I., 1978, pp. 55–60.

[SW19] Marko Stosic and Paul Wedrich. "Rational links and DT invariants of quivers". In: *Int. Math. Res. Not.* 2021.6 (2019). arXiv:1711.03333, pp. 4169–4210.

[SW21] Marko Stosic and Paul Wedrich. "Tangle addition and the knots-quivers correspondence". In: *J. London Math. Soc.* (2021). doi.org/10.1112/jlms.12433. arXiv:2004.10837. arXiv: 2004.10837 [math.QA].

[Tur02] Vladimir Turaev. *Torsions of 3-dimensional manifolds*. Vol. 208. Progress in Mathematics. Birkhäuser Verlag, Basel, 2002, pp. x+196. ISBN: 3-7643-6911-6. DOI: 10.1007/978-3-0348-7999-6. URL: https://doi.org/10.1007/978-3-0348-7999-6.

[Tur94] V. G. Turaev. *Quantum invariants of knots and 3-manifolds*. Vol. 18. De Gruyter Studies in Mathematics. Walter de Gruyter & Co., Berlin, 1994, pp. x+588. ISBN: 3-11-013704-6.

[Wal60] Andrew H. Wallace. "Modifications and cobounding manifolds". In: *Canadian J. Math.* 12 (1960), pp. 503–528. ISSN: 0008-414X. DOI: 10.4153/CJM-1960-045-7. URL: https://doi.org/10.4153/CJM-1960-045-7.

[Wil22] Sonny Willetts. "A unification of the ADO and colored Jones polynomials of a knot". In: *Quantum Topol.* 13.1 (2022), pp. 137–181. ISSN: 1663-487X. DOI: 10.4171/qt/161. URL: https://doi.org/10.4171/qt/161.

[Wit88] Edward Witten. "Topological quantum field theory". In: *Comm. Math. Phys.* 117.3 (1988), pp. 353–386. ISSN: 0010-3616. URL: http://projecteuclid.org/euclid.cmp/1104161738.

[Wit89] Edward Witten. "Quantum field theory and the Jones polynomial". In: *Comm. Math. Phys.* 121.3 (1989), pp. 351–399. ISSN: 0010-3616. URL: http://projecteuclid.org/euclid.cmp/1104178138.

[Wit95] E. Witten. "Chern-Simons gauge theory as a string theory". In: *The Floer memorial volume*. Vol. 133. Progr. Math. Birkhäuser, Basel, 1995, pp. 637–678.